# Spatial coalescent connectivity through multi-generation dispersal modelling predicts gene flow across marine phyla

Térence Legrand, Anne Chenuil, Enrico Ser-Giacomi, Sophie Arnaud-Haond, Nicolas Bierne, Vincent Rossi

# Title:

Spatial coalescent connectivity through multi-generation dispersal modelling predicts gene flow across marine phyla

# Author list :

Térence Legrand[1]*; Anne Chenuil[2]; Enrico Ser-Giacomi[3]; Sophie Arnaud-Haond[4]; Nicolas Bierne[5]; Vincent Rossi[6]*

# Affiliations :

[1]Aix Marseille University, Universite de Toulon, CNRS, IRD, Mediterranean Institute of Oceanography (UMR 7294), Marseille, France. (legrandterence@gmail.com).

[2] Institut Méditerranéen de Biodiversité et d'Ecologie Marine et Continentale, CNRS (UMR 7263), Station Marine d'Endoume, Marseille, France. (anne.chenuil@imbe.fr).

[3]Department of Earth, Atmospheric and Planetary Sciences, Massachusetts Institute of Technology, 54-1514 MIT, Cambridge, Massachusetts, USA. (enrico.sergiacomi@gmail.com).

[4] MARBEC (Marine Biodiversity, Exploitation and Conservation, UMR 9190) Univ. Montpellier, IFREMER, IRD, CNRS, Sète, France. (sophie.arnaud-haond@umontpellier.fr).

[5]ISEM, Univ Montpellier, CNRS, IRD, Montpellier, France. (nicolas.bierne@umontpellier.fr).

[6]Aix Marseille University, Universite de Toulon, CNRS, IRD, Mediterranean Institute of Oceanography (UMR 7294), Marseille, France (vincent.rossi@mio.osupytheas.fr).

*Corresponding authors.

## Abstract:

Gene flow governs the contemporary spatial structure and dynamic of populations as well as their long-term evolution. For species that disperse using atmospheric or oceanic flows, biophysical models allow predicting the migratory component of gene flow, which facilitates the interpretation of broad-scale spatial structure inferred from observed allele frequencies among populations. However, frequent mismatches between dispersal estimates and observed genetic diversity prevent an operational synthesis for eco-evolutionary projections. Here we use an extensive compilation of 58 population genetic studies of 47 phylogenetically divergent marine sedentary species over the Mediterranean basin to assess how genetic differentiation is predicted by Isolation-By-Distance, single-generation dispersal and multi-generation dispersal models. Unlike previous approaches, the latter unveil explicit parents-to-offspring links (filial connectivity) and implicit links among siblings from a common ancestor (coalescent connectivity). We find that almost 70 % of observed variance in genetic differentiation is explained by coalescent connectivity over multiple generations, significantly outperforming other models. Our results offer great promises to untangle the eco-evolutionary forces that shape sedentary population structure and to anticipate climate-driven redistributions, altogether improving spatial conservation planning.

## Introduction:

Gene flow counterbalances natural selection and genetic drift, reshuffles mutations among spatial locations and contributes to shaping the contemporary spatial patterns of biodiversity [1–5]. By introducing foreign alleles to local populations, gene flow spreads adaptative changes and tends to alleviate the effect of inbreeding depression [1–3]. Simultaneously, gene flow homogenises allele frequency among populations, which counteracts the effects of local adaptation, reducing the mean fitness of populations (i.e. migration load) [2]. Fundamentally, gene flow is ensured when dispersal is followed by reproduction and subsequent offspring survival [6]. A common confusion prevails between demographic connectivity (i.e. the number of migrants exchanged among populations), which is usually assessed by direct detection of individuals (field observations and parentage analyses of genetic data), and genetic connectivity (i.e. the efficient transfer of genetic material between distant populations), which is indirectly estimated thanks to population genetics analyses [1,3,4,7–10]. In this way, demographic and genetic connectivity seem to interact on specific -yet poorly appreciated- temporal and spatial scales [3,11–14]. This may explain the numerous mismatches reported between demographic connectivity and gene flow estimates [7–9].

This paradox could stem from the fact that dispersal is a complex and multi-aspect process involving interlocked ecological and evolutionary mechanisms [6,15,16]. Dispersal results from movements of individuals themselves or those induced by third-parties categorized as biotic, (e.g. thanks to other moving organisms [17,18]), or abiotic, that is driven by winds and ocean currents [8,16,19]. This study focuses on species that, as adults, have no or little displacement abilities (hereafter called sedentary species) so that their connectivity is mostly ensured by the abiotic dispersal of propagules, like numerous marine and terrestrial taxa. This alleviates the difficulties in appraising the movements of wild populations and biotic third parties. In marine sedentary populations, early-life non-motile stages (e.g. seeds, eggs, larvae) are regularly released in the water column and are then passively transported across the seascape by anisotropic currents over various spatial scales [20,21], ensuring the replenishment

of both local and distant populations [22,23]. As such, the proper evaluation of current-driven dispersal should help us disentangling the evolutionary forces (gene flow, selection, genetic drift or mutation) shaping marine biodiversity and its climate-driven redistributions [24]. The inherent spatial scales of genetic structures are generally a few orders of magnitude higher than potential dispersal distances over a single generation [25], even for species exhibiting rare long-distance dispersal [26,27]. Likewise, a single generation dispersal event does not allow to evaluate the evolutionary timescale over which gene flow shapes genetic diversity [6]. Theory predicts instead that consecutive dispersal events of numerous propagules, acting in synergy with other evolutionary forces, shape together the genetic diversity observed at broad-scale [26,28]. Consequently, modelling genetic diversity from the unique perspective of water-borne dispersal should enlighten the typical scales and relative importance of evolutionary forces that shape the spatial structure of marine sedentary populations.

Modelling water-borne dispersal is a multidisciplinary challenge sharing tight commonalities with air-borne dispersal [29]. First, it requires to jointly account for the spatio-temporal variability of currents, the species-specific early-life traits, the habitat patchiness [9,30], as well as to consider all possible connectivity pathways [31]. Second, it must simulate consecutive dispersal events by considering multiple generations of migrants where each intermediary connected population acts as a stepping-stone. Third, it must simulate all possibly existing populations, not just known or sampled ones. Bio-physical models, which simulate explicitly the dispersal of propagules by oceanic chaotic flows, have been widely used in the last few decades to derive physical connectivity metrics such as dispersal kernels [20,23,32,33]. Simulations of single-generation dispersal commonly provide quantitative estimates of how distant populations are connected with each other. However they rarely match observed gene flows [8], possibly due to intrinsic flaws such as disregarding the multi-generational character of successive dispersal events [34–36], while overlooking intermediate stepping-stone connections.

In the marine realm, current models considering multi-generational dispersal are seldom used, concern only a few specific species or taxa, and still inadequately explain genetic differentiation

measures. They rely on the computation of connectivity matrices, which are mathematical objects describing dispersal of propagules exchanged between discrete populations, hereafter called localities. Such matrices can be interpreted as adjacency matrices of directed and weighted networks (or graphs). Thus, an approach consists in considering network theory tools such as shortest paths analysis to estimate the strength of connections among two distinct localities over multiple dispersal events [34,37,38]. As shortest and most-probable paths of such networks differ [39], these methods neglect all other possible pathways that may drastically change the resulting connectivity [40]. Another approach uses Markov chains and matrix multiplications to estimate the probability of connection between locality-pairs over a given number of generations [35,41–43]. Studies using this method did not consider all the inherent dispersal pathways as they only assessed the connection probabilities occurring at a given number of generations (equivalent to the exact number of multiplication) while neglecting all intermediate connections associated to any number of generations lower or equal to the prescribed number of dispersal events [44]. Moreover, and to our knowledge, all present modelling approaches simulate stepping-stone dispersal of single lineages; in other words, they estimate the connectivity resulting from explicit parents-to-offspring connections, i.e. filial connectivity. However, it is conspicuous that two fully disconnected localities, which are both replenished by migrants originating from the same source locality, should share common alleles and thus display similar allele frequencies.

The consideration in dispersal models of this conceptual view of coalescent connectivity [44], that highlights implicit links among siblings through common ancestors has been overlooked to-date, although it could largely alter gene flow predictions and contribute to the aforementioned discrepancies between predicted dispersal and realized gene flow assessments [1]. Note that here the term “coalescent” refers to the dispersal model, not to the genetic model. Modelling such implicit connections would permit going beyond the concept of pairwise interactions addressing higher-order dynamics, a perspective that is lately attracting lots of interests, both in Network Theory [45] and Theoretical Ecology [46,47].

In this work, we present an exhaustive comparison between demographic and genetic basin-scale connectivity based on classical and novel dispersal metrics across a meta-analysis of several marine taxa. While our results mainly apply to marine sedentary populations whose dispersal is mediated by ocean currents, our models and conclusions have the potential to transform how water- as well as air-borne dispersal of sedentary terrestrial populations are evaluated. Here, we introduce state-of-the-art multi-generation dispersal models that evaluate all connections among locality-pairs for a fixed number of generations while simultaneously accounting for those accumulated by previous generations [44]. Our models provide not only a precise estimation of the explicit links (filial connectivity) but also allow computing, for the first time, the implicit links existing between any locality-pair having common source localities through multi-generational dispersal (coalescent connectivity). After parameterizing our model with the main dispersal traits of various taxa encompassing seagrasses, algae and metazoans, we test modelled gene flow predictions against an extensive compilation of observed genetic structures (i.e. genetic differentiation estimates given by $F_{st}$ between locality-pairs [48]) over the whole Mediterranean Sea. We find that coalescent connectivity through multi-generation dispersal explains almost 70 % of the observed variance of genetic structures, substantially improving gene flow predictions with respect to previous approaches. Furthermore, the optimal number of generations to best predict gene flow significantly correlates with the sampling coverage scaled by the species-specific dispersal abilities, enlightening the typical scales of eco-evolutionary processes. It suggests that our model could be used to infer population genetic structures, a key pre-requisite for management and protection.

## Results:

We test the predictions of our multi-generation explicit and implicit dispersal models [44], simulating filial and coalescent connectivity respectively, against an extensive compilation of 58 genetic structures observed in the Mediterranean Sea. The dataset contains 3821 observed $F_{st}$ measures ($F_{st}^{obs}$) between locality-pairs for 47 marine species (Fig. 1a) which are characterized by a biphasic life-cycle, i.e. early-life free-swimming dispersing propagules and full to semi-sedentary adult (Fig. 2a). We model the full range of variability of current-driven dispersal over the whole Mediterranean basin for each species using a fine-tuned particle-tracking model [23,49–52], fed by the horizontal multi-year velocity field from an operational data-assimilative ocean model [53]. Each species is characterized by three main dispersal traits: Pelagic Larval Duration (PLD, i.e. the time propagules spend drifting with ocean currents, Fig. 2a), spawning seasons and adult habitats (Fig. 1b,c). These biological factors were identified as the major ones governing how the variability of ocean currents reflect on our probabilistic connectivity metrics [39,50].

Among the 58 compiled basin-scale population genetic studies (Fig. 1), we test for prediction of $F_{st}^{obs}/(1-F_{st}^{obs})$ [48,54] by our cumulative explicit and implicit dispersal models (Fig. 2b,c) considering both single- and multi-generation estimates thanks to a maximum-likelihood population-effects (MLPE) linear mixed model. We also test for conventional Isolation-By-Distance (IBD) models, using either Euclidian or sea-least cost distances (i.e. the shortest overwater distances). The number of significant $R^2$ is 16 for single-generation explicit, 30 for Euclidian IBD, 31 for sea least-cost IBD, 37 for multi-generation explicit and implicit models respectively (Fig. 3). Among the significant MLPE linear mixed model $R^2$, the lowest mean $R^2$ is found for the single-generation explicit dispersal model (0.50, i.e. 95% confidence intervals), followed by both sea-least cost (0.58) and Euclidian (0.59) IBD models. The highest mean $R^2$ stem from both multi-generation models, with 0.68 for explicit dispersal and 0.69 for implicit dispersal models.

Next, we evaluate the quality (i.e. predictive ability) of each model relative to each of the other models, and then to all models together, thanks to the AIC estimator. To do so, the same expected value, $F_{st}^{obs}/(1-F_{st}^{obs})$, is considered among the five different models of gene flow when using MLPE linear mixed models. The best model is the multi-generation implicit dispersal model in 25 cases, the multi-generation explicit dispersal model in 18 cases, the Euclidian IBD model in 10 cases, the sea least-cost IBD model in 7 cases, and the single-generation explicit dispersal model in only 3 cases. The relative likelihood permits to evaluate that among the five candidate models, the multi-generation implicit dispersal model is the one that minimises the information lost with a mean relative likelihood of 0.75 at the meta-analysis scale. Moreover, the multi-generation implicit dispersal model is the only one that displays positive relative likelihood difference in pairwise comparisons with the four other models (Fig. 3). Hence, our multi-generation implicit dispersal model provides the best predictions of $F_{st}^{obs}$.

When inspecting the study-specific accuracy of the best multi-generation implicit dispersal model, $R^2$ values range from 0.11 for the colonial ascidian *Botryllus schlosseri* [55] to 1 for the ascidian *Halocynthia papillosa* [56], the sea cucumber *Holothuria mammata* [57] and the sea snail *Phorcus turbinatus* [56] (Fig. 4a). For studies that include abundant genetic markers, it is possible to identify markers with particularly high $F_{st}^{obs}$ values (i.e. outliers; based on appropriate models), suggesting that natural selection filtered alleles differentially among localities. For a sea urchin *Paracentrotus lividus* [58], $F_{st}^{obs}$ outlier loci returns a $R^2$ of 0.93***, which is higher than the $R^2$ of 0.80*** obtained considering all the loci. Note that two studies focusing on the same species both using microsatellite markers, can display contradictory results: *Corallium rubrum* is characterized by a highly significant and tight correlation ($R^2$ = 0.54***, [59]) as well as a non-significant loose correlation ($R^2$ = $0.27^{ns}$,[60] ; Fig. 4a), exemplifying inter-study variability. For the flathead grey mullet *Mugil cephalus* [61], which have been sampled homogeneously across the Mediterranean basin (i.e. the mean straight-line geographical distance between sampled localities, $D_{btw}$, is 1279 km, Supplementary Table 1), the network representation of modelled $F_{st}$ ($F_{st}^{mod}$) mimics well the one of $F_{st}^{obs}$ (Fig. 4b). $F_{st}^{obs}$ are low for locality-

pairs located in the western basin but relatively high between western and eastern Mediterranean localities, suggesting spatial genetic structuring that is well predicted by coalescent connectivity (see the scatter plot of Fig. 4b, $R^2 = 0.73$***). Similar results are obtained for instance for a seagrass species, *Cymodocea nodosa* [62] (Fig. 4c). Although in this case spatial sampling is less balanced (sampled locality mostly clustered along the Spanish coast but with two distant localities in the Eastern Mediterranean, $D_{btw}$ = 1601 km), the genetic structure (high $F_{st}^{obs}$) between the Adriatic and Spanish localities is well reproduced by $F_{st}^{mod}$ ($R^2 = 0.77$***).

We then test the robustness of the multi-generation implicit dispersal model with respect to the species and studies attributes. None of these factors (taxa, PLD, spawning season, genetic marker, and $D_{btw}$) has a significant effect on model fit results ($R^2$, *p-value*, Supplementary Table 10). Yet, we find a significant linear negative correlation between the logarithm of MLPE linear mixed models *p-values* and the number of sampled localities ($R^2 = 0.40$***) as well as with the range of $F_{st}^{obs}$ ($R^2 = 0.18$***, Supplementary Table 10). Furthermore, the probability to obtain a significant $R^2$, i.e. successful gene flow predictions, as a function of categories of number of sampled localities is well predicted by a logit model using a binomial distribution ($R^2 = 0.72$***, Supplementary Figure 10). Finally, we find a positive linear relationship between the PLDs categories and $D_{btw}$ divided by the optimal number of modelled generations ($R^2 = 0.31$***, Fig.5), considering the 37 studies whose model predictions of genetic observations are significant. This surprisingly tight relationship has several interesting implications. First, if the spatial structures of two species are evaluated through the same sampling design, our dispersal model needs more generations for short PLD than for long PLD species to properly represent genetic observations. Consequently, our model conforms to the intuitive view that a species needs more successive events of dispersion across generations to disperse widely across the seascape. Moreover, if two species have similar PLDs, our model requires a higher number of generations to accurately simulate the genetic structure of the one whose sampling is wider and more comprehensive. Last, when parameterized to fit the dispersal ability (i.e. PLD) of the target species, the predictive ability of the implicit dispersal model scales with the $D_{btw.}$ The metric $D_{btw}$/(optimal number

of generation) could be interpreted as the average velocity of genetic connectivity in km.generations$^{-1}$. Altogether and assuming that the species-specific dispersal traits have been accurately parametrized, it suggests that the non-significant gene flow predictions (e.g. 21 studies among the meta-analysis) could be attributed to too scarcely and spatially-restricted sampling rather than to the models abilities themselves.

## Discussion:

For gene flow predictions at the meta-analysis scale, the cumulative multi-generation implicit dispersal model [44], which evaluates coalescent connectivity, significantly outperformed explicit dispersal models, which assess filial connectivity, as well as IBD models. Nearly two thirds of the predicted genetic differentiation estimates are significant, even though observations span a wide phylogenetic range of sedentary taxa with contrasted dispersal traits. It is more than twice the proportion displayed by the explicit single-generation dispersal model, which emerges as the worst model in our meta-analysis. Overall, the best models are the multi-generation implicit and explicit dispersal, suggesting unambiguously that modelling multiple generations is crucial to accurately predict genetic connectivity [36]. To our knowledge, the only other model that considers both coalescent and filial connectivity uses circuit theory to approximate how barriers and corridors of habitat affect genetic connectivity through a process called Isolation-By-Resistance [63]. While this empirical model helped interpreting gene flow for self-dispersing organisms across a well-known and relatively stable landscape [40], it has not yet been applied to the marine realm probably because the seascape is highly variable and in perpetual movement. Contrarily, our dispersal models are mechanistic and plainly consider the dynamical properties of ocean currents that drive water-borne dispersal, so that it can be readily applied to air-borne dispersal [29].

We find that multi-generation dispersal models performed significantly better than IBD models. Similar results are found when using explicit multi-generation models for the seagrass *Zostera marina* in the North Sea [35], and the mollusc *Kelletia kelletii* along the Californian shores [43]. Yet, Boulanger et al. (2020) found a tighter and more significant correlation of observed genetic structure with sea least-cost IBD model than with their explicit multi-generation dispersal model for the fish *Mullus surmuletus* [64]. By contrast, when using the same data of $F_{st}^{obs}$, our multi-generation implicit dispersal model returns a better correlation than IBD models.

Our results also show that IBD models (Euclidian and sea-least cost distance) better explain observed genetic differentiation than the single-generation dispersal model, in accord with previous studies [34,35]. Slightly more than half of the compiled studies displayed significant IBD predictions. The mean Mantel $R^2$ computed from these studies (Supplementary Table 5 and 6) is comparable to previous meta-analysis [65,66]. Still, for some previous studies which do not consider multi-generation, single-generation dispersal models were reported to improve gene flow prediction as compared to IBD models (e.g [67–69]). The apparent contradiction with the present results may be due to a publication bias: single-generation dispersal predictions that were worse than IBD's ones could have been withheld by authors. Single-generation dispersal models are worse than IBD models probably because broad-scale single-generation dispersal modelling studies often reported that most distant localities were not connected at all, suggesting genetic isolation. This was often explained by dispersal barriers due to major oceanographic features such as fronts and jet-like currents [70]. Our results contradict this view: multi-generation dispersal models suggest that these locality-pairs can be connected through stepping-stone dispersal despite the supposed physical barriers [44]. Notwithstanding, our models showed that physical barriers still can limit the levels of connectivity (see Fig. 8 of Ser-Giacomi *et al*., 2021) as reflected in observed genetic differentiation and as predicted by theoretical gene flow magnitudes [3,7]. Consequently, the reduced gene flow measured across these barriers is probably due to the large environmental gradients (affecting negatively propagules survival and settlement) they symbolize rather than to intrinsic transport barriers (since propagules dispersal is effective through them, [44]). Since IBD is an analytical model with little biological meaning as it tentatively explains genetic differentiation by only accounting for geographical distances, it does not allow disentangling the relative importance of evolutionary processes that control gene flow. In line with the distinction between IBD and Isolation-by-Environment [71], and since our mechanistic multi-generation dispersal models realistically simulate stepping-stone dispersal, one can tease apart the respective role of evolutionary forces in driving gene flow. In fact, the non-significant predictions of observed genetic differentiation suggests that strong evolutionary forces (such as natural selection) not considered in

266 our approach are at play. Moreover, our analysis indicates that addressing implicit connections and
267 thus going beyond simple pairwise perspectives (i.e. such as explicit connections) [45], can significantly
268 improve the understanding of biogeographical and genetic patterns [47]. Altogether, our results suggest
269 that the–supposed physical barriers often underlined in seascape analyses are more permeable to
270 dispersal than previously thought [70], and that genetic isolation in the marine realm could be rather due
271 to environmental selection acting on drifting propagules and settled adults as well as intrinsic
272 reproductive isolation [72]. Since both ocean currents [73], transport and mixing [74] and temperatures [75] are
273 already changing fast, the structure of marine populations is expected to fluctuate accordingly,
274 consistently with the recent evidence of spatial reorganization of marine biodiversity [24].

275 Our models perform better than previous ones probably also because they consider properly the
276 mesoscale variability of ocean currents, they are parametrized with species-specific dispersal traits,
277 and they allow testing explicitly what number of generations maximise correlations with observed
278 data. Since there is no consensus on the adequate number of generations required to comprehend
279 gene flow, previous multi-generational approaches used shortest path algorithms (minimum number
280 of steps to connect sampled locality-pairs) with 25 or less intermediate steps [34,37] or set arbitrarily the
281 number of generations from dozens (as it was considered sufficient to span the studied domain, [35]) to
282 thousands (i.e. the number of Markov chain iterations needed to reach convergence) of generations
283 [43]. It illustrates that the typical time-scales over which demographic connectivity interplays with
284 genetic connectivity are difficult to infer [1,3]. The relationship between the main dispersal trait (PLD)
285 and the $D_{btw}$ (evaluating the spatial extent of the sampling) divided by the optimal number of
286 generations implies that the temporal scales estimated with our implicit model (from 1 to several tens
287 of generations, e.g. ecological time) and spatial scales derived from genetic methods (over typical
288 evolutionary scales, from a hundred to a few thousands of kilometres) are tightly linked. This is aligned
289 with estimates of dispersal kernels that were found congruent over ecological and evolutionary time
290 [14]. Indeed, the averaged genetic connectivity velocities, in km.generation$^{-1}$, match the demographic
291 connectivity scales for similar PLD (an order of 100 km for two coastal fishes [23]). Moreover, island

model theory assumes that the metapopulation has reached an equilibrium between gene flow and genetic drift [76], suggesting that the implicit model should predict best $F_{st}^{obs}/(1-F_{st}^{obs})$ for long-term multi-generation dispersal, that is when dispersal probabilities reach convergence [43] (i.e. after about 500 generations in our case; see Fig. 9 of Ser-Giacomi *et al*., 2021). The relatively low median optimal number of generations disclosed here (~ 20, Supplementary Figure 7) further suggests that gene flow and drift have insufficient time to reach equilibrium due to environmental stochasticity and rapidly changing ecological forces [10]. Moreover, the substantial impacts of ecological processes on genetic structures shown here could explain why chaotic genetic patchiness has been recently documented at small space and time scales [11,77–81], which are also the scales over which dispersal and environment co-vary. As such, dispersal could be characterized as one of the evolutionary forces shaping the contemporary spatial patterns of biodiversity, along with natural selection, providing evolutionary changes occurring over ecological timescales of few generations [78,82].

Last but not least, our multi-generation mechanistic dispersal models, which allow assessing both filial and coalescent connectivity and are applicable to other taxonomic groups and ecosystems, could serve as future guidelines to optimize sampling design for population genetic studies and anticipate the structure of wild sedentary populations. Moreover, while higher-order interactions can stabilize competitive ecosystems [83], they can also foster abrupt transitions [45]. Investigating such aspects in marine ecosystems would provide crucial information about how they could react to future perturbations and open the way to novel approaches to spatial ecology. In the context of biodiversity loss [84] and spatial reorganization [24], it is indeed urgent to better understand the eco-evolutionary dynamics that continuously shape population structures to improve protection strategies [85] and management of natural resources such as forestry and fisheries [86].

# Methods:

**Studies characteristics.**

We screen the published literature over the last two decades to gather population genetic studies focussing on marine species at basin-scale in the Mediterranean Sea. While our meta-analysis intends to be the most comprehensive possible in terms of collected data and taxa covered, pre-selected studies are filtered out based on two criteria: the biological traits of the species and the sampling design. In this way, we exclude datasets that are not appropriate to address our research question while optimizing statistical discriminatory power. More specifically, we select studies (i) whose target poorly mobile species, i.e. that is characterized by a biphasic life cycle with early-life free-swimming dispersing propagules (e.g. seeds, eggs, larvae or body fragments) and sessile to sedentary adult behaviour (Fig. 1a), and (ii) which must present at least four distinct localities where at least 15 individuals were sampled (see the PRISMA flow diagram depicting our systematic review in Supplementary Notes 1). As a result, this meta-analysis compiles 58 population genetic studies published between 2002 and 2020, encompassing 47 different marine species distributed in nine taxonomic groups: Algae, Anthozoa, Ascidiacea, Crustacea, Demospongiae, Echinodermata, Fish, Mollusca and Phanerogam (Fig. 1a). In total, 559 localities were sampled across the basin (dark green dots in Fig. 1b,c), representing 3821 locality-pairs. $F_{st}$ fixation index allows evaluating the genetic differentiation (i.e. observed genetic differentiation, $F_{st}^{obs}$) between locality-pairs using five types of genetic markers (allozymes, microsatellites, mitochondrial DNA sequences, nuclear DNA sequences and SNPs from high throughput sequencing). Note that, when applicable, we analyse separately different genetic markers extracted from the same study, i.e. mitochondrial DNA sequences and nuclear DNA sequences for *Ophioderma longicauda* [87] and *Hexaplex trunculus* [88].

To gauge the sampling strategy of each selected study, we compute the mean straight-line geographical distance (in km) between sampled localities. This geometrical metric, that we called $D_{btw}$, quantitatively evaluates the spatial coverage of the sampling strategy carried out in each study.

**Species characteristics.**

Based on literature review (Supplementary Table 2), all species are classified according to their main dispersal traits. Reproductive phenology comprises five groups to reflect seasonal (spring, summer, fall, winter) and annual spawning strategies. Pelagic Larval Durations (PLD) are categorized in five groups: very-low (1 day), low (10 days), low-to-medium (20 days), medium-to-high (30 days) and high (45 days) dispersal abilities. Finally, two broad-scale classes of habitats are distinguished (Supplementary Methods 2): the shallow coastal habitat (inner continental shelf whose depths span 0-50 m; Fig. 1b) and the neritic shelf habitat (mid to outer continental shelf whose depths range is 50-200 m; Fig. 1c).

**Bio-physical modelling.**

Tracking passive Lagrangian particles is a common approach to characterize flow-driven dispersal of propagules [20,23,29,49,51,89] (Fig. 2a). To provide synthetic -yet realistic- views of basin-scale propagules dispersal while encompassing the full variability of ocean currents and for various dispersal abilities, we use the Lagrangian Flow Network framework (LFN [23,39,49–52]). It combines a particle-tracking model with graph theory tools to generate and analyse connectivity matrices (Supplementary Methods 3), allowing us to investigate oceanic dispersal in a robust and efficient manner [50].

The Mediterranean Sea surface characterized by favourable habitats is subdivided into several ¼° sub-areas that are considered in our analysis as theoretically isolated marine localities, resulting in n = 1170 localities in the shallow coastal habitat (Fig. 1b) while the neritic shelf habitat is composed of n = 1163 localities (Fig. 1c; see Supplementary Methods 2). For each LFN experiment, we track 100 propagules per localities (i.e. totalling ~ 120,000 propagules considering all the localities contained in each habitat) by integrating daily gridded velocity fields generated by a data-assimilative operational ocean model implemented in the Mediterranean Sea at a 1⁄16° horizontal resolution [53]. We use the horizontal flow field at 10 m and 100 m for species inhabiting shallow coastal and neritic shelf habitats, respectively. Overall, virtual propagules trajectories are modelled at two specific depths during the five

PLDs groups defined previously, simulating consecutive propagule release events with a 10-day periodicity over 2000 to 2010. Assuming that the long-term (e.g. decadal, centennial and longer) variability of ocean currents is negligible as compared to their inter- and intra-annual variations, our approximation using 10 recent years allows comprehending the full variability of both contemporary and past oceanic flows. By computing billions of Lagrangian trajectories and recording their initial and final positions, the LFN constructs 402 connectivity matrices for each of the 10 habitat/PLD combinations, resulting in 4020 matrices in total. The elements $m_{ij}$ of each raw n x n connectivity matrix encode the number of propagules advected between all locality-pairs; they are converted into backward-in-time dispersal probabilities thanks to a column-normalization:

$$m_{ij} = \frac{m_{ij}}{\sum_{i=1}^{n} m_{ij}} \quad (1)$$

Then connectivity matrices *M* are aggregated (i.e. element-by-element averaged) according to their starting dates to match each species-specific spawning phenology. We average 402 matrices for year-round release and about 100 matrices for seasonal release (i.e. 402 and about 100 Lagrangian experiments respectively, Supplementary Table 4). In other words, we compute for each species a composite matrix *P* (i.e. a 1170 x 1170 matrix for the shallow coastal habitat and a 1163 x 1163 matrix for the neritic shelf habitat, encompassing both sampled and non-sampled localities) that fits best its dispersal traits, averaging ten years of realistic current-driven dispersal in the Mediterranean Sea. Single-generation dispersal estimates are directly extracted from one of these composite matrices. As explained next, multi-generational dispersal estimates are finally obtained by applying additional computations on these composite matrices.

**Cumulating implicit and explicit links in multi-generation dispersal models.**

Explicit links, [44], evaluate filial connectivity from parents to children, assuming unique lineage (Fig. 2b). It is the usual proxy of connectivity used in other multi-generation models to assess gene flow between localities [34–38,41–43]. Implicit links, [44], evaluate coalescent connectivity among siblings with common parents, considering multiple lineages (Fig. 2c). To estimate multi-generation dispersal

probabilities between all locality-pairs, considering explicit or implicit links, we apply the theoretical formulations described in Ser-Giacomi *et al*., 2021 on composite matrices. The main novelties of this approach are i) the adequate consideration of putative intermediate connections or steps between any of the non-sampled localities of both habitats (Fig. 1b,c) and ii) the fact that it allows cumulating connectivity pathways over each consecutive generation, i.e. from one generation to a fixed number of generations. For example, the connection between two localities over three generations of dispersal also accounts for connections over two and one generations. Analytical formulations for both cumulative explicit and implicit probabilities for any number of generations are established in Ser-Giacomi *et al*., 2021 and are theoretically bounded to 1 for an infinite number of generations.

- The general expression of explicit dispersal probabilities over G = 2 generations based on the composite matrix *P* is:

$$P^{G=2} = P + P(L \circ P) \quad (2)$$

The circle denotes the Hadamard product, and *L* is the all-ones matrix minus the identity matrix. When applying equation (2) for two localities A and B (example illustrated in Fig. 2b), explicit link cumulates: (i) the sampled locality-pair explicit probability ($P_{AB}$) and (ii) the products of probabilities between sampled localities and their second generation intermediate locality ($P_{Ak_1}P_{k_1B}$, Fig. 2b), that is:

$$P_{AB}^{G=2} = P_{AB} + P_{Ak_1}P_{k_1B} \quad (3)$$

- The general expression of implicit dispersal probabilities over G = 2 generations based on the composite matrix *P* is:

$$P^{G=2} = P^{\,T}P + P\left[L \circ \left(P^{\,T}P\right)\right]^{T}P \quad (4)$$

As before, the circle denotes the Hadamard product, and *L* is the all-ones matrix minus the identity matrix. When applying equation (4) for two localities A and B (example illustrated in Fig. 2c) implicit link cumulates: (i) the product of probability between sampled localities and

their common source (i.e. parent) localities $\left(P_{Ak_1}P_{Bk_1}\right)$; and (ii) the product of probability between sampled localities and their common source localities through two generations ($P_{AI_A}P_{I_Ak_2}P_{BI_B}P_{I_Bk_2}$, Fig. 2c), that is:

$$P_{AB}^{G=2} = P_{Ak_1}P_{Bk_1} + P_{AI_A}P_{I_Ak_2}P_{BI_B}P_{I_Bk_2} \quad (5)$$

The Hadamard product vanished in equation (3) and equation (() because there is no self-loop (i.e. self-recruitment) in none of our simplified exemplary localities. If self-recruitment exists, e.g. if $k_1 = A$ in Fig. 2c, siblings are found in both origin and destination localities implying that implicit links also encompass explicit links. Since $F_{st}$ are theoretically symmetrical (i.e. $F_{st_{AB}}$ equals $F_{st_{BA}}$), explicit dispersal probabilities have been transformed following $1-(1-P_{AB})*(1-P_{BA})$ to be symmetrical. Note that implicit dispersal probabilities between locality-pairs are already symmetrical by construction [44]. Both multi-generation explicit and implicit dispersal models are computed for 1, 5, 10, 20, 40, 60, 80, 100, 150, 200, 300, 400 and 500 generations using species-specific composite matrices.

**Reciprocal transformation of dispersal probabilities into modelled $F_{st}$**

We perform a reciprocal transformation of dispersal probabilities to compare them against $F_{st}^{obs}/(1-F_{st}^{obs})$ with linear models. As such, dispersal probabilities are linearized and transformed into modelled $F_{st}$ ( $F_{st}^{mod}$) following:

$$F_{st}^{mod} = \frac{1}{\alpha * P_{AB}^{G} + \frac{1}{max(F_{st}^{obs}) - min\,(F_{st}^{obs})}} + min(F_{st}^{obs}) \quad (6)$$

Where $P_{AB}^{G}$ is the symmetrical dispersal probability of connection between localities A and B for a fixed number of generations G (derived either from single generation explicit or multi-generation explicit or implicit dispersal models); α is a coefficient modulating the reciprocal transformation. The sensitivity of $F_{st}^{mod}$ to a wide range of α value has been thoroughly tested in order to retain the optimal value for each study (see Supplementary Figure 4 and 5). The maximal and minimal $F_{st}^{obs}$ values averaged across the meta-analysis are included so that (i) when the dispersal probability is null, the reciprocal

transformation returns a $F_{st}^{mod}$ equal to the mean maximal $F_{st}^{obs}$ (i.e. the average of all maximal $F_{st}^{obs}$ values of the 58 compiled studies, which is 0.1414) and (ii) when the probability of connection is 1, the $F_{st}^{mod}$ tends toward the mean minimal $F_{st}^{obs}$ (i.e. the average of all minimal $F_{st}^{obs}$ values of the 58 compiled species, which is 0.0127). Note that our goal here is not to scale each study's reciprocal transformation of pairwise probabilities into $F_{st}^{mod}$ by its own extrema $F_{st}^{obs}$, but rather to optimize robustness across the meta-analysis using the mean maximal and minimal $F_{st}^{obs}$ over 58 population genetics studies.

**Screening for the best models predicting observed genetic differentiation**

We test for the predictions of $F_{st}^{obs}/(1-F_{st}^{obs})$ by $F_{st}^{mod}$ derived from multi-generation dispersal models for 1 to 500 generations for all studies of the meta-analysis using maximum-likelihood population-effects (MLPE) linear mixed models. In addition of enabling the cross-comparison of several models for their predictive abilities, this statistical approach accounts for non-independence of pairwise comparisons, a distinguished feature of $F_{st}$ between localities [8,34,36,68]. We also search for correlations between $F_{st}^{mod}$ and $F_{st}^{obs}/(1-F_{st}^{obs})$ using classical Mantel tests (see Supplementary Table 7, 8 and 9). For each study, we parametrize our models by (i) selecting the optimal α value for which the model AIC displays the lowest value (Supplementary Figure 4 and 5, Supplementary Table 7, 8 and 9) and (ii) selecting the optimal number of generations for which the AIC displays the lowest value (Supplementary Figure 6 and 7, Supplementary Table 7, 8 and 9). In addition, we perform Isolation-By-Distance (IBD) analyses of all compiled genetic structures with two proxies of distance between locality pairs: the Euclidian distance (i.e. straight-line geographical distances) and the sea least-cost distance, which corresponds to the length of the shortest path considering only maritime areas. Sea least-cost distances are calculated thanks to the Marmap package [90] (version 1.0.4) on R (version 4.0.2). For the IBD analyses, we consider a two-dimensional dispersal model and thus test for predictions of $F_{st}^{obs}/(1-F_{st}^{obs})$ by $\log_e$(distance) [48,54].

To estimate the quality (predictive power) of each model relative to each of the other models, we also test for predictions of $F_{st}^{obs}/(1-F_{st}^{obs})$ by $F_{st}^{mod}$ obtained with the dispersal models (one-generation explicit, multi-generation explicit, and multi-generation implicit). We fit the five predictors to $F_{st}^{obs}/(1-F_{st}^{obs})$ with MLPE linear mixed models, considering a random effect on the locality level, thanks to the 'lmer' function of the lmerTest package (version 3.1.3). The coefficient of determination $R^2$ is computed with the function 'r.squaredGLMM' of the MuMIn package (version 1.43.17). All these tests are computed using the R software (version 4.0.5). For each study, we compare MLPE model predictions to determine the best model ability to predict gene flow. More specifically, we compute for each study the relative likelihood $\exp((AIC_{min}-AIC_i)/2)$ to determine the probability of each model *i* (IBDs, one-generation explicit, multi-generation explicit and multi-generation implicit) to minimize the information loss of being the best one. We cross-compare model predictions across the entire meta-analysis by computing (i) the relative likelihood for each model against the four others (i.e. $AIC_{min}$ being the minimal value among IBDs, one-generation explicit, multi-generation explicit, and multi-generation implicit models) and (ii) the non-symmetrical pair-wise relative likelihood difference (i.e. $AIC_{min}$ being the minimal value among both models under comparison). For example, for models A and B whose relative likelihood are 1 and 0.7 respectively, the relative likelihood difference between A and B is 0.3 and the relative likelihood difference between B and A is -0.3.

We test the sensitivity of MLPE model results ($R^2$ and *p-values*) against species-specific (taxonomic group, PLD, spawning season) and studies-specific (marker, number of sampled localities, $D_{btw}$ and $F_{st}^{obs}$ range) factors with ANOVA and linear regressions (Supplementary Table 10). Sensitivity tests are performed using the Matlab software (version 9.4).

Throughout the entire manuscript, asterisks inform about the significance of all statistical tests, as follows: * ≤ 0.05; ** ≤ 0.005 ; *** ≤ 0.0005 and "ns" stands for statistically non-significant.

## Data availability:

The population genetic data generated in this study is provided as a Supplementary Information (Supplementary Data 1). Genetic population studies references are provided as a Supplementary Information, as well as literature references used to categorize species characteristics (Supplementary Methods 1). We also used FishBase (Froese and Pauly 2000, https://www.fishbase.se/search.php) and Doris (Willis et al., 2016, https://doris.ffessm.fr/) websites for global information about the species of interest. Source and raw data relevant for each figure are provided with this paper.

## Code availability:

The Python codes used to compute multi-generation explicit and implicit dispersal probabilities have been already published (Ser-Giacomi et al. 2021 ; doi:10.1103/PhysRevE.103.042309) and are available online here: https://github.com/serjaaa/cumulated-net-conn.

## References:


1. Hellberg, M. E. Gene Flow and Isolation among Populations of Marine Animals. *Annu. Rev. Ecol. Evol. Syst.* **40**, 291–310 (2009).
2. Lenormand, T. Gene flow and the limits to natural selection. *Trends Ecol. Evol.* **17**, 183–189 (2002).
3. Lowe, W. H., Kovach, R. P. & Allendorf, F. W. Population Genetics and Demography Unite Ecology and Evolution. *Trends Ecol. Evol.* **32**, 141–152 (2017).
4. Slatkin, M. Gene flow and the geographic structure of natural populations. *Science* **236**, 787–792 (1987).
5. Slatkin, M. Gene Flow in Natural Populations. *Annu. Rev. Ecol. Syst.* **1**, 393–430 (1985).
6. Duputié, A. & Massol, F. An empiricist's guide to theoretical predictions on the evolution of dispersal. *Interface Focus* **3**, 20130028 (2013).
7. Lowe, W. H. & Allendorf, F. W. What can genetics tell us about population connectivity? *Mol. Ecol.* **19**, 3038–3051 (2010).
8. Selkoe, K. A. *et al.* A decade of seascape genetics: contributions to basic and applied marine connectivity. *Mar. Ecol. Prog. Ser.* **554**, 1–19 (2016).
9. Weersing, K. & Toonen, R. J. Population genetics, larval dispersal, and connectivity in marine systems. *Mar. Ecol. Prog. Ser.* **393**, 1–12 (2009).
10. Whitlock, M. C. & Mccauley, D. E. Indirect measures of gene flow and migration: FST≠1/(4Nm+1). *Heredity* **82**, 117–125 (1999).
11. Benestan, L. *et al.* Restricted dispersal in a sea of gene flow. *Proc. R. Soc. B Biol. Sci.* **288**, 20210458 (2021).
12. Bode, M. *et al.* Successful validation of a larval dispersal model using genetic parentage data. *PLOS Biol.* **17**, e3000380 (2019).
13. Gagnaire, P.-A. Comparative genomics approach to evolutionary process connectivity. *Evol. Appl.* **13**, 1320–1334 (2020).

519 14. Pinsky, M. L. *et al.* Marine Dispersal Scales Are Congruent over Evolutionary and Ecological Time.
520 *Curr. Biol.* **27**, 149–154 (2017).
521 15. Baguette, M., Blanchet, S., Legrand, D., Stevens, V. M. & Turlure, C. Individual dispersal, landscape
522 connectivity and ecological networks. *Biol. Rev.* **88**, 310–326 (2013).
523 16. Cowen, R. K. & Sponaugle, S. Larval Dispersal and Marine Population Connectivity. *Annu. Rev. Mar.*
524 *Sci.* **1**, 443–466 (2009).
525 17. Tomback, D. F., Anderies, A. J., Carsey, K. S., Powell, M. L. & Mellmann-Brown, S. Delayed Seed
526 Germination in Whitebark Pine and Regeneration Patterns Following the Yellowstone Fires.
527 *Ecology* **82**, 2587–2600 (2001).
528 18. Viana, D. S., Santamaría, L. & Figuerola, J. Migratory Birds as Global Dispersal Vectors. *Trends Ecol.*
529 *Evol.* **31**, 763–775 (2016).
530 19. Nathan, R. *et al.* Mechanisms of long-distance dispersal of seeds by wind. *Nature* **418**, 409–413
531 (2002).
532 20. Cowen, R. K., Paris, C. B. & Srinivasan, A. Scaling of connectivity in marine populations. *Science*
533 **311**, 522–527 (2006).
534 21. Shanks, A. L. Pelagic Larval Duration and Dispersal Distance Revisited. *Biol. Bull.* **216**, 373–385
535 (2009).
536 22. Hidalgo, M. *et al.* Accounting for ocean connectivity and hydroclimate in fish recruitment
537 fluctuations within transboundary metapopulations. *Ecol. Appl.* **29**, (2019).
538 23. Legrand, T., Di Franco, A., Ser-Giacomi, E., Caló, A. & Rossi, V. A multidisciplinary analytical
539 framework to delineate spawning areas and quantify larval dispersal in coastal fish. *Mar. Environ.*
540 *Res.* **151**, 104761 (2019).
541 24. Blowes, S. A. *et al.* The geography of biodiversity change in marine and terrestrial assemblages.
542 *Science* **366**, 339–345 (2019).
543 25. Marshall, D. J., Monro, K., Bode, M., Keough, M. J. & Swearer, S. Phenotype–environment
544 mismatches reduce connectivity in the sea. *Ecol. Lett.* **13**, 128–140 (2010).

26. Crandall, E. D., Treml, E. A. & Barber, P. H. Coalescent and biophysical models of stepping-stone gene flow in neritid snails. *Mol. Ecol.* **21**, 5579–5598 (2012).
27. Smith, T. M. *et al.* Rare long-distance dispersal of a marine angiosperm across the Pacific Ocean. *Glob. Ecol. Biogeogr.* **27**, 487–496 (2018).
28. Saura, S., Bodin, Ö. & Fortin, M.-J. EDITOR'S CHOICE: Stepping stones are crucial for species' long-distance dispersal and range expansion through habitat networks. *J. Appl. Ecol.* **51**, 171–182 (2014).
29. Lett, C., Barrier, N. & Bahlali, M. Converging approaches for modeling the dispersal of propagules in air and sea. *Ecol. Model.* **415**, 108858 (2020).
30. D'Aloia, C. C. *et al.* Patterns, causes, and consequences of marine larval dispersal. *Proc. Natl. Acad. Sci.* **112**, 13940–13945 (2015).
31. Kool, J. T., Moilanen, A. & Treml, E. A. Population connectivity: recent advances and new perspectives. *Landsc. Ecol.* **28**, 165–185 (2013).
32. Mari, L., Melià, P., Fraschetti, S., Gatto, M. & Casagrandi, R. Spatial patterns and temporal variability of seagrass connectivity in the Mediterranean Sea. *Divers. Distrib.* **26**, 169–182 (2020).
33. Nathan, R., Klein, E. K., Robledo-Arnuncio, J. J. & Revilla, E. *Dispersal kernels*. vol. 15 (Oxford University Press Oxford, UK, 2012).
34. Boulanger, E., Dalongeville, A., Andrello, M., Mouillot, D. & Manel, S. Spatial graphs highlight how multi-generational dispersal shapes landscape genetic patterns. *Ecography* **43**, 1167–1179 (2020).
35. Jahnke, M. *et al.* Seascape genetics and biophysical connectivity modelling support conservation of the seagrass Zostera marina in the Skagerrak–Kattegat region of the eastern North Sea. *Evol. Appl.* **11**, 645–661 (2018).
36. Jahnke, M. & Jonsson, P. R. Biophysical models of dispersal contribute to seascape genetic analyses. *Philos. Trans. R. Soc. B Biol. Sci.* **377**, 20210024 (2022).

37. Buonomo, R. *et al.* Habitat continuity and stepping-stone oceanographic distances explain population genetic connectivity of the brown alga Cystoseira amentacea. *Mol. Ecol.* **26**, 766–780 (2017).
38. Assis, J. *et al.* Ocean currents shape the genetic structure of a kelp in southwestern Africa. *J. Biogeogr.* **49**, 822–835 (2022).
39. Ser-Giacomi, E., Vasile, R., Hernández-García, E. & López, C. Most probable paths in temporal weighted networks: An application to ocean transport. *Phys. Rev. E* **92**, 012818 (2015).
40. McRae, B. H. & Beier, P. Circuit theory predicts gene flow in plant and animal populations. *Proc. Natl. Acad. Sci.* **104**, 19885–19890 (2007).
41. Foster, N. L. *et al.* Connectivity of Caribbean coral populations: complementary insights from empirical and modelled gene flow. *Mol. Ecol.* **21**, 1143–1157 (2012).
42. Kool, J. T., Paris, C. B., Andréfouët, S. & Cowen, R. K. Complex migration and the development of genetic structure in subdivided populations: an example from Caribbean coral reef ecosystems. *Ecography* **33**, 597–606 (2010).
43. White, J. W., Botsford, L. W., Hastings, A. & Largier, J. L. Population persistence in marine reserve networks: incorporating spatial heterogeneities in larval dispersal. *Mar. Ecol. Prog. Ser.* **398**, 49–67 (2010).
44. Ser-Giacomi, E., Legrand, T., Hernández-Carrasco, I. & Rossi, V. Explicit and implicit network connectivity: Analytical formulation and application to transport processes. *Phys. Rev. E* **103**, 042309 (2021).
45. Battiston, F. *et al.* Networks beyond pairwise interactions: Structure and dynamics. *Phys. Rep.* **874**, 1–92 (2020).
46. Levine, J. M., Bascompte, J., Adler, P. B. & Allesina, S. Beyond pairwise mechanisms of species coexistence in complex communities. *Nature* **546**, 56–64 (2017).
47. Mayfield, M. M. & Stouffer, D. B. Higher-order interactions capture unexplained complexity in diverse communities. *Nat. Ecol. Evol.* **1**, 1–7 (2017).

48. Rousset, F. Inferences from spatial population genetics. in *Handbook of statistical genetics* vol. 4 23 (2001).
49. Dubois, M. *et al.* Linking basin-scale connectivity, oceanography and population dynamics for the conservation and management of marine ecosystems. *Glob. Ecol. Biogeogr.* **25**, 503–515 (2016).
50. Monroy, P., Rossi, V., Ser-Giacomi, E., López, C. & Hernández-García, E. Sensitivity and robustness of larval connectivity diagnostics obtained from Lagrangian Flow Networks. *ICES J. Mar. Sci.* **74**, 1763–1779 (2017).
51. Rossi, V., Ser-Giacomi, E., López, C. & Hernández-García, E. Hydrodynamic provinces and oceanic connectivity from a transport network help designing marine reserves. *Geophys. Res. Lett.* **41**, 2883–2891 (2014).
52. Ser-Giacomi, E., Rossi, V., Lopez, C. & Hernandez-Garcia, E. Flow networks: A characterization of geophysical fluid transport. *Chaos Interdiscip. J. Nonlinear Sci.* **25**, 036404 (2015).
53. Oddo, P. *et al.* A nested Atlantic-Mediterranean Sea general circulation model for operational forecasting. *Ocean Sci.* (2009).
54. Rousset, F. Genetic Differentiation and Estimation of Gene Flow from F-Statistics Under Isolation by Distance. *Genetics* **145**, 1219–1228 (1997).
55. Reem, E., Douek, J., Paz, G., Katzir, G. & Rinkevich, B. Phylogenetics, biogeography and population genetics of the ascidian Botryllus schlosseri in the Mediterranean Sea and beyond. *Mol. Phylogenet. Evol.* **107**, 221–231 (2017).
56. Villamor, A., Costantini, F. & Abbiati, M. Genetic Structuring across Marine Biogeographic Boundaries in Rocky Shore Invertebrates. *PLOS ONE* **9**, e101135 (2014).
57. Borrero-Pérez, G. H., González-Wangüemert, M., Marcos, C. & Pérez-Ruzafa, A. Phylogeography of the Atlanto-Mediterranean sea cucumber Holothuria (Holothuria) mammata: the combined effects of historical processes and current oceanographical pattern: PHYLOGEOGRAPHY OF HOLOTHURIA MAMMATA. *Mol. Ecol.* **20**, 1964–1975 (2011).

58. Carreras, C. *et al.* East is East and West is West: Population genomics and hierarchical analyses reveal genetic structure and adaptation footprints in the keystone species *Paracentrotus lividus* (Echinoidea). *Divers. Distrib.* **26**, 382–398 (2020).
59. Aurelle, D. *et al.* Phylogeography of the red coral (Corallium rubrum): inferences on the evolutionary history of a temperate gorgonian. *Genetica* **139**, 855–869 (2011).
60. Costantini, F., Carlesi, L. & Abbiati, M. Quantifying Spatial Genetic Structuring in Mesophotic Populations of the Precious Coral Corallium rubrum. *PLoS ONE* **8**, e61546 (2013).
61. Durand, J., Blel, H., Shen, K., Koutrakis, E. & Guinand, B. Population genetic structure of Mugil cephalus in the Mediterranean and Black Seas: a single mitochondrial clade and many nuclear barriers. *Mar. Ecol. Prog. Ser.* **474**, 243–261 (2013).
62. Alberto, F. *et al.* Genetic differentiation and secondary contact zone in the seagrass Cymodocea nodosa across the Mediterranean–Atlantic transition region. *J. Biogeogr.* **35**, 1279–1294 (2008).
63. McRae, B. H. Isolation by Resistance. *Evolution* **60**, 1551–1561 (2006).
64. Dalongeville, A. *et al.* Geographic isolation and larval dispersal shape seascape genetic patterns differently according to spatial scale. *Evol. Appl.* **11**, 1437–1447 (2018).
65. Jenkins, D. G. *et al.* A meta-analysis of isolation by distance: relic or reference standard for landscape genetics? *Ecography* **33**, 315–320 (2010).
66. Selkoe, K. A. & Toonen, R. J. Marine connectivity: a new look at pelagic larval duration and genetic metrics of dispersal. *Mar. Ecol. Prog. Ser.* **436**, 291–305 (2011).
67. Alberto, F. *et al.* Isolation by oceanographic distance explains genetic structure for Macrocystis pyrifera in the Santa Barbara Channel. *Mol. Ecol.* **20**, 2543–2554 (2011).
68. Selkoe, K. A. *et al.* Taking the chaos out of genetic patchiness: seascape genetics reveals ecological and oceanographic drivers of genetic patterns in three temperate reef species. *Mol. Ecol.* **19**, 3708–3726 (2010).

644 69. Xuereb, A. *et al.* Asymmetric oceanographic processes mediate connectivity and population
645 genetic structure, as revealed by RADseq, in a highly dispersive marine invertebrate (Parastichopus
646 californicus). *Mol. Ecol.* **27**, 2347–2364 (2018).
647 70. Pascual, M., Rives, B., Schunter, C. & Macpherson, E. Impact of life history traits on gene flow: A
648 multispecies systematic review across oceanographic barriers in the Mediterranean Sea. *PLOS*
649 *ONE* **12**, e0176419 (2017).
650 71. Wang, I. J., Glor, R. E. & Losos, J. B. Quantifying the roles of ecology and geography in spatial
651 genetic divergence. *Ecol. Lett.* **16**, 175–182 (2013).
652 72. Bierne, N., Welch, J., Loire, E., Bonhomme, F. & David, P. The coupling hypothesis: why genome
653 scans may fail to map local adaptation genes. *Mol. Ecol.* **20**, 2044–2072 (2011).
654 73. Sen Gupta, A. *et al.* Future changes to the upper ocean Western Boundary Currents across two
655 generations of climate models. *Sci. Rep.* **11**, 9538 (2021).
656 74. Ser-Giacomi, E. *et al.* Impact of Climate Change on Surface Stirring and Transport in the
657 Mediterranean Sea. *Geophys. Res. Lett.* **47**, e2020GL089941 (2020).
658 75. Jorda, G. *et al.* Ocean warming compresses the three-dimensional habitat of marine life. *Nat. Ecol.*
659 *Evol.* **4**, 109–114 (2020).
660 76. Wright, S. Evolution in Mendelian Populations. *Genetics* **16**, 97–159 (1931).
661 77. Eldon, B., Riquet, F., Yearsley, J., Jollivet, D. & Broquet, T. Current hypotheses to explain genetic
662 chaos under the sea. *Curr. Zool.* **62**, 551–566 (2016).
663 78. Schunter, C. *et al.* A novel integrative approach elucidates fine-scale dispersal patchiness in marine
664 populations. *Sci. Rep.* **9**, 1–10 (2019).
665 79. Jackson, T. M., Roegner, G. C. & O'Malley, K. G. Evidence for interannual variation in genetic
666 structure of Dungeness crab (Cancer magister) along the California Current System. *Mol. Ecol.* **27**,
667 352–368 (2018).
668 80. Pascual, M. *et al.* Temporal and spatial genetic differentiation in the crab Liocarcinus depurator
669 across the Atlantic-Mediterranean transition. *Sci. Rep.* **6**, 29892 (2016).

81. Pérez-Portela, R. *et al.* Spatio-temporal patterns of genetic variation in Arbacia lixula, a thermophilous sea urchin in expansion in the Mediterranean. *Heredity* **122**, 244–259 (2019).
82. Carroll, S. P., Hendry, A. P., Reznick, D. N. & Fox, C. W. Evolution on ecological time-scales. *Funct. Ecol.* **21**, 387–393 (2007).
83. Grilli, J., Barabás, G., Michalska-Smith, M. J. & Allesina, S. Higher-order interactions stabilize dynamics in competitive network models. *Nature* **548**, 210–213 (2017).
84. Butchart, S. H. M. *et al.* Global Biodiversity: Indicators of Recent Declines. *Science* **328**, 1164–1168 (2010).
85. Sala, E. *et al.* Protecting the global ocean for biodiversity, food and climate. *Nature* **592**, 397–402 (2021).
86. Hauser, L. & Carvalho, G. R. Paradigm shifts in marine fisheries genetics: ugly hypotheses slain by beautiful facts. *Fish Fish.* **9**, 333–362 (2008).
87. Weber, A. a.-T., Mérigot, B., Valière, S. & Chenuil, A. Influence of the larval phase on connectivity: strong differences in the genetic structure of brooders and broadcasters in the Ophioderma longicauda species complex. *Mol. Ecol.* **24**, 6080–6094 (2015).
88. Marzouk, Z., Aurelle, D., Said, K. & Chenuil, A. Cryptic lineages and high population genetic structure in the exploited marine snail Hexaplex trunculus (Gastropoda: Muricidae). *Biol. J. Linn. Soc.* **122**, 411–428 (2017).
89. Cowen, R. K., Lwiza, K. M., Sponaugle, S., Paris, C. B. & Olson, D. B. Connectivity of marine populations: open or closed? *Science* **287**, 857–859 (2000).
90. Pante, E. & Simon-Bouhet, B. marmap: A Package for Importing, Plotting and Analyzing Bathymetric and Topographic Data in R. *PLOS ONE* **8**, e73051 (2013).
91. Susini, M.-L., Thibaut, T., Meinesz, A. & Forcioli, D. A preliminary study of genetic diversity in Cystoseira amentacea (C. Agardh) Bory var. stricta Montagne (Fucales, Phaeophyceae) using random amplified polymorphic DNA. *Phycologia* **46**, 605–611 (2007).

## Acknowledgements:

T.L. is funded by a Doctoral fellowship obtained through Aix-Marseille University. T.L., A.C. and V.R acknowledge financial support from the European project SEAMoBB (Solutions for sEmi-Automated Monitoring of Benthic Biodiversity), funded by ERA-Net Mar-TERA (id. 145) and managed by the ANR (Grant No. ANR-17-MART0001-02, P.I.: A. Chenuil). V.R., E.S-G., N.B. and S. A-H. acknowledge financial support obtained through the HYDROGENCONNECT project (P.I. V. Rossi) funded by the French program MISTRALS ENVI-Med. E.S-G. thanks C. Payrató Borrás and S. Meloni for stimulating discussions on Network Theory. E.S-G. is very grateful for support from the Simons Foundation: the Simons Collaboration on Computational BIOgeochemical modeling of Marine EcosystemS (CBIOMES #549931). T.L. and V.R. warmly thank Madiop Lo for the technical improvements implemented in the LFN model. T.L. thanks E. Boulanger for the advice on the mixed model implementation. V.R., A.C., S.A.-H. and N.B. thank the GDR iMarCo for the initiation of this work, with a particular mention to Barbara Porro and Neil Alloncle for their implications in the first steps of the data compilation.

## Author contributions statement:

T.L. and V.R. planned and designed research with important contributions from A.C. and building upon earlier discussions with N.B. and S.A-H. T.L., A.C. and S.A-H. contributed substantially to the compilation of genetic population studies. E.S-G. developed the theoretical formulations of the multi-generation dispersal models. T.L. performed data analysis with important contributions from V.R. and A.C. The manuscript was written by T.L. and V.R., and A.C., E.S-G, S.A-H and N.B. provided important contributions and critical revisions. All authors approved the final version of this manuscript.

## Competing Interests Statement:

The authors declare no competing interests.

718 Figures:

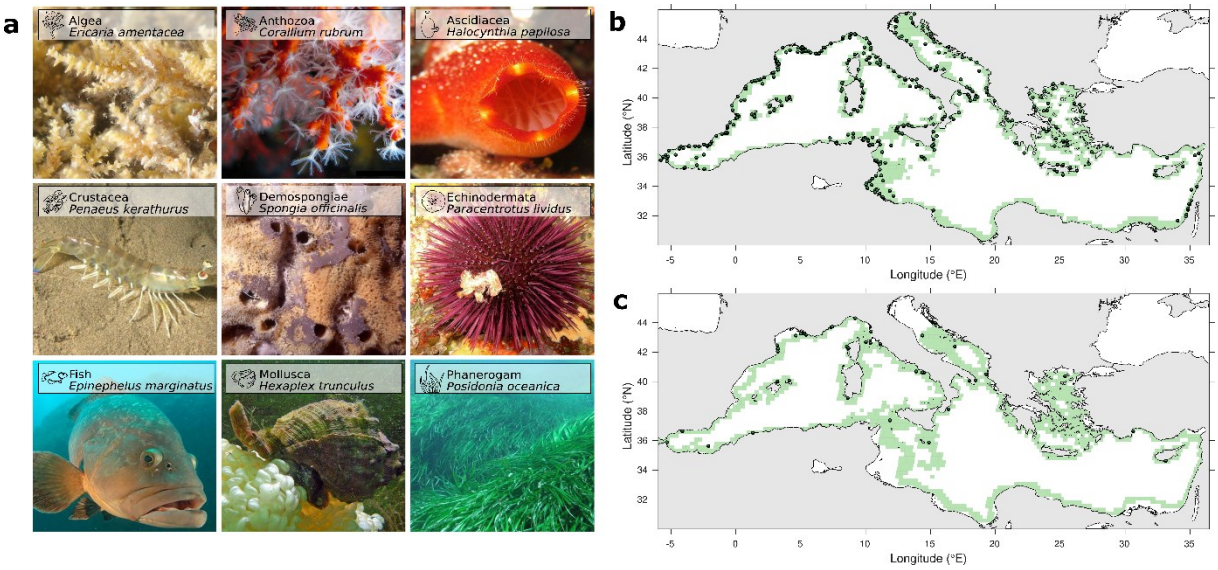


719

720 Figure 1: **Meta-analysis summary, estimated habitats and geographical locations of the sampled**
721 **populations**. **a** Exemplary pictures of marine species belonging to the nine taxonomic groups
722 comprised in the compilation of 58 population genetics studies. **b** Basin-scale view of all sampled
723 populations compiled in the meta-analysis (dark green dots) and putative localities (light green
724 squares) that act as steppingstones in our multi-generation dispersal model for the shallow coastal
725 habitat. **c**, same as **b** but for the neritic shelf habitat. Source data are provided as a Source Data file.
726 Photos credit (from left to right, top to bottom): © Veronique Lamare 2015, © Alain-Pierre Sittler 2004,
727 © Alain-Pierre Sittler 2005, © Gilles Cavignaux 2007, © Jean-Georges Harmelin 1999, © Frédéric André
728 2007, © Christophe Dehondt 2006, © Jean-Claude Wolles 2007 and © Jean-Georges Harmelin 2005
729 (published on the DORIS web site, https://doris.ffessm.fr/).

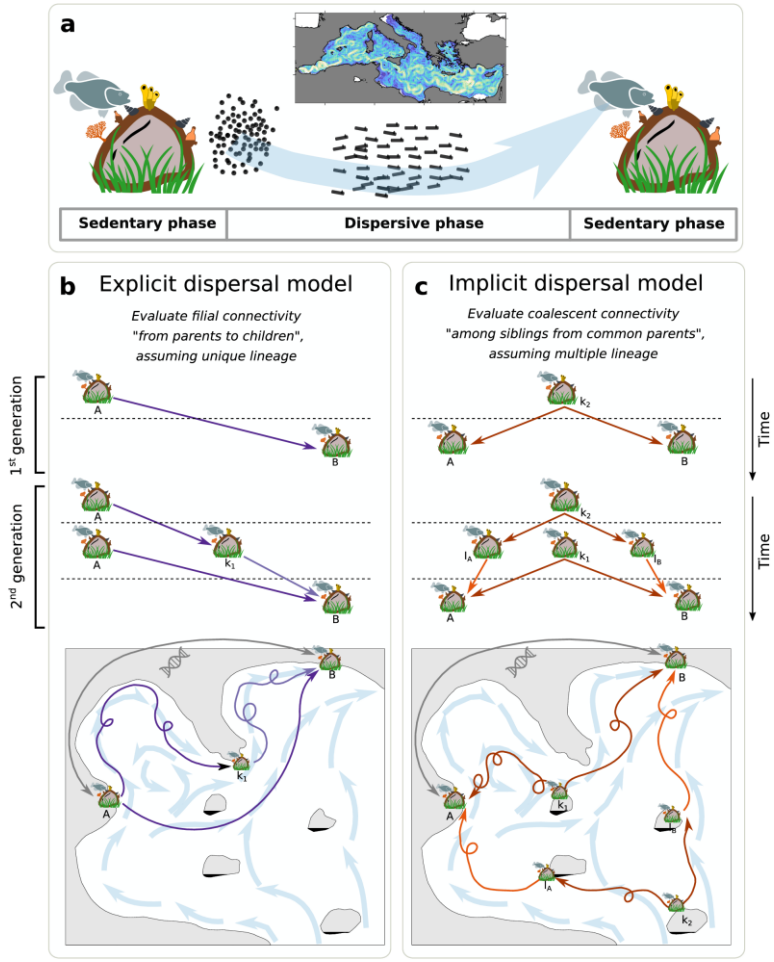


730

731 Figure 2: **Modelling multi-generational water-borne dispersal. a** Schematic representation of a
732 biphasic life cycle composed of sedentary adults and dispersive early-life stages, that is a distinctive
733 feature of all species included in the meta-analysis. During the dispersive phase, numerous individuals
734 are dispersed across the seascape by turbulent currents (represented in the Mediterranean miniature).
735 **b** Explicit dispersal model evaluates filial connections between locality-pairs. **c** Implicit dispersal model
736 estimates coalescent connections between locality-pairs. Schematics highlight the simulated
737 genealogy over two generations and illustrate one of many multi-generational dispersal pathways that
738 are considered by our models when estimating the connectivity between distant localities A and B.
739 Icons credit: © vectors market, © Agne Alesiute, © Elisabetta Calabritto, © Luis Prado, © Joi Stack, ©
740 Tatina Vazest, © mindgraphy, © Oleksandr Panasovskyi, © ProSymbols, © Sean Maldjian (changes
741 were made on all the icons, Creative Commons BY 4.0 license).

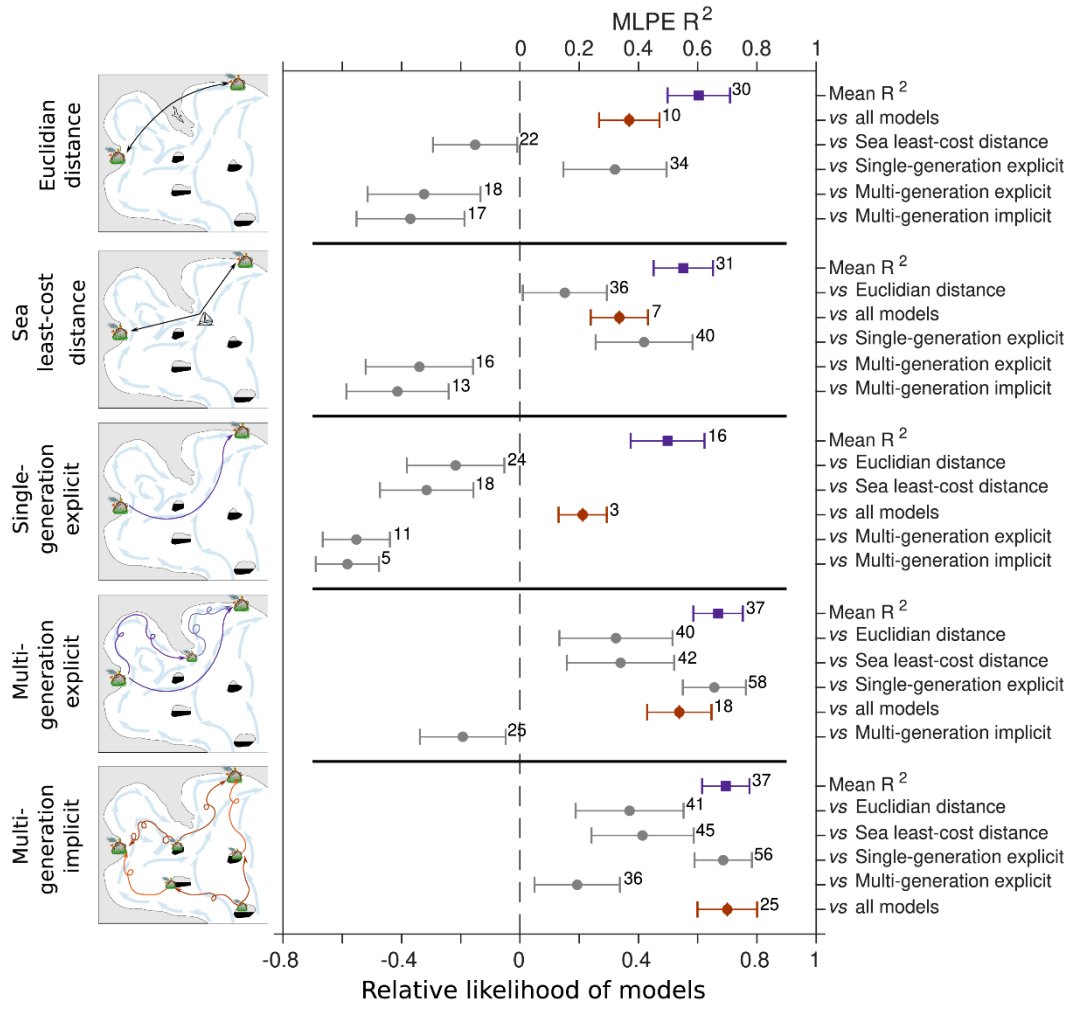


742

743 Figure 3: **Cross-comparison of gene flow predictive models**. Purple squares indicate mean MLPE linear
744 mixed model $R^2$, red diamonds indicate the relative likelihood of the reference model (depicted on the
745 left) vs the four remaining models, and grey dots indicate the relative likelihood difference of the
746 reference model (depicted on the left) vs each of the four remaining models. Comparative analyses
747 are made for **a** IBD (Euclidian) model, **b** IBD (sea least-cost) model, **c** single-generation explicit dispersal
748 connectivity, **d** multi-generation explicit dispersal model and **e** multi-generation implicit dispersal
749 model. Only the significant predictions (p-value*) of each reference model (left) are considered to
750 compute the mean $R^2$, while all the 58 studies are used to compute the relative likelihood and the
751 relative likelihood difference. The number of significant predictions per model (over the total of 58
752 studies) is reported on the right of each purple square. The number of times the reference model
753 displays the lowest AIC among all the four other models is reported on the right of each red diamond.

754 The number of times the reference model displays the lower AIC among each of the four remaining
755 models is reported on the right of each grey dots. Error-bars represent the 95 % confidence intervals.
756 Source data are provided as a Source Data file. Icons credit: © vectors market, © Agne Alesiute, ©
757 Elisabetta Calabritto, © Luis Prado, © Joi Stack, © Tatina Vazest, © mindgraphy, © Sean Maldjian
758 (changes were made on all the icons, Creative Commons BY 4.0 license).

759

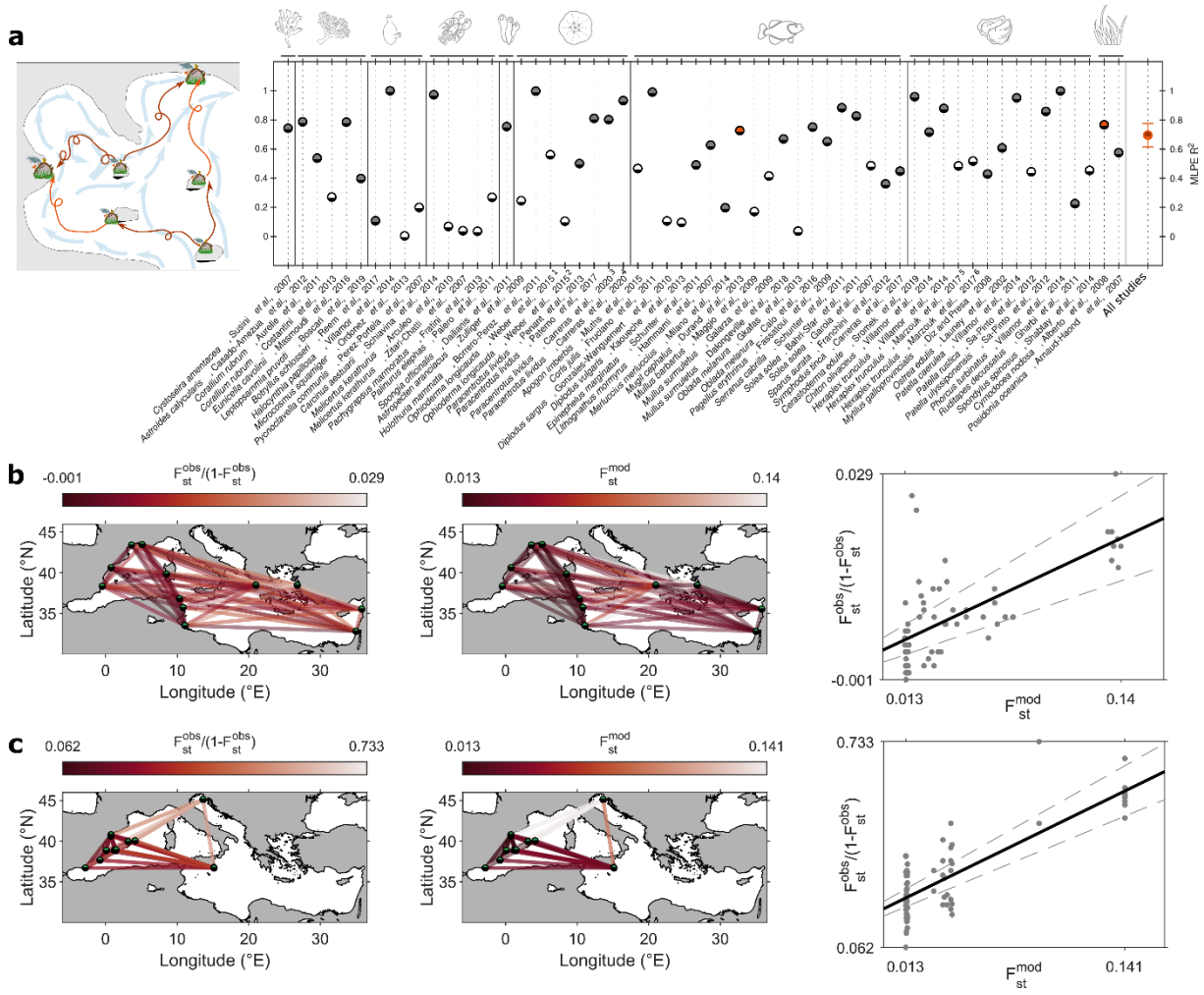


Figure 4: **Accuracy of the multi-generation implicit dispersal model in explaining compiled genetic structures. a** MLPE linear mixed model R² between $F_{st}^{mod}$ and $F_{st}^{obs}/(1-F_{st}^{obs})$. Filled dots highlight the 37 significant correlations (p-value*). Note that some results reported by a given study are analysed separately: (i) Weber et al., 2015 used nuclear DNA marker ([1]) and mtDNA marker ([2]); (ii) Carreras et al., 2020 considered all the loci together ([3]) and then only the Mediterranean outliers loci ([4]); (iii) Marzouk et al., 2017 analysed nuclear DNA marker ([5]) and mtDNA marker ([6]). Error-bars for all studies represent the 95 % confidence intervals. **b** Network representation of $F_{st}^{obs}/(1-F_{st}^{obs})$ (observed $F_{st}$, left) and $F_{st}^{mod}$ (modelled $F_{st}$, right) and their corresponding scatterplot for the flathead grey mullet (*Mugil cephalus* [61]; red dot in a). **c** same as **b** but for a seagrass (*Cymodocea nodosa* [62]; red dot in **a**). Source data are provided as a Source Data file. Icons credit: © vectors market, © Agne Alesiute, © Elisabetta Calabritto, © Luis Prado, © Joi Stack, © Tatina Vazest, © mindgraphy, ©

772 Oleksandr Panasovskyi, © ProSymbols, © Sean Maldjian (changes were made on all the icons, Creative

773 Commons BY 4.0 license).

774

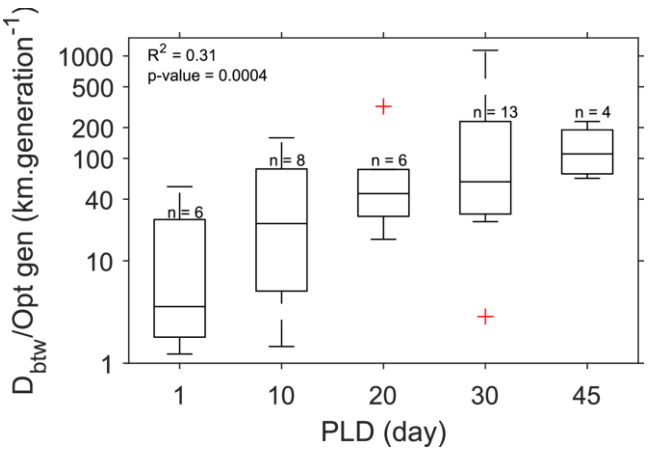


775

776 Figure 5: **Sensitivity of the multi-generation implicit dispersal model predictions to dispersal trait and**
777 **sampling design.** Correlation ($R^2$ = 0.31*** using a linear regression model fit) between the PLDs
778 categories (x-axis) and the proxy of sampling extent $D_{btw}$ divided by the optimal number of modelled
779 generations (y-axis). n = number of studies whose model predictions of genetic observations are
780 significant per PLD categories. On each box, the central mark, the bottom and top edges indicate the
781 indicates the median, the 25$^{th}$ and the 75$^{th}$ percentiles, respectively. The whiskers extend to the most
782 extreme data points not considered outliers, and the outliers are plotted individually using a cross
783 symbol. Note that Susini et al. (2007) [91] has been removed from this figure as it displays the minimal
784 number of localities of our compilation (i.e. three localities while two sampled populations are indeed
785 compassed in the same locality), which does not permit a robust evaluation of ($D_{btw}$)/(Opt gen) ratio.
786 When considering this study, $R^2$=0.23***. Source data are provided as a Source Data file.

# Supplementary Information:

# Spatial coalescent connectivity through multi-generation dispersal modelling predicts gene flow across marine phyla

Térence Legrand[1]*; Anne Chenuil[2]; Enrico Ser-Giacomi[3]; Sophie Arnaud-Haond[4]; Nicolas Bierne[5]; Vincent Rossi[6]*

Affiliations :

[1]Aix Marseille University, Universite de Toulon, CNRS, IRD, Mediterranean Institute of Oceanography (UMR 7294), Marseille, France. (legrandterence@gmail.com).

[2] Institut Méditerranéen de Biodiversité et d'Ecologie Marine et Continentale, CNRS (UMR 7263), Station Marine d'Endoume, Marseille, France. (anne.chenuil@imbe.fr).

[3]Department of Earth, Atmospheric and Planetary Sciences, Massachusetts Institute of Technology, 54-1514 MIT, Cambridge, Massachusetts, USA. (enrico.sergiacomi@gmail.com).

[4] MARBEC (Marine Biodiversity, Exploitation and Conservation, UMR 9190) Univ. Montpellier, IFREMER, IRD, CNRS, Sète, France. (sophie.arnaud-haond@umontpellier.fr).

[5]ISEM, Univ Montpellier, CNRS, IRD, Montpellier, France. (nicolas.bierne@umontpellier.fr).

[6]Aix Marseille University, Universite de Toulon, CNRS, IRD, Mediterranean Institute of Oceanography (UMR 7294), Marseille, France (vincent.rossi@mio.osupytheas.fr).

*Corresponding authors

# Supplementary Methods 1: Selected references, model parameterization and literature review

*Supplementary Table 1:* ***Summarized description of the 58 population genetic studies included in the meta-analysis****. Note that some results reported by a given study are analysed separately: (i) Weber et al., 2015 used SNPs marker ([1]) and mtDNA marker ([2]); (ii) Carrera et al., 2020 considered all the loci together ([3]) and then only the Mediterranean outliers loci ([4]); (iii) Marzouk et al., 2017 analyzed SNPs marker ([5]) and mtDNA marker ([6]). Dbtw is the mean straight-line geographical distance (in km) between sampled localities. Source data are provided as a Source Data file.*

| Species characteristics | | | | | Study characteristics | | | |
|---|---|---|---|---|---|---|---|---|
| **Taxa** | **Species** | **Habitat** | **PLD** | **Season** | **Study** | **Marker** | **Nbr of populations** | **$D_{btw}$** |
| Algea | Cystoseira amentacea | shallow coastal | 1 | all | Susini et al., 2007 | RAPD | 4 | 223 |
| Anthozoa | Astroides calycularis | shallow coastal | 1 | summer | Casado-Amezua et al., 2012 | microsat | 16 | 617 |
| Anthozoa | Corallium rubrum | neritic shelf | 10 | summer | Aurelle et al., 2011 | microsat | 24 | 729 |
| Anthozoa | Corallium rubrum | neritic shelf | 10 | summer | Costantini et al., 2013 | microsat | 5 | 716 |
| Anthozoa | Eunicella cavolinii | shallow coastal | 1 | all | Masmoudi et al., 2016 | microsat | 18 | 715 |
| Anthozoa | Leptopsammia pruvoti | shallow coastal | 10 | spring | Boscari et al., 2019 | SNP/RAD_GBS_transc | 10 | 793 |
| Ascidiacea | Botryllus schlosseri | shallow coastal | 1 | all | Reem et al., 2017 | microsat | 11 | 1020 |
| Ascidiacea | Halocynthia papillosa | neritic shelf | 20 | summer | Villamor et al., 2014 | mtDNA | 4 | 1018 |
| Ascidiacea | Microcosmus squamiger | shallow coastal | 1 | summer | Ordóñez et al., 2013 | microsat | 6 | 970 |
| Ascidiacea | Pycnoclavella communis | shallow coastal | 1 | all | Pérez-Portela et al., 2007 | microsat | 4 | 983 |
| Crustacea | Carcinus aestuarii | shallow coastal | 30 | fall | Schiavina et al., 2014 | microsat | 8 | 965 |
| Crustacea | Melicertus kerathurus | shallow coastal | 20 | all | Arculeo et al., 2010 | microsat | 9 | 996 |
| Crustacea | Melicertus kerathurus | shallow coastal | 20 | all | Zitari-Chatti et al., 2007 | allozymes | 9 | 911 |
| Crustacea | Pachygrapsus marmoratus | shallow coastal | 30 | all | Fratini et al., 2013 | microsat | 8 | 896 |
| Crustacea | Palinurus elephas | shallow coastal | 45 | spring | Palero et al., 2011 | microsat | 5 | 945 |
| Demospongiae | Spongia officinalis | shallow coastal | 1 | summer | Dailianis et al., 2011 | microsat | 9 | 1059 |
| Echinodermata | Astropecten aranciacus | shallow coastal | 45 | all | Zulliger et al., 2009 | microsat | 7 | 1076 |
| Echinodermata | Holothuria mammata | shallow coastal | 20 | spring | Borrero-Pérez et al., 2011 | microsat | 4 | 1087 |
| Echinodermata | Ophioderma longicauda | shallow coastal | 10 | spring | Weber et al., 2015[1] | mtDNA | 13 | 1047 |

| Species characteristics | | | | | Study characteristics | | | |
|---|---|---|---|---|---|---|---|---|
| **Taxa** | **Species** | **Habitat** | **PLD** | **Season** | **Study** | **Marker** | **Nbr of populations** | **$D_{btw}$** |
| Echinodermata | Ophioderma longicauda | shallow coastal | 10 | spring | Weber et al., 2015[2] | nuclearDNAseq | 11 | 1127 |
| Echinodermata | Paracentrotus lividus | shallow coastal | 30 | spring | Penant et al., 2013 | mtDNA | 12 | 1134 |
| Echinodermata | Paracentrotus lividus | shallow coastal | 30 | spring | Paterno et al., 2017 | SNP/RAD_GBS_transc | 10 | 1094 |
| Echinodermata | Paracentrotus lividus | shallow coastal | 30 | spring | Carreras et al., 2020[3] | SNP/RAD_GBS_transc | 8 | 1183 |
| Echinodermata | Paracentrotus lividus | shallow coastal | 30 | spring | Carreras et al., 2020[4] | SNP/RAD_GBS_transc | 8 | 1183 |
| Fish | Apogon imberbis | shallow coastal | 20 | summer | Muths et al., 2015 | microsat | 4 | 1178 |
| Fish | Coris julis | shallow coastal | 30 | summer | Fruciano et al., 2011 | mtDNA | 10 | 1144 |
| Fish | Diplodus sargus | shallow coastal | 20 | spring | González-Wangüemert et al., 2010 | microsat | 5 | 1141 |
| Fish | Diplodus vulgaris | shallow coastal | 45 | winter | Kaouèche et al., 2013 | allozymes | 6 | 1103 |
| Fish | Epinephelus marginatus | shallow coastal | 30 | summer | Schunter et al., 2011 | microsat | 9 | 1149 |
| Fish | Lithognathus mormyrus | shallow coastal | 30 | all | Hammami et al., 2007 | allozymes | 4 | 1144 |
| Fish | Merluccius merluccius | neritic shelf | 45 | all | Milano et al., 2014 | SNP/RAD_GBS_transc | 14 | 1147 |
| Fish | Mugil cephalus | shallow coastal | 45 | all | Durand et al., 2013 | microsat | 12 | 1279 |
| Fish | Mullus barbartus | shallow coastal | 30 | spring | Maggio et al., 2009 | microsat | 14 | 882 |
| Fish | Mullus surmuletus | shallow coastal | 30 | spring | Galarza et al., 2009 | microsat | 6 | 919 |
| Fish | Mullus surmuletus | shallow coastal | 30 | spring | Dalongeville et al., 2018 | SNP/RAD_GBS_transc | 47 | 1559 |
| Fish | Oblada melanura | shallow coastal | 20 | spring | Gkafas et al., 2013 | microsat | 8 | 1555 |
| Fish | Oblada melanura | shallow coastal | 20 | spring | Calò et al., 2016 | microsat | 9 | 1561 |
| Fish | Pagellus erythrinus | shallow coastal | 45 | spring | Fassatoui et al., 2009 | allozymes | 6 | 1561 |
| Fish | Serranus cabrilla | shallow coastal | 30 | spring | Schunter et al., 2011 | microsat | 13 | 1592 |
| Fish | Solea solea | shallow coastal | 30 | winter | Bahri-Sfar et al., 2011 | allozymes | 10 | 1603 |
| Fish | Solea solea | shallow coastal | 30 | winter | Garoia et al., 2007 | microsat | 4 | 1607 |
| Fish | Sparus aurata | shallow coastal | 45 | fall | Franchini et al., 2012 | microsat | 12 | 1569 |
| Fish | Symphodus tinca | shallow coastal | 10 | spring | Carreras et al., 2017 | SNP/RAD_GBS_transc | 6 | 1569 |
| Mollusca | Cerastoderma edule | shallow coastal | 10 | all | Sromek et al., 2019 | SNP/RAD_GBS_transc | 7 | 1583 |
| Mollusca | Chiton olivaceus | shallow coastal | 10 | spring | Villamor et al., 2014 | mtDNA | 4 | 1583 |

| Species characteristics | | | | | Study characteristics | | | |
|---|---|---|---|---|---|---|---|---|
| **Taxa** | **Species** | **Habitat** | **PLD** | **Season** | **Study** | **Marker** | **Nbr of populations** | **$D_{btw}$** |
| Mollusca | Hexaplex trunculus | shallow coastal | 1 | all | Villamor et al., 2014 | mtDNA | 4 | 1583 |
| Mollusca | Hexaplex trunculus | shallow coastal | 1 | all | Marzouk et al., 2017[5] | nuclearDNAseq | 15 | 1627 |
| Mollusca | Hexaplex trunculus | shallow coastal | 1 | all | Marzouk et al., 2017[6] | mtDNA | 15 | 1627 |
| Mollusca | Mytilus galloprovincialis | shallow coastal | 20 | spring | Diz and Presa, 2008 | microsat | 8 | 1609 |
| Mollusca | Ostrea edulis | shallow coastal | 10 | summer | Launey et al., 2002 | microsat | 5 | 1617 |
| Mollusca | Patella caerulea | shallow coastal | 20 | fall | Villamor et al., 2014 | mtDNA | 6 | 1612 |
| Mollusca | Patella rustica | shallow coastal | 20 | fall | Sá-Pinto et al., 2012 | allozymes | 6 | 1623 |
| Mollusca | Patella ulyssiponensis | shallow coastal | 20 | summer | Sá-Pinto et al., 2012 | allozymes | 5 | 1624 |
| Mollusca | Phorcus turbinatus | shallow coastal | 10 | all | Villamor et al., 2014 | mtDNA | 4 | 1620 |
| Mollusca | Ruditapes decussatus | shallow coastal | 10 | summer | Gharbi et al., 2011 | allozymes | 11 | 1589 |
| Mollusca | Spondylus spinosus | shallow coastal | 20 | all | Shabtay et al., 2014 | mtDNA | 5 | 1587 |
| Phanerogam | Cymodocea nodosa | shallow coastal | 30 | all | Alberto et al., 2008 | microsat | 13 | 1601 |
| Phanerogam | Posidonia oceanica | shallow coastal | 30 | all | Arnaud-Haond et al., 2007 | microsat | 29 | 1588 |

*Supplementary Table 2: Literature reference used to configure species characteristics (i.e. habitat, PLD, spawning season). We also use FishBase (Froese and Pauly 2000, https://www.fishbase.se/search.php) and Doris (Willis et al., 2016, https://doris.ffessm.fr/) webpages for global information about the species of interest.*

| Species | References |
|---|---|
| *Apogon imberbis* | (Macpherson and Raventos, 2006; Raventos, 2007) |
| *Astroides calycularis* | (Casado-Amezúa et al., 2012; Goffredo et al., 2010) |
| *Astropecten aranciacus* | (Baeta et al., 2016; Zulliger et al., 2009) |
| *Balanophyllia europaea* | (Goffredo et al., 2004) |
| *Botryllus schlosseri* | (Reem et al., 2017) |
| *Perforatus perforatus* | (Villamor et al., 2014) |
| *Carcinus aestuarii* | (Carlton and Cohen, 2003; Schiavina et al., 2014) |
| *Cerastoderma edule* | (Boyden and Russell, 1972) |
| *Chiton olivaceus* | (Villamor et al., 2014; Wanninger and Haszprunar, 2002) |
| *Chondrosia reniformis* | (Lazoski et al., 2001; Villamor et al., 2014) |
| *Cladocora caespitosa* | (Casado-Amezúa et al., 2012; Kersting et al., 2013; Kružić et al., 2008) |
| *Corallium rubrum* | (Coelho and Lasker, 2016; Costantini et al., 2013; Teixidó et al., 2011) |
| *Coris julis* | (Fruciano et al., 2011; Macpherson and Raventos, 2006) |
| *Crassostrea gigas* | (Ernande et al., 2003) |
| *Cymodocea nodosa* | (Alberto et al., 2008; Orth et al., 2006) |
| *Cystoseira amentacea* | (Susini et al., 2007; Thibaut et al., 2016) |
| *Diplodus puntazzo* | (Di Franco and Guidetti, 2011) |
| *Diplodus sargus* | (Di Franco et al., 2013) |
| *Diplodus vulgaris* | (Di Franco et al., 2013; Macpherson and Raventos, 2006) |
| *Eunicella cavolinii* | (Cánovas-Molina et al., 2018; Masmoudi et al., 2016) |
| *Fistularia commersonii* | (Bernardi et al., 2016) |
| *Epinephelus marginatus* | (Macpherson and Raventos, 2006) |
| *Halocynthia papillosa* | (Villamor et al., 2014) |
| *Hexaplex trunculus* | (Vasconcelos et al., 2004) |
| *Holothuria mammata* | (Borrero-Pérez et al., 2011; Santos et al., n.d.) |
| *Leptopsammia pruvoti* | (Boscari et al., 2019; Goffredo et al., 2006) |
| *Lithognathus mormyrus* | Fishbase & Doris |
| *Melicertus kerathurus* | (Arculeo et al., 2010; Roberts et al., 2012; Zitari-Chatti et al., 2007) |
| *Merluccius merluccius* | (Hidalgo et al., 2019; Morales-Nin and Moranta, 2004) |
| *Microcosmus squamiger* | (Rius et al., 2010, 2009) |
| *Mugil cephalus* | (Kuo et al., 1973) |
| *Mullus barbartus* | (Félix-Hackradt et al., 2013; Maggio et al., 2009) |
| *Mullus surmuletus* | (Félix-Hackradt et al., 2013; Macpherson and Raventos, 2006) |
| *Mytilus galloprovincialis* | (Caceres-Martinez et al., 1993) |
| *Oblada melanura* | (Macpherson and Raventos, 2006) |
| *Phorcus turbinatus* | (Villamor et al., 2014) |
| *Ophioderma longicauda* | (Weber et al., 2014, 2015) |
| *Ostrea edulis* | (Bierne et al., 1998) |
| *Pachygrapsus marmoratus* | (Cuesta and Rodríguez, 2000) |
| *Pagellus erythrinus* | (Macpherson and Raventos, 2006) |
| *Palinurus elephas* | (Hunter, 1999) |
| *Paracentrotus lividus* | (Pedrotti, 1993) |

| Species | References |
|---|---|
| *Patella caerulea* | (Villamor et al., 2014) |
| *Patella rustica* | (Sá-Pinto et al., 2012) |
| *Patella ulyssiponensis* | (Sá-Pinto et al., 2012) |
| *Posidonia oceanica* | (Melià et al., 2016; Serra et al., 2010) |
| *Pycnoclavella communis* | (Pérez-Portela et al., 2007) |
| *Ruditapes decussatus* | (Gharbi et al., 2011) |
| *Scopalina lophyropoda* | (Garoia et al., 2004) |
| *Serranus cabrilla* | (Macpherson and Raventos, 2006) |
| *Solea solea* | (Bahri-Sfar et al., 2011; Vaz et al., 2019) |
| *Sparus aurata* | (Franchini et al., 2012) |
| *Spondylus spinosus* | (Soria et al., 2010) |
| *Spongia officinalis* | (Baldacconi et al., 2007; Gaino et al., 2007) |
| *Symphodus tinca* | (Macpherson and Raventos, 2006; Pallaoro and Jardas, 2003) |

# Supplementary Notes 1: PRISMA 2020 flow diagram for updated systematic reviews

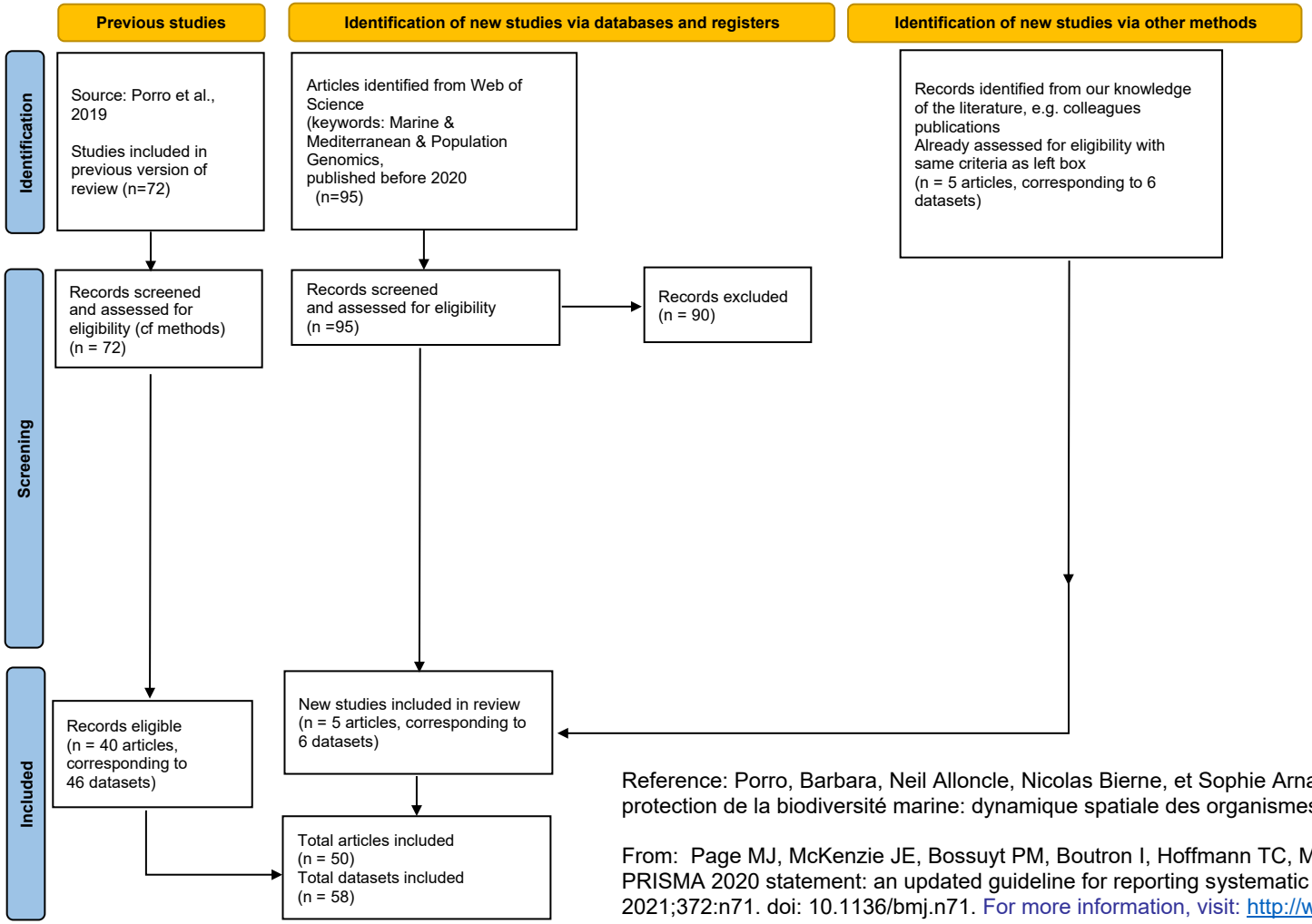


Reference: Porro, Barbara, Neil Alloncle, Nicolas Bierne, et Sophie Arnaud-Haond. Connectivité et protection de la biodiversité marine: dynamique spatiale des organismes marins. Quae, 2019

From: Page MJ, McKenzie JE, Bossuyt PM, Boutron I, Hoffmann TC, Mulrow CD, et al. The PRISMA 2020 statement: an updated guideline for reporting systematic reviews. BMJ 2021;372:n71. doi: 10.1136/bmj.n71. For more information, visit: http://www.prisma-statement.org/

# Supplementary Methods 2: Shallow coastal and neritic shelf habitat description

## Species-specific habitat

Based on the compiled literature of Supplementary Table 2, we attribute to each species pertaining to our meta-analysis (Supplementary Table 1) one habitat chosen between two broad types: shallow coastal habitat or neritic shelf habitat. If a species could fall into both habitat types, we select only one by (i) for fishes, retaining the habitat that contains the depth where the post-settlers/juveniles inhabit; (ii) for other organisms, retaining the habitat that comprises the most frequent sampling depths.

## Network habitat filter

### i. Bathymetric filter

Gridded bathymetry data provided by ETOPO1 1 Arc-Minute Global Relief Model (doi:10.7289/V5C8276M) are co-located with on our network grid to select all the topographic values encompassed in each node. Nodes whose shallowest depth is between 0 m and 50 m are kept in the shallow coastal bathymetric filter and those whose shallowest depth is between 50 m and 200 m are filtered in our neritic shelf bathymetric filter; the remaining deeper nodes are excluded.

### ii. Substrate filter

We use EMODnet Seabed Habitats data[1] to define our substrate filter combining both the EUNIS classification and the MSFD Benthic Broad Habitat typology. We distinguish *infralittoral* and *circalittoral* substrate categories, while considering all substrates together including rocks, fine muds, coarse sediments, etc. (Supplementary Table 3). By co-locating substrate data on our network grid, nodes which encompass *infralittoral* substrate are filtered in our shallow coastal substrate filter and nodes which encompass *circalittoral* substrate are filtered in our neritic shelf substrate filter.

*Supplementary Table 3:* ***Substrate typology used to define the two composite substrates****, called shallow coastal and neritic shelf substrates, following EUNIS and MFSD classifications referenced in EMODnet Seabed Habitats data.*

| Classifications | Shallow coastal substrate | Neritic shelf substrate |
|---|---|---|
| EUNIS | -'A3: Infralittoral rock and other hard substrata'<br>-'A4.26 or A4.32: Mediterranean coralligenous communities moderately exposed to hydrodynamic action or Mediterranean coralligenous communities sheltered from hydrodynamic action' | -'A4.26 or A4.32: Mediterranean coralligenous communities moderately exposed to hydrodynamic action or Mediterranean coralligenous communities sheltered from hydrodynamic action'<br>-'A4.27: Faunal communities on deep moderate energy circalittoral rock' |

[1] *Information contained here has been derived from data that is made available under the European Marine Observation Data Network (EMODnet) Seabed Habitats initiative (http://www.emodnet-seabedhabitats.eu/), financed by the European Union under Regulation (EU) No 508/2014 of the European Parliament and of the Council of 15 May 2014 on the European Maritime and Fisheries Fund.*

| Classifications | Shallow coastal substrate | Neritic shelf substrate |
|---|---|---|
| | -'A5.13: Infralittoral coarse sediment'<br>-'A5.23 or A5.33 or A5.34: Infralittoral fine sands or Infralittoral sandy mud or Infralittoral fine mud'<br>-'A5.23: Infralittoral fine sands'<br>-'A5.33: Infralittoral sandy mud'<br>-'A5.34: Infralittoral fine mud'<br>-'A5.5353: Facies of dead "mattes" of [Posidonia oceanica]'<br>-'A5.535: [Posidonia] beds' | -'A4: Circalittoral rock and other hard substrata<br>-'A5.14: Circalittoral coarse sediment'<br>-'A5.25: Circalittoral fine sand'<br>-'A5.26: Circalittoral muddy sand'<br>-'A5.35: Circalittoral sandy mud'<br>-'A5.36: Circalittoral fine mud' |
| MFSD | -'Infralittoral coarse sediment'<br>-'Infralittoral mixed sediment'<br>-'Infralittoral mud'<br>-'Infralittoral rock and biogenic reef'<br>-'Infralittoral sand' | -'Circalittoral coarse sediment'<br>-'Circalittoral mixed sediment'<br>-'Circalittoral mud'<br>-'Circalittoral mud or Offshore circalittoral mud'<br>-'Circalittoral rock and biogenic reef'<br>-'Circalittoral sand'<br>-'Offshore circalittoral coarse sediment'<br>-'Offshore circalittoral mixed sediment'<br>-'Offshore circalittoral mud'<br>-'Offshore circalittoral rock and biogenic reef'<br>-'Offshore circalittoral sand' |

1.

iii. Habitat filter

The final habitat filter consists in the superposition of both bathymetric and substrate filters: coloured nodes characterize the shallow coastal habitat (Supplementary Figure 1 and Figure 1b main manuscript) and the neritic shelf habitat (Supplementary Figure 2, Figure 1c main manuscript). All nodes selected in the bathymetric filter are coloured in transparent light grey, those belonging to the substrate filter are displayed in red, while pink nodes represent the superposition of both filters.

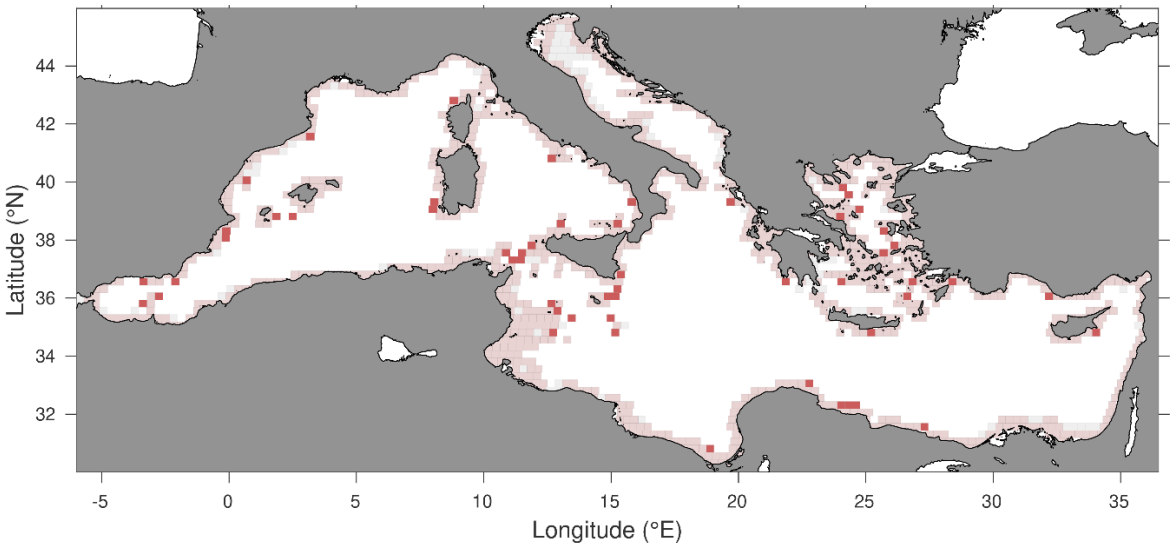


*Supplementary Figure 1:* ***Shallow coastal habitat*** *represented by a bathymetric filter (light grey nodes) and a substrate filter (red nodes). Pink nodes characterize the superposition of both bathymetric and substrate filters.*

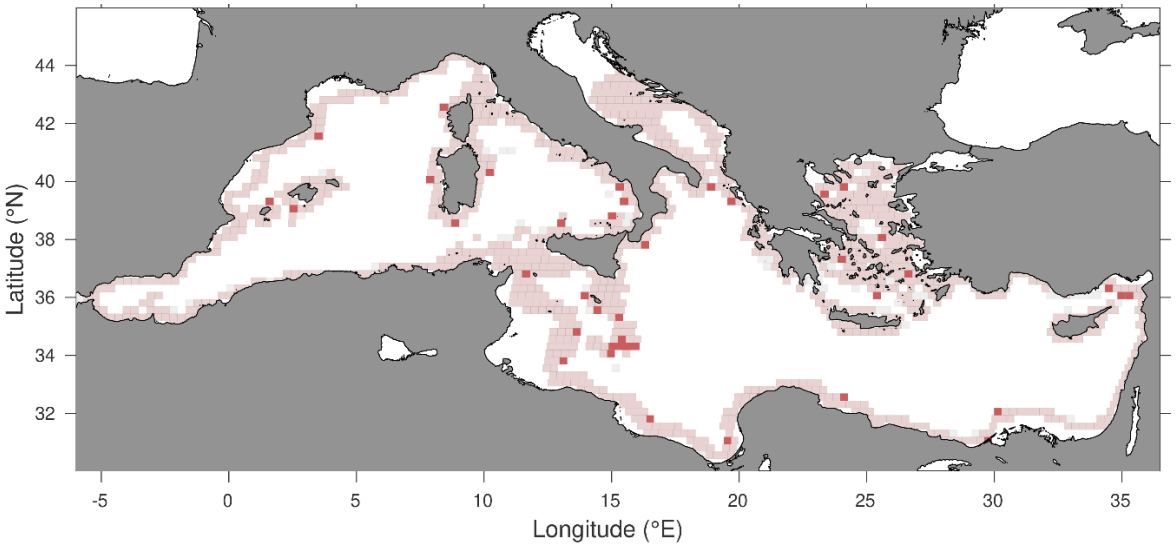


*Supplementary Figure 2:* ***Neritic shelf habitat*** *represented by a bathymetric filter (light grey nodes) and a substrate filter (red nodes). Pink nodes characterize the superposition of both bathymetric and substrate filters.*

# Supplementary Methods 3: Bio-physical modelling

## Hydrodynamical model

We use the hydrodynamic model Mediterranean Forecasting System (MFS) based on NEMO-OPA (Nucleus for European Modelling of the Ocean-PArellelis, version 3.2; Madec, 2008). This data-assimilative operational model has been implemented in the Mediterranean at 1/16° degree horizontal regular resolution and 72 unevenly spaced verticals levels (Oddo et al., 2009). We use the physics reanalysis products for years spanning 2000-2010 downloaded from Marine Copernicus website (https://marine.copernicus.eu/).

## Lagrangian modelling

Following the procedure described in Ser-Giacomi et al., (2015), we discretise the Mediterranean basin on a network of 8196 nodes of 1/4° degree horizontal resolution. About 100 numerical particles are evenly initialised in each node. Horizontal trajectories are simulated by integrating the velocity field, bilinearly interpolated using a *Runge-Kutta* 4 algorithm with a time step of 0.3 h, fulfilling the Courant-Friedrichs-Lewy condition (CFL, Courant et al., (1928)) over the period of interest (Supplementary Figure 3). We use the MFS horizontal velocity fields of the 3$^{rd}$ and 17$^{th}$ vertical levels, which correspond to about 12 m for the shallow coastal habitat and 102 m for the neritic shelf habitat, respectively. Numerical propagules are tracked over five different drifting times (simulating different Pelagic Larval Durations): 1, 10, 20, 30 and 45 days considering successive starting times with a 10-day periodicity over years 2000 to 2010. Altogether, it represents 402 Lagrangian experiments per PLD and per vertical layer, that is 4020 numerical experiments in total (Supplementary Table 4).

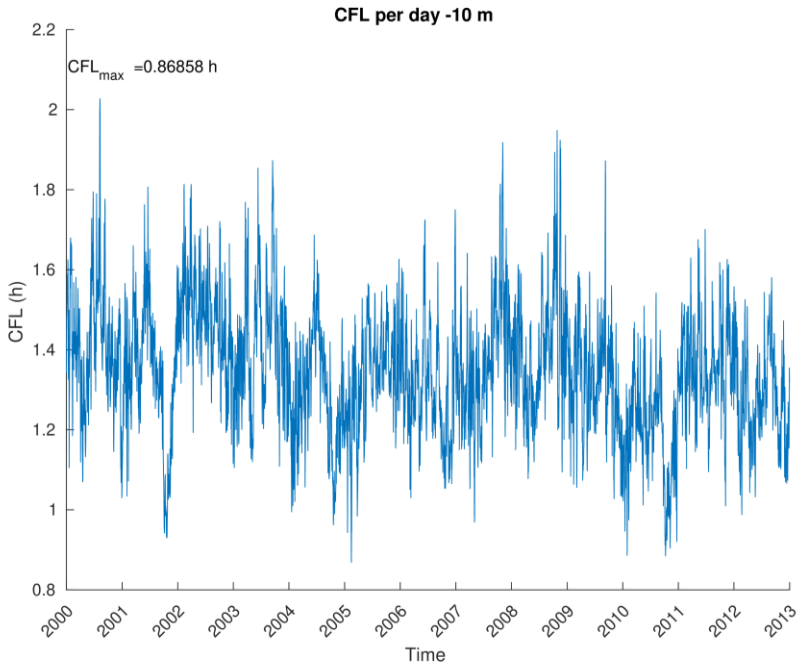


*Supplementary Figure 3:* ***CFL condition indexed for each MFS daily velocity field at 12 m deep between 2000 and 2010****. The maximum time-step value to fulfil CFL condition is 0.87 h, we use a time-step of 0.3 h in our Lagrangian experiments.*

*Supplementary Table 4:* ***Summary of the numerical experiments performed*** *using a 10-day periodicity over 2000-2010. In total, 402 Lagrangian experiments were performed for each PLD/habitat combination (i.e. five PLDs and two habitats, meaning 4020 Lagrangian experiments in total). All the 402 Lagrangian experiments were used to summarize dispersal for all year spawning species. For species characterised by seasonal spawning, we considered only Lagrangian experiments conducted during the spawning season (~ 100 experiments for each study).*

| Season | Winter | Spring | Summer | Fall | All year |
|---|---|---|---|---|---|
| Start date | 01/01 | 01/04 | 01/07 | 01/10 | 01/01 |
| End date | 31/03 | 30/06 | 30/09 | 31/12 | 31/12 |
| Nbr of Lagrangian experiment | 100 | 99 | 100 | 103 | 402 |
| Total mean nbr of particles | 12,000,000 | 12,000,000 | 12,000,000 | 12,000,000 | 48,000,000 |

# Supplementary Methods 4: Parametrization of our multi-generation dispersal models

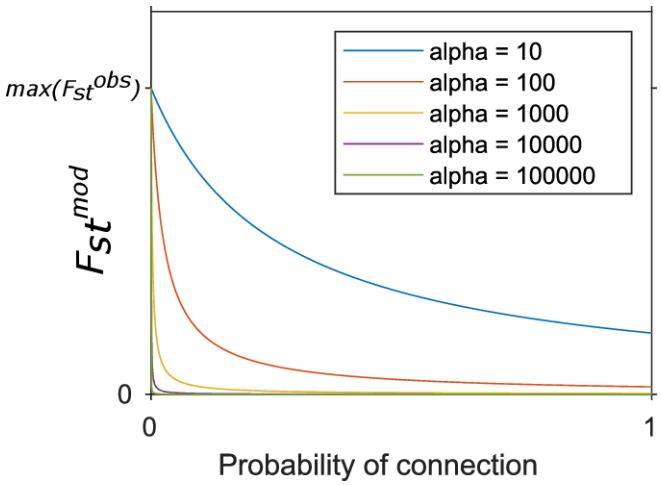


*Supplementary Figure 4:* ***Sensitivity of the reciprocal transformation applied on dispersal probabilities to obtain*** $F_{st}^{mod}$ ***with respect to the value of alpha.***

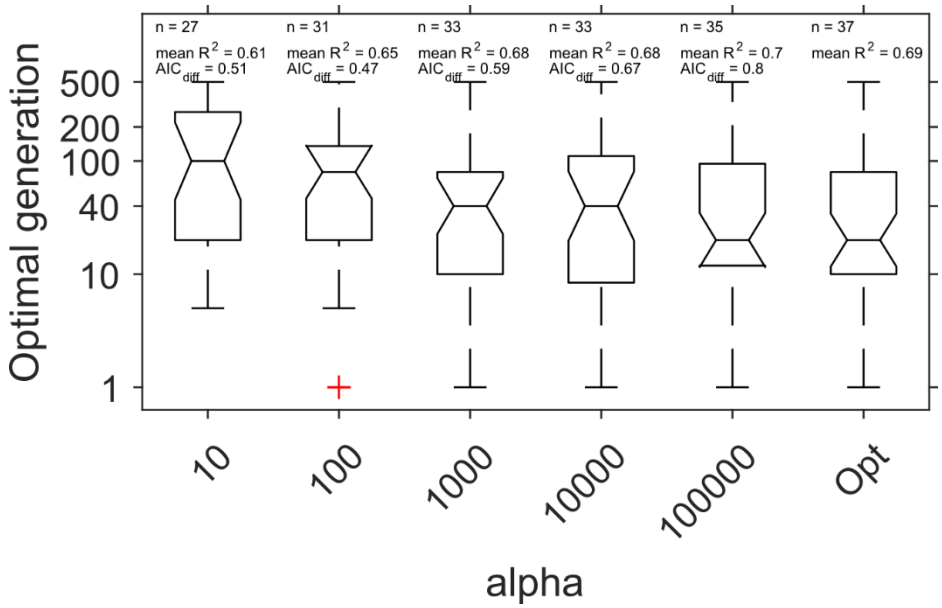


*Supplementary Figure 5:* ***Boxplot of the optimal generations obtained when varying alpha (reciprocal transformation of dispersal probabilities into*** $F_{st}^{mod}$ ***when comparing the multi-generation implicit dispersal model predictions (R², p-value and AIC) against*** $F_{st}^{obs}/(1-F_{st}^{obs})$ ***across the whole meta-analysis.*** *n = number of studies whose model predictions of genetic observations are significant. On each box, the central mark, the bottom and top edges indicate the indicates the median, the 25th and the 75th percentiles, respectively. The whiskers extend to the most extreme data points not considered outliers, and the outliers are plotted individually using a cross symbol. Source data are provided as a Source Data file.*

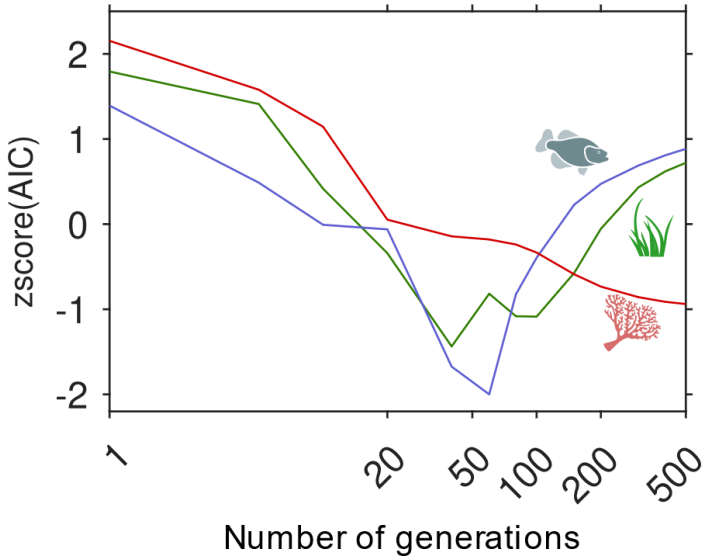


*Supplementary Figure 6:* ***Multi-generation implicit dispersal model AIC values as a function of the number of generations for three specific studies: Aurelle et al., 2011 (*****Corallium rubrum*** ***in red), Dalongeville et al., 2018 (*****Mullus surmuletus*** ***in blue) and Arnaud-Haond et al., 2007 (*****Posidonia oceanica*** ***in green).*** *Source data are provided as a Source Data file. Icons credit: © vectors market, © Agne Alesiute, © Luis Prado (changes were made on all the icons, Creative Commons BY 4.0 license).*

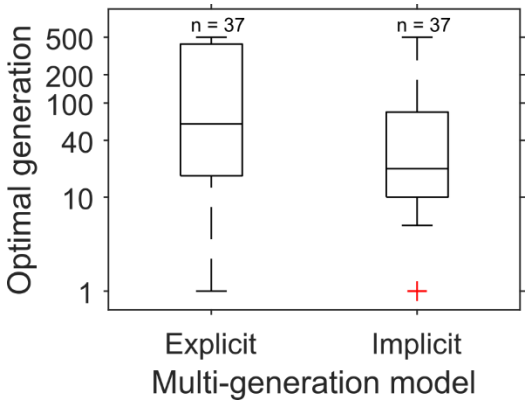


*Supplementary Figure 7:* ***Statistical distribution (boxplot) of the optimal generations for significant predictions of*** $F_{st}^{obs}/(1-F_{st}^{obs})$ ***across the meta-analysis, as obtained using the multi-generation explicit and implicit dispersal models.*** *n = number of studies whose model predictions of genetic observations are significant. On each box, the central mark, the bottom and top edges indicate the indicates the median, the 25th and the 75th percentiles, respectively. The whiskers extend to the most extreme data points not considered outliers, and the outliers are plotted individually using a cross symbol. Source data are provided as a Source Data file.*

# Supplementary Methods 5: Screening for the best models predicting observed genetic differentiation

*Supplementary Table 5:* ***Accuracy of the Isolation-by-Euclidian Distance model in explaining observed genetic structure across the meta-analysis.*** *Mantel r and MLPE linear mixed model R² between Euclidian distance and $F_{st}^{obs}/(1-F_{st}^{obs})$ and theirs associated p-value are indexed for all the studies. Note that (i) Weber et al., 2015 use SNPs marker ([1]) and mtDNA marker ([2]), (ii) Carrera et al., 2019 considers all the loci ([3]) and only the Mediterranean outliers loci ([4]), and (iii) Marzouk et al., 2017 use SNPs marker ([5]) and mtDNA marker ([6]). Significant studies (p-values*) are highlighted in grey. Source data are provided as a Source Data file.*

| Species | Study | Mantel *r* | Mantel p-value | MLPE $R^2$ | MLPE p-value |
|---|---|---|---|---|---|
| *Cystoseira amentacea* | Susini et al., 2007 | 0,78 | 0,0417 | 0,85 | 0,0148 |
| *Astroides calycularis* | Casado-Amezua et al., 2012 | 0,72 | 0,001 | 0,84 | 0 |
| *Corallium rubrum* | Aurelle et al., 2011 | 0,42 | 0,001 | 0,43 | 0 |
| *Corallium rubrum* | Costantini et al., 2013 | 0,54 | 0,1 | 0,31 | 0,0653 |
| *Eunicella cavolinii* | Masmoudi et al., 2016 | 0,76 | 0,001 | 0,58 | 0 |
| *Leptopsammia pruvoti* | Boscari et al., 2019 | 0,22 | 0,125 | 0,09 | 0,1201 |
| *Botryllus schlosseri* | Reem et al., 2017 | 0,36 | 0,099 | 0,17 | 0,0056 |
| *Halocynthia papillosa* | Villamor et al., 2014 | 0,87 | 0,125 | 1 | 0 |
| *Microcosmus squamiger* | Ordóñez et al., 2013 | -0,32 | 0,8972 | 0,11 | 0,1982 |
| *Pycnoclavella communis* | Pérez-Portela et al., 2007 | -0,37 | 0,7917 | 0,16 | 0,3488 |
| *Carcinus aestuarii* | Schiavina et al., 2014 | 0,46 | 0,008 | 0,93 | 0,5072 |
| *Melicertus kerathurus* | Arculeo et al., 2010 | -0,04 | 0,523 | 0 | 0,8016 |
| *Melicertus kerathurus* | Zitari-Chatti et al., 2007 | 0,11 | 0,219 | 0,05 | 0,4783 |
| *Pachygrapsus marmoratus* | Fratini et al., 2013 | 0,44 | 0,002 | 0,2 | 0,0132 |
| *Palinurus elephas* | Palero et al., 2011 | 0,24 | 0,3167 | 0,06 | 0,4472 |
| *Spongia officinalis* | Dailianis et al., 2011 | 0,72 | 0,005 | 0,68 | 0 |
| *Astropecten aranciacus* | Zulliger et al., 2009 | 0,44 | 0,014 | 0,2 | 0,0327 |
| *Holothuria mammata* | Borrero-Pérez et al., 2011 | 0,96 | 0,125 | 0,97 | 0,0001 |
| *Ophioderma longicauda* | Weber et al., 2015[1] | -0,16 | 0,777 | 0,56 | 0,8773 |
| *Ophioderma longicauda* | Weber et al., 2015[2] | -0,22 | 0,871 | 0,12 | 0,1357 |

| Species | Study | Mantel *r* | Mantel p-value | MLPE $R^2$ | MLPE p-value |
|---|---|---|---|---|---|
| *Paracentrotus lividus* | Penant et al., 2013 | -0,33 | 0,933 | 0,56 | 0,0001 |
| *Paracentrotus lividus* | Paterno et al., 2017 | 0,66 | 0,03 | 0,85 | 0,0397 |
| *Paracentrotus lividus* | Carreras et al., 2020[3] | 0,52 | 0,001 | 0,81 | 0 |
| *Paracentrotus lividus* | Carreras et al., 2020[4] | 0,56 | 0,006 | 0,81 | 0 |
| *Apogon imberbis* | Muths et al., 2015 | -0,17 | 0,625 | 0,61 | 0,9141 |
| *Coris julis* | Fruciano et al., 2011 | 0,61 | 0,044 | 0,98 | 0,7393 |
| *Diplodus sargus* | González-Wangüemert et al., 2010 | 0,26 | 0,175 | 0,08 | 0,3955 |
| *Diplodus vulgaris* | Kaouèche et al., 2013 | 0,22 | 0,2014 | 0,05 | 0,391 |
| *Epinephelus marginatus* | Schunter et al., 2011 | 0,22 | 0,173 | 0,48 | 0,0331 |
| *Lithognathus mormyrus* | Hammami et al., 2007 | 0,68 | 0,1667 | 0,51 | 0,0515 |
| *Merluccius merluccius* | Milano et al., 2014 | 0,55 | 0,001 | 0,37 | 0 |
| *Mugil cephalus* | Durand et al., 2013 | 0,29 | 0,05 | 0,14 | 0,0144 |
| *Mullus barbartus* | Maggio et al., 2009 | 0,12 | 0,215 | 0,24 | 0,0714 |
| *Mullus surmuletus* | Galarza et al., 2009 | -0,04 | 0,4514 | 0,15 | 0,9186 |
| *Mullus surmuletus* | Dalongeville et al., 2018 | 0,21 | 0,001 | 0,61 | 0,0199 |
| *Oblada melanura* | Gkafas et al., 2013 | 0,04 | 0,382 | 0 | 0,8142 |
| *Oblada melanura* | Calò et al., 2016 | 0,2 | 0,118 | 0,23 | 0,1709 |
| *Pagellus erythrinus* | Fassatoui et al., 2009 | 0,35 | 0,1792 | 0,13 | 0,1659 |
| *Serranus cabrilla* | Schunter et al., 2011 | 0,33 | 0,07 | 0,75 | 0 |
| *Solea solea* | Bahri-Sfar et al., 2011 | 0,57 | 0,009 | 0,65 | 0 |
| *Solea solea* | Garoia et al., 2007 | 0,99 | 0,0417 | 0,98 | 0 |
| *Sparus aurata* | Franchini et al., 2012 | 0,15 | 0,195 | 0,23 | 0,111 |
| *Symphodus tinca* | Carreras et al., 2017 | 0,37 | 0,175 | 0,36 | 0,4087 |
| *Cerastoderma edule* | Sromek et al., 2019 | 0,71 | 0,003 | 0,89 | 0 |
| *Chiton olivaceus* | Villamor et al., 2014 | 0,78 | 0,2083 | 0,65 | 0,0175 |
| *Hexaplex trunculus* | Villamor et al., 2014 | 0,82 | 0,125 | 0,71 | 0,0396 |
| *Hexaplex trunculus* | Marzouk et al., 2017[5] | 0,17 | 0,154 | 0,48 | 0,5448 |
| *Hexaplex trunculus* | Marzouk et al., 2017[6] | 0,2 | 0,111 | 0,52 | 0,6864 |

| Species | Study | Mantel *r* | Mantel p-value | MLPE $R^2$ | MLPE p-value |
|---|---|---|---|---|---|
| *Mytilus galloprovincialis* | Diz and Presa, 2008 | 0,5 | 0,009 | 0,3 | 0,0064 |
| *Ostrea edulis* | Launey et al., 2002 | 0,4 | 0,2167 | 0,83 | 0,0097 |
| *Patella caerulea* | Villamor et al., 2014 | 0,37 | 0,1 | 0,39 | 0,0992 |
| *Patella rustica* | Sá-Pinto et al., 2012 | 0,05 | 0,3736 | 0,18 | 0,7239 |
| *Patella ulyssiponensis* | Sá-Pinto et al., 2012 | 0,39 | 0,0667 | 0,16 | 0,201 |
| *Phorcus turbinatus* | Villamor et al., 2014 | 0,84 | 0,2917 | 1 | 0,0001 |
| *Ruditapes decussatus* | Gharbi et al., 2011 | 0,42 | 0,006 | 0,18 | 0,0048 |
| *Spondylus spinosus* | Shabtay et al., 2014 | -0,05 | 0,5167 | 0,5 | 0,7273 |
| *Cymodocea nodosa* | Alberto et al., 2008 | 0,37 | 0,014 | 0,36 | 0,0002 |
| *Posidonia oceanica* | Arnaud-Haond et al., 2007 | 0,36 | 0,001 | 0,25 | 0 |

*Supplementary Table 6:* ***Accuracy of the Isolation-by-sea least cost Distance model in explaining observed genetic structure across the meta-analysis.*** *Mantel r and MLPE linear mixed model R² between sea least-cost distance and $F_{st}^{obs}/(1-F_{st}^{obs})$ and theirs associated p-value are indexed for all the studies. Note that (i) Weber et al., 2015 use SNPs marker ([1]) and mtDNA marker ([2]), (ii) Carrera et al., 2019 considers all the loci ([3]) and only the Mediterranean outliers loci ([4]), and (iii) Marzouk et al., 2017 use SNPs marker ([5]) and mtDNA marker ([6]). Significant studies (p-values*) are highlighted in grey. Source data are provided as a Source Data file.*

| Species | Study | Mantel *r* | Mantel p-value | MLPE $R^2$ | MLPE p-value |
|---|---|---|---|---|---|
| *Cystoseira amentacea* | Susini et al., 2007 | 0,78 | 0,0417 | 0,85 | 0,0148 |
| *Astroides calycularis* | Casado-Amezua et al., 2012 | 0,72 | 0,001 | 0,84 | 0 |
| *Corallium rubrum* | Aurelle et al., 2011 | 0,42 | 0,001 | 0,43 | 0 |
| *Corallium rubrum* | Costantini et al., 2013 | 0,54 | 0,1 | 0,31 | 0,0653 |
| *Eunicella cavolinii* | Masmoudi et al., 2016 | 0,76 | 0,001 | 0,58 | 0 |
| *Leptopsammia pruvoti* | Boscari et al., 2019 | 0,22 | 0,125 | 0,09 | 0,1201 |
| *Botryllus schlosseri* | Reem et al., 2017 | 0,36 | 0,099 | 0,17 | 0,0056 |
| *Halocynthia papillosa* | Villamor et al., 2014 | 0,87 | 0,125 | 1 | 0 |
| *Microcosmus squamiger* | Ordóñez et al., 2013 | -0,32 | 0,8972 | 0,11 | 0,1982 |
| *Pycnoclavella communis* | Pérez-Portela et al., 2007 | -0,37 | 0,7917 | 0,16 | 0,3488 |
| *Carcinus aestuarii* | Schiavina et al., 2014 | 0,46 | 0,008 | 0,93 | 0,5072 |
| *Melicertus kerathurus* | Arculeo et al., 2010 | -0,04 | 0,523 | 0 | 0,8016 |
| *Melicertus kerathurus* | Zitari-Chatti et al., 2007 | 0,11 | 0,219 | 0,05 | 0,4783 |
| *Pachygrapsus marmoratus* | Fratini et al., 2013 | 0,44 | 0,002 | 0,2 | 0,0132 |
| *Palinurus elephas* | Palero et al., 2011 | 0,24 | 0,3167 | 0,06 | 0,4472 |
| *Spongia officinalis* | Dailianis et al., 2011 | 0,72 | 0,005 | 0,68 | 0 |
| *Astropecten aranciacus* | Zulliger et al., 2009 | 0,44 | 0,014 | 0,2 | 0,0327 |
| *Holothuria mammata* | Borrero-Pérez et al., 2011 | 0,96 | 0,125 | 0,97 | 0,0001 |
| *Ophioderma longicauda* | Weber et al., 2015[1] | -0,16 | 0,777 | 0,56 | 0,8773 |
| *Ophioderma longicauda* | Weber et al., 2015[2] | -0,22 | 0,871 | 0,12 | 0,1357 |
| *Paracentrotus lividus* | Penant et al., 2013 | -0,33 | 0,933 | 0,56 | 0,0001 |
| *Paracentrotus lividus* | Paterno et al., 2017 | 0,66 | 0,03 | 0,85 | 0,0397 |
| *Paracentrotus lividus* | Carreras et al., 2020[3] | 0,52 | 0,001 | 0,81 | 0 |
| *Paracentrotus lividus* | Carreras et al., 2020[4] | 0,56 | 0,006 | 0,81 | 0 |

| Species | Study | Mantel *r* | Mantel p-value | MLPE $R^2$ | MLPE p-value |
|---|---|---|---|---|---|
| *Apogon imberbis* | Muths et al., 2015 | -0,17 | 0,625 | 0,61 | 0,9141 |
| *Coris julis* | Fruciano et al., 2011 | 0,61 | 0,044 | 0,98 | 0,7393 |
| *Diplodus sargus* | González-Wangüemert et al., 2010 | 0,26 | 0,175 | 0,08 | 0,3955 |
| *Diplodus vulgaris* | Kaouèche et al., 2013 | 0,22 | 0,2014 | 0,05 | 0,391 |
| *Epinephelus marginatus* | Schunter et al., 2011 | 0,22 | 0,173 | 0,48 | 0,0331 |
| *Lithognathus mormyrus* | Hammami et al., 2007 | 0,68 | 0,1667 | 0,51 | 0,0515 |
| *Merluccius merluccius* | Milano et al., 2014 | 0,55 | 0,001 | 0,37 | 0 |
| *Mugil cephalus* | Durand et al., 2013 | 0,29 | 0,05 | 0,14 | 0,0144 |
| *Mullus barbartus* | Maggio et al., 2009 | 0,12 | 0,215 | 0,24 | 0,0714 |
| *Mullus surmuletus* | Galarza et al., 2009 | -0,04 | 0,4514 | 0,15 | 0,9186 |
| *Mullus surmuletus* | Dalongeville et al., 2018 | 0,21 | 0,001 | 0,61 | 0,0199 |
| *Oblada melanura* | Gkafas et al., 2013 | 0,04 | 0,382 | 0 | 0,8142 |
| *Oblada melanura* | Calò et al., 2016 | 0,2 | 0,118 | 0,23 | 0,1709 |
| *Pagellus erythrinus* | Fassatoui et al., 2009 | 0,35 | 0,1792 | 0,13 | 0,1659 |
| *Serranus cabrilla* | Schunter et al., 2011 | 0,33 | 0,07 | 0,75 | 0 |
| *Solea solea* | Bahri-Sfar et al., 2011 | 0,57 | 0,009 | 0,65 | 0 |
| *Solea solea* | Garoia et al., 2007 | 0,99 | 0,0417 | 0,98 | 0 |
| *Sparus aurata* | Franchini et al., 2012 | 0,15 | 0,195 | 0,23 | 0,111 |
| *Symphodus tinca* | Carreras et al., 2017 | 0,37 | 0,175 | 0,36 | 0,4087 |
| *Cerastoderma edule* | Sromek et al., 2019 | 0,71 | 0,003 | 0,89 | 0 |
| *Chiton olivaceus* | Villamor et al., 2014 | 0,78 | 0,2083 | 0,65 | 0,0175 |
| *Hexaplex trunculus* | Villamor et al., 2014 | 0,82 | 0,125 | 0,71 | 0,0396 |
| *Hexaplex trunculus* | Marzouk et al., 2017[5] | 0,17 | 0,154 | 0,48 | 0,5448 |
| *Hexaplex trunculus* | Marzouk et al., 2017[6] | 0,2 | 0,111 | 0,52 | 0,6864 |
| *Mytilus galloprovincialis* | Diz and Presa, 2008 | 0,5 | 0,009 | 0,3 | 0,0064 |
| *Ostrea edulis* | Launey et al., 2002 | 0,4 | 0,2167 | 0,83 | 0,0097 |
| *Patella caerulea* | Villamor et al., 2014 | 0,37 | 0,1 | 0,39 | 0,0992 |
| *Patella rustica* | Sá-Pinto et al., 2012 | 0,05 | 0,3736 | 0,18 | 0,7239 |

| Species | Study | Mantel *r* | Mantel p-value | MLPE $R^2$ | MLPE p-value |
|---|---|---|---|---|---|
| *Patella ulyssiponensis* | Sá-Pinto et al., 2012 | 0,39 | 0,0667 | 0,16 | 0,201 |
| *Phorcus turbinatus* | Villamor et al., 2014 | 0,84 | 0,2917 | 1 | 0,0001 |
| *Ruditapes decussatus* | Gharbi et al., 2011 | 0,42 | 0,006 | 0,18 | 0,0048 |
| *Spondylus spinosus* | Shabtay et al., 2014 | -0,05 | 0,5167 | 0,5 | 0,7273 |
| *Cymodocea nodosa* | Alberto et al., 2008 | 0,37 | 0,014 | 0,36 | 0,0002 |
| *Posidonia oceanica* | Arnaud-Haond et al., 2007 | 0,36 | 0,001 | 0,25 | 0 |

*Supplementary Table 7:* ***Accuracy of our single-generation explicit dispersal model in explaining observed genetic structure across the meta-analysis.*** *Mantel r and MLPE linear mixed model R² between $F_{st}^{mod}$ and $F_{st}^{obs}/(1-F_{st}^{obs})$ and theirs associated p-value are indexed for all the studies. The "opt alpha" stands for the optimal alpha value of the reciprocal transformation that minimizes the AIC estimator (see Supplementary Figure 5). Note that (i) Weber et al., 2015 use SNPs marker ([1]) and mtDNA marker ([2]), (ii) Carrera et al., 2019 considers all the loci ([3]) and only the Mediterranean outliers loci ([4]), and (iii) Marzouk et al., 2017 use SNPs marker ([5]) and mtDNA marker ([6]). Significant studies (p-values*) are highlighted in grey. Source data are provided as a Source Data file.*

| Species | Study | Mantel *r* | Mantel p-value | Mantel opt alpha | MLPE $R^2$ | MLPE p-value | MLPE opt alpha |
|---|---|---|---|---|---|---|---|
| *Cystoseira amentacea* | Susini et al., 2007 | 0,74 | 0,1667 | 10 | 0,59 | 0,0304 | 10 |
| *Astroides calycularis* | Casado-Amezua et al., 2012 | 0,44 | 0,001 | 10000 | 0,66 | 0 | 1000 |
| *Corallium rubrum* | Aurelle et al., 2011 | 0,3 | 0,001 | 1000 | 0,4 | 0 | 100000 |
| *Corallium rubrum* | Costantini et al., 2013 | 0,49 | 0,1 | 10 | 0,26 | 0,1029 | 10 |
| *Eunicella cavolinii* | Masmoudi et al., 2016 | 0,68 | 0,001 | 100000 | 0,46 | 0 | 100000 |
| *Leptopsammia pruvoti* | Boscari et al., 2019 | 0,27 | 0,012 | 100000 | 0,11 | 0,0642 | 100000 |
| *Botryllus schlosseri* | Reem et al., 2017 | NaN | NaN | NaN | NaN | NaN | NaN |
| *Halocynthia papillosa* | Villamor et al., 2014 | NaN | NaN | NaN | NaN | NaN | NaN |
| *Microcosmus squamiger* | Ordóñez et al., 2013 | -0,07 | 0,6667 | 10 | 0 | 0,7982 | 10 |
| *Pycnoclavella communis* | Pérez-Portela et al., 2007 | -0,41 | 0,8333 | 10 | 0,2 | 0,2879 | 10 |
| *Carcinus aestuarii* | Schiavina et al., 2014 | 0,37 | 0,028 | 100000 | 0,94 | 0,3879 | 100 |
| *Melicertus kerathurus* | Arculeo et al., 2010 | 0,04 | 0,597 | 10 | 0,01 | 0,5952 | 100000 |
| *Melicertus kerathurus* | Zitari-Chatti et al., 2007 | 0,13 | 0,237 | 100000 | 0,06 | 0,4233 | 100000 |
| *Pachygrapsus marmoratus* | Fratini et al., 2013 | 0,01 | 0,52 | 10 | 0,01 | 0,6935 | 100000 |
| *Palinurus elephas* | Palero et al., 2011 | NaN | NaN | NaN | NaN | NaN | NaN |
| *Spongia officinalis* | Dailianis et al., 2011 | 0,25 | 0,068 | 100000 | 0,31 | 0,0364 | 100000 |
| *Astropecten aranciacus* | Zulliger et al., 2009 | NaN | NaN | NaN | NaN | NaN | NaN |
| *Holothuria mammata* | Borrero-Pérez et al., 2011 | 0,44 | 0,3333 | 10 | 0,22 | 0,2543 | 10 |
| *Ophioderma longicauda* | Weber et al., 2015[1] | -0,06 | 0,662 | 10 | 0,56 | 0,1217 | 100000 |
| *Ophioderma longicauda* | Weber et al., 2015[2] | -0,16 | 0,782 | 100000 | 0,11 | 0,1647 | 10 |
| *Paracentrotus lividus* | Penant et al., 2013 | -0,24 | 0,906 | 10 | 0,46 | 0,0024 | 100000 |
| *Paracentrotus lividus* | Paterno et al., 2017 | 0,43 | 0,038 | 100000 | 0,88 | 0,0971 | 1000 |
| *Paracentrotus lividus* | Carreras et al., 2020[3] | 0,35 | 0,038 | 10 | 0,68 | 0,0005 | 1000 |

| Species | Study | Mantel *r* | Mantel p-value | Mantel opt alpha | MLPE $R^2$ | MLPE p-value | MLPE opt alpha |
|---|---|---|---|---|---|---|---|
| *Paracentrotus lividus* | Carreras et al., 2020[4] | 0,51 | 0,04 | 100000 | 0,73 | 0,0001 | 100000 |
| *Apogon imberbis* | Muths et al., 2015 | -0,65 | 1 | 10 | 0,47 | 0,2004 | 10 |
| *Coris julis* | Fruciano et al., 2011 | 0,12 | 0,113 | 100000 | 0,98 | 0,7344 | 100000 |
| *Diplodus sargus* | González-Wangüemert et al., 2010 | 0,11 | 0,6 | 10 | 0,01 | 0,7217 | 10 |
| *Diplodus vulgaris* | Kaouèche et al., 2013 | 0,21 | 0,2417 | 100000 | 0,06 | 0,3602 | 100000 |
| *Epinephelus marginatus* | Schunter et al., 2011 | 0,16 | 0,16 | 10 | 0,45 | 0,1263 | 10000 |
| *Lithognathus mormyrus* | Hammami et al., 2007 | 0,69 | 0,2083 | 100000 | 0,53 | 0,0476 | 100000 |
| *Merluccius merluccius* | Milano et al., 2014 | 0,18 | 0,022 | 100000 | 0,14 | 0,069 | 100000 |
| *Mugil cephalus* | Durand et al., 2013 | 0,16 | 0,074 | 100000 | 0,04 | 0,1277 | 100000 |
| *Mullus barbartus* | Maggio et al., 2009 | 0,08 | 0,201 | 10 | 0,15 | 0,2698 | 10 |
| *Mullus surmuletus* | Galarza et al., 2009 | 0,29 | 0,0806 | 1000 | 0,2 | 0,2659 | 1000 |
| *Mullus surmuletus* | Dalongeville et al., 2018 | 0,01 | 0,379 | 100000 | 0,62 | 0,3775 | 10 |
| *Oblada melanura* | Gkafas et al., 2013 | -0,07 | 0,589 | 10 | 0,04 | 0,2833 | 10000 |
| *Oblada melanura* | Calò et al., 2016 | 0,21 | 0,138 | 10000 | 0,61 | 0,1171 | 10000 |
| *Pagellus erythrinus* | Fassatoui et al., 2009 | 0,46 | 0,0389 | 100000 | 0,23 | 0,0534 | 100000 |
| *Serranus cabrilla* | Schunter et al., 2011 | 0,2 | 0,036 | 100 | 0,81 | 0 | 10 |
| *Solea solea* | Bahri-Sfar et al., 2011 | 0,38 | 0,003 | 100000 | 0,14 | 0,0089 | 100000 |
| *Solea solea* | Garoia et al., 2007 | NaN | NaN | NaN | NaN | NaN | NaN |
| *Sparus aurata* | Franchini et al., 2012 | 0,32 | 0,044 | 100000 | 0,38 | 0,0004 | 100000 |
| *Symphodus tinca* | Carreras et al., 2017 | 0,32 | 0,1139 | 100000 | 0,41 | 0,3075 | 100000 |
| *Cerastoderma edule* | Sromek et al., 2019 | 0,36 | 0,048 | 1000 | 0,13 | 0,0897 | 10 |
| *Chiton olivaceus* | Villamor et al., 2014 | 0,44 | 0,3333 | 10 | 0,23 | 0,2523 | 10 |
| *Hexaplex trunculus* | Villamor et al., 2014 | NaN | NaN | NaN | NaN | NaN | NaN |
| *Hexaplex trunculus* | Marzouk et al., 2017[5] | 0 | 0,545 | 100000 | 0,5 | 0,2692 | 100000 |
| *Hexaplex trunculus* | Marzouk et al., 2017[6] | 0,05 | 0,328 | 100000 | 0,52 | 0,4083 | 10 |
| *Mytilus galloprovincialis* | Diz and Presa, 2008 | 0,41 | 0,006 | 1000 | 0,28 | 0,0245 | 1000 |
| *Ostrea edulis* | Launey et al., 2002 | 0,41 | 0,2 | 10 | 0,55 | 0,0723 | 10000 |

| Species | Study | Mantel *r* | Mantel p-value | Mantel opt alpha | MLPE $R^2$ | MLPE p-value | MLPE opt alpha |
|---|---|---|---|---|---|---|---|
| *Patella caerulea* | Villamor et al., 2014 | 0,47 | 0,0444 | 1000 | 0,23 | 0,055 | 1000 |
| *Patella rustica* | Sá-Pinto et al., 2012 | 0,31 | 0,0667 | 10 | 0,18 | 0,2184 | 10 |
| *Patella ulyssiponensis* | Sá-Pinto et al., 2012 | 0,25 | 0,2 | 10 | 0,07 | 0,4257 | 10 |
| *Phorcus turbinatus* | Villamor et al., 2014 | 0,91 | 0,3333 | 100000 | 1 | 0 | 100000 |
| *Ruditapes decussatus* | Gharbi et al., 2011 | 0,17 | 0,089 | 1000 | 0,16 | 0,3376 | 100000 |
| *Spondylus spinosus* | Shabtay et al., 2014 | 0,24 | 0,4333 | 10 | 0,46 | 0,6774 | 10 |
| *Cymodocea nodosa* | Alberto et al., 2008 | 0,44 | 0,002 | 100000 | 0,36 | 0 | 100000 |
| *Posidonia oceanica* | Arnaud-Haond et al., 2007 | 0,3 | 0,001 | 100000 | 0,19 | 0 | 100000 |

*Supplementary Table 8:* ***Accuracy of our multi-generation explicit dispersal model in explaining observed genetic structure across the meta-analysis.*** *Mantel r and MLPE linear mixed model R² between $F_{st}^{mod}$ and $F_{st}^{obs}/(1-F_{st}^{obs})$ and theirs associated p-value are indexed for all the studies. The "opt alpha" stands for the alpha value of the reciprocal transformation that minimizes the AIC estimator (see Supplementary Figure 5). The "opt M" stands for the number of generations that minimizes the AIC estimator (see Supplementary Figure 6). Note that (i) Weber et al., 2015 use SNPs marker ([1]) and mtDNA marker ([2]), (ii) Carrera et al., 2019 considers all the loci ([3]) and only the Mediterranean outliers loci ([4]), and (iii) Marzouk et al., 2017 use SNPs marker ([5]) and mtDNA marker ([6]). Significant studies (p-values*) are highlighted in grey. Source data are provided as a Source Data file.*

| Species | Study | Mantel *r* | Mantel p-value | Mantel opt M | Mantel opt alpha | MLPE $R^2$ | MLPE p-value | MLPE opt M | MLPE opt alpha |
|---|---|---|---|---|---|---|---|---|---|
| *Cystoseira amentacea* | Susini et al., 2007 | 0,77 | 0,1667 | 1 | 10 | 0,59 | 0,0304 | 1 | 10 |
| *Astroides calycularis* | Casado-Amezua et al., 2012 | 0,57 | 0,001 | 300 | 100000 | 0,66 | 0 | 300 | 100000 |
| *Corallium rubrum* | Aurelle et al., 2011 | 0,71 | 0,001 | 40 | 100000 | 0,5 | 0 | 40 | 100000 |
| *Corallium rubrum* | Costantini et al., 2013 | 0,5 | 0,1 | 1 | 10 | 0,26 | 0,1029 | 1 | 10 |
| *Eunicella cavolinii* | Masmoudi et al., 2016 | 0,88 | 0,001 | 300 | 1000 | 0,78 | 0 | 300 | 1000 |
| *Leptopsammia pruvoti* | Boscari et al., 2019 | 0,59 | 0,002 | 400 | 100000 | 0,35 | 0 | 400 | 100000 |
| *Botryllus schlosseri* | Reem et al., 2017 | 0,36 | 0,006 | 500 | 100000 | 0,11 | 0,0118 | 500 | 100000 |
| *Halocynthia papillosa* | Villamor et al., 2014 | 0,9 | 0,125 | 200 | 10 | 1 | 0 | 200 | 100000 |
| *Microcosmus squamiger* | Ordóñez et al., 2013 | -0,07 | 0,6667 | 1 | 10 | 0 | 0,7982 | 1 | 10 |
| *Pycnoclavella communis* | Pérez-Portela et al., 2007 | -0,41 | 0,75 | 500 | 100000 | 0,2 | 0,2879 | 500 | 10 |
| *Carcinus aestuarii* | Schiavina et al., 2014 | 0,99 | 0,017 | 40 | 100000 | 0,97 | 0 | 40 | 100000 |
| *Melicertus kerathurus* | Arculeo et al., 2010 | 0,03 | 0,479 | 5 | 10 | 0,06 | 0,1444 | 5 | 100000 |
| *Melicertus kerathurus* | Zitari-Chatti et al., 2007 | 0,14 | 0,206 | 1 | 100000 | 0,06 | 0,4233 | 1 | 100000 |
| *Pachygrapsus marmoratus* | Fratini et al., 2013 | 0,04 | 0,327 | 500 | 10 | 0,05 | 0,2558 | 500 | 100000 |
| *Palinurus elephas* | Palero et al., 2011 | 0,29 | 0,2333 | 40 | 100000 | 0,36 | 0,0414 | 40 | 10 |

| Species | Study | Mantel *r* | Mantel p-value | Mantel opt M | Mantel opt alpha | MLPE $R^2$ | MLPE p-value | MLPE opt M | MLPE opt alpha |
|---|---|---|---|---|---|---|---|---|---|
| *Spongia officinalis* | Dailianis et al., 2011 | 0,62 | 0,009 | 500 | 100000 | 0,74 | 0 | 500 | 10000 |
| *Astropecten aranciacus* | Zulliger et al., 2009 | 0,34 | 0,075 | 5 | 10 | 0,12 | 0,1038 | 5 | 10 |
| *Holothuria mammata* | Borrero-Pérez et al., 2011 | 1 | 0,0417 | 100 | 100000 | 0,99 | 0 | 100 | 100000 |
| *Ophioderma longicauda* | Weber et al., 2015[1] | 0,05 | 0,415 | 500 | 100000 | 0,56 | 0,1217 | 500 | 100000 |
| *Ophioderma longicauda* | Weber et al., 2015[2] | 0,01 | 0,449 | 150 | 100000 | 0,11 | 0,1647 | 150 | 10 |
| *Paracentrotus lividus* | Penant et al., 2013 | 0,06 | 0,454 | 80 | 100000 | 0,49 | 0,0012 | 80 | 1000 |
| *Paracentrotus lividus* | Paterno et al., 2017 | 0,89 | 0,008 | 40 | 10000 | 0,9 | 0,0001 | 40 | 1000 |
| *Paracentrotus lividus* | Carreras et al., 2020[3] | 0,4 | 0,036 | 20 | 100000 | 0,8 | 0 | 20 | 100000 |
| *Paracentrotus lividus* | Carreras et al., 2020[4] | 0,63 | 0,008 | 5 | 100000 | 0,92 | 0 | 5 | 100000 |
| *Apogon imberbis* | Muths et al., 2015 | 0,65 | 0,25 | 5 | 10 | 0,47 | 0,2004 | 5 | 10 |
| *Coris julis* | Fruciano et al., 2011 | 0,4 | 0,049 | 80 | 100000 | 0,99 | 0,0479 | 80 | 10000 |
| *Diplodus sargus* | González-Wangüemert et al., 2010 | 0,32 | 0,2167 | 10 | 10000 | 0,44 | 0,0204 | 10 | 10 |
| *Diplodus vulgaris* | Kaouèche et al., 2013 | 0,34 | 0,1306 | 5 | 100000 | 0,13 | 0,1686 | 5 | 100000 |
| *Epinephelus marginatus* | Schunter et al., 2011 | 0,24 | 0,163 | 10 | 100000 | 0,49 | 0,0491 | 10 | 1000 |
| *Lithognathus mormyrus* | Hammami et al., 2007 | 0,84 | 0,0833 | 5 | 100000 | 0,75 | 0,0058 | 5 | 100000 |
| *Merluccius merluccius* | Milano et al., 2014 | 0,28 | 0,001 | 40 | 10 | 0,2 | 0,011 | 40 | 100000 |
| *Mugil cephalus* | Durand et al., 2013 | 0,61 | 0,002 | 20 | 100000 | 0,72 | 0 | 20 | 100000 |
| *Mullus barbartus* | Maggio et al., 2009 | 0,1 | 0,164 | 5 | 10 | 0,1 | 0,1825 | 5 | 1000 |

| Species | Study | Mantel *r* | Mantel p-value | Mantel opt M | Mantel opt alpha | MLPE $R^2$ | MLPE p-value | MLPE opt M | MLPE opt alpha |
|---|---|---|---|---|---|---|---|---|---|
| *Mullus surmuletus* | Galarza et al., 2009 | 0,34 | 0,1986 | 500 | 100 | 0,25 | 0,1794 | 500 | 10000 |
| *Mullus surmuletus* | Dalongeville et al., 2018 | 0,21 | 0,017 | 60 | 100000 | 0,67 | 0 | 60 | 100000 |
| *Oblada melanura* | Gkafas et al., 2013 | 0,01 | 0,447 | 500 | 10 | 0,04 | 0,2833 | 500 | 10000 |
| *Oblada melanura* | Calò et al., 2016 | 0,21 | 0,113 | 1 | 10000 | 0,77 | 0,0084 | 1 | 100000 |
| *Pagellus erythrinus* | Fassatoui et al., 2009 | 0,46 | 0,0389 | 1 | 100000 | 0,23 | 0,0534 | 1 | 100000 |
| *Serranus cabrilla* | Schunter et al., 2011 | 0,2 | 0,024 | 1 | 100 | 0,88 | 0 | 1 | 10 |
| *Solea solea* | Bahri-Sfar et al., 2011 | 0,9 | 0,005 | 20 | 10000 | 0,86 | 0 | 20 | 10000 |
| *Solea solea* | Garoia et al., 2007 | 0,49 | 0,1667 | 5 | 10 | 0,47 | 0,0686 | 5 | 100000 |
| *Sparus aurata* | Franchini et al., 2012 | 0,41 | 0,043 | 400 | 100 | 0,43 | 0 | 400 | 10 |
| *Symphodus tinca* | Carreras et al., 2017 | 0,35 | 0,0764 | 5 | 10 | 0,52 | 0,1206 | 5 | 100000 |
| *Cerastoderma edule* | Sromek et al., 2019 | 0,66 | 0,018 | 5 | 100000 | 0,67 | 0,0002 | 5 | 100000 |
| *Chiton olivaceus* | Villamor et al., 2014 | 0,82 | 0,1667 | 500 | 10000 | 0,71 | 0,01 | 500 | 1000 |
| *Hexaplex trunculus* | Villamor et al., 2014 | 0,94 | 0,0833 | 200 | 100000 | 0,88 | 0,0023 | 200 | 10000 |
| *Hexaplex trunculus* | Marzouk et al., 2017[5] | 0,25 | 0,093 | 150 | 10 | 0,49 | 0,0984 | 150 | 100000 |
| *Hexaplex trunculus* | Marzouk et al., 2017[6] | 0,31 | 0,048 | 300 | 10 | 0,52 | 0,1023 | 300 | 10 |
| *Mytilus galloprovincialis* | Diz and Presa, 2008 | 0,41 | 0,006 | 1 | 1000 | 0,28 | 0,0245 | 1 | 1000 |
| *Ostrea edulis* | Launey et al., 2002 | 0,71 | 0,0333 | 40 | 1000 | 0,59 | 0,0059 | 40 | 10000 |
| *Patella caerulea* | Villamor et al., 2014 | 0,91 | 0,0153 | 40 | 100000 | 0,86 | 0 | 40 | 100000 |
| *Patella rustica* | Sá-Pinto et al., 2012 | 0,34 | 0,0389 | 5 | 10 | 0,45 | 0,1975 | 5 | 100000 |
| *Patella ulyssiponensis* | Sá-Pinto et al., 2012 | 0,64 | 0,05 | 80 | 100000 | 0,88 | 0,0016 | 80 | 100000 |
| *Phorcus turbinatus* | Villamor et al., 2014 | 0,95 | 0,3333 | 40 | 100000 | 1 | 0 | 40 | 100000 |
| *Ruditapes decussatus* | Gharbi et al., 2011 | 0,41 | 0,006 | 5 | 100000 | 0,17 | 0,0073 | 5 | 100000 |
| *Spondylus spinosus* | Shabtay et al., 2014 | 0,38 | 0,1667 | 5 | 100000 | 0,45 | 0,4206 | 5 | 100000 |
| *Cymodocea nodosa* | Alberto et al., 2008 | 0,75 | 0,011 | 10 | 10000 | 0,77 | 0 | 10 | 100000 |
| *Posidonia oceanica* | Arnaud-Haond et al., 2007 | 0,58 | 0,001 | 40 | 10000 | 0,58 | 0 | 40 | 10000 |

*Supplementary Table 9:* ***Accuracy of our multi-generation implicit dispersal models in explaining observed genetic structure across the meta-analysis.*** *Mantel r and MLPE linear mixed model R² between $F_{st}^{mod}$ and $F_{st}^{obs}/(1-F_{st}^{obs})$ and theirs associated p-value are indexed for all the studies. The "opt alpha" stands for the alpha value of the reciprocal transformation that minimizes the AIC estimator (see Supplementary Figure 5). The "opt M" stands for the number of generations that minimizes the AIC estimator (see Supplementary Figure 6). Note that (i) Weber et al., 2015 use SNPs marker ([1]) and mtDNA marker ([2]), (ii) Carrera et al., 2019 considers all the loci ([3]) and only the Mediterranean outliers loci ([4]), and (iii) Marzouk et al., 2017 use SNPs marker ([5]) and mtDNA marker ([6]). Significant studies (p-values*) are highlighted in grey. Source data are provided as a Source Data file.*

| Species | Study | Mantel *r* | Mantel p-value | Mantel opt M | Mantel opt alpha | MLPE $R^2$ | MLPE p-value | MLPE opt M | MLPE opt alpha |
|---|---|---|---|---|---|---|---|---|---|
| *Cystoseira amentacea* | Susini et al., 2007 | 0,81 | 0,0833 | 1 | 100000 | 0,74 | 0,0194 | 1 | 100000 |
| *Astroides calycularis* | Casado-Amezua et al., 2012 | 0,67 | 0,005 | 500 | 100000 | 0,79 | 0 | 500 | 100000 |
| *Corallium rubrum* | Aurelle et al., 2011 | 0,71 | 0,001 | 40 | 10000 | 0,54 | 0 | 40 | 100000 |
| *Corallium rubrum* | Costantini et al., 2013 | 0,51 | 0,1 | 1 | 10 | 0,27 | 0,0928 | 1 | 10 |
| *Eunicella cavolinii* | Masmoudi et al., 2016 | 0,88 | 0,001 | 300 | 1000 | 0,78 | 0 | 300 | 10000 |
| *Leptopsammia pruvoti* | Boscari et al., 2019 | 0,6 | 0,002 | 40 | 10 | 0,4 | 0 | 40 | 100000 |
| *Botryllus schlosseri* | Reem et al., 2017 | 0,36 | 0,006 | 500 | 100000 | 0,11 | 0,0132 | 500 | 100000 |
| *Halocynthia papillosa* | Villamor et al., 2014 | 0,9 | 0,1667 | 20 | 100 | 1 | 0 | 20 | 10 |
| *Microcosmus squamiger* | Ordóñez et al., 2013 | -0,07 | 0,6667 | 1 | 10 | 0 | 0,7982 | 1 | 10 |
| *Pycnoclavella communis* | Pérez-Portela et al., 2007 | -0,27 | 0,5833 | 500 | 100000 | 0,2 | 0,2879 | 500 | 10 |
| *Carcinus aestuarii* | Schiavina et al., 2014 | 0,98 | 0,022 | 40 | 10000 | 0,97 | 0 | 40 | 10000 |
| *Melicertus kerathurus* | Arculeo et al., 2010 | 0,14 | 0,32 | 40 | 10 | 0,07 | 0,113 | 40 | 10000 |
| *Melicertus kerathurus* | Zitari-Chatti et al., 2007 | 0,19 | 0,206 | 10 | 10 | 0,04 | 0,2453 | 10 | 10 |
| *Pachygrapsus marmoratus* | Fratini et al., 2013 | 0,19 | 0,142 | 1 | 10 | 0,04 | 0,3206 | 1 | 10 |
| *Palinurus elephas* | Palero et al., 2011 | 0,26 | 0,4333 | 20 | 100000 | 0,27 | 0,0909 | 20 | 10 |

| Species | Study | Mantel *r* | Mantel p-value | Mantel opt M | Mantel opt alpha | MLPE $R^2$ | MLPE p-value | MLPE opt M | MLPE opt alpha |
|---|---|---|---|---|---|---|---|---|---|
| *Spongia officinalis* | Dailianis et al., 2011 | 0,63 | 0,006 | 500 | 10000 | 0,75 | 0 | 500 | 100000 |
| *Astropecten aranciacus* | Zulliger et al., 2009 | 0,33 | 0,043 | 10 | 100000 | 0,25 | 0,0567 | 10 | 100000 |
| *Holothuria mammata* | Borrero-Pérez et al., 2011 | 0,99 | 0,0833 | 40 | 100000 | 1 | 0 | 40 | 100000 |
| *Ophioderma longicauda* | Weber et al., 2015[1] | 0,05 | 0,307 | 500 | 100000 | 0,56 | 0,0957 | 500 | 100000 |
| *Ophioderma longicauda* | Weber et al., 2015[2] | 0,02 | 0,46 | 500 | 100000 | 0,11 | 0,1507 | 500 | 100 |
| *Paracentrotus lividus* | Penant et al., 2013 | 0,11 | 0,467 | 40 | 100000 | 0,5 | 0,0008 | 40 | 100000 |
| *Paracentrotus lividus* | Paterno et al., 2017 | 0,88 | 0,004 | 40 | 10000 | 0,81 | 0,0251 | 40 | 10000 |
| *Paracentrotus lividus* | Carreras et al., 2020[3] | 0,39 | 0,045 | 20 | 100000 | 0,8 | 0 | 20 | 100000 |
| *Paracentrotus lividus* | Carreras et al., 2020[4] | 0,6 | 0,011 | 20 | 100000 | 0,93 | 0 | 20 | 1000 |
| *Apogon imberbis* | Muths et al., 2015 | -0,65 | 1 | 1 | 10 | 0,47 | 0,2004 | 1 | 10 |
| *Coris julis* | Fruciano et al., 2011 | 0,62 | 0,05 | 400 | 10000 | 0,99 | 0,0005 | 400 | 100000 |
| *Diplodus sargus* | González-Wangüemert et al., 2010 | 0,31 | 0,1333 | 10 | 10000 | 0,11 | 0,3129 | 10 | 100000 |
| *Diplodus vulgaris* | Kaouèche et al., 2013 | 0,3 | 0,1167 | 1 | 10000 | 0,1 | 0,2328 | 1 | 1000 |
| *Epinephelus marginatus* | Schunter et al., 2011 | 0,24 | 0,137 | 40 | 10 | 0,49 | 0,0497 | 40 | 1000 |
| *Lithognathus mormyrus* | Hammami et al., 2007 | 0,71 | 0,0417 | 5 | 10 | 0,63 | 0,0218 | 5 | 100000 |
| *Merluccius merluccius* | Milano et al., 2014 | 0,3 | 0,014 | 500 | 10 | 0,2 | 0,0037 | 500 | 100000 |
| *Mugil cephalus* | Durand et al., 2013 | 0,68 | 0,02 | 20 | 100000 | 0,73 | 0 | 20 | 10000 |
| *Mullus barbartus* | Maggio et al., 2009 | 0,14 | 0,109 | 5 | 1000 | 0,17 | 0,0921 | 5 | 100 |

| Species | Study | Mantel *r* | Mantel p-value | Mantel opt M | Mantel opt alpha | MLPE $R^2$ | MLPE p-value | MLPE opt M | MLPE opt alpha |
|---|---|---|---|---|---|---|---|---|---|
| *Mullus surmuletus* | Galarza et al., 2009 | 0,24 | 0,3194 | 1 | 10 | 0,42 | 0,1082 | 1 | 100000 |
| *Mullus surmuletus* | Dalongeville et al., 2018 | 0,34 | 0,004 | 500 | 100 | 0,67 | 0 | 500 | 100000 |
| *Oblada melanura* | Gkafas et al., 2013 | 0,1 | 0,24 | 100 | 10 | 0,04 | 0,3129 | 100 | 10000 |
| *Oblada melanura* | Calò et al., 2016 | 0,3 | 0,021 | 20 | 10 | 0,75 | 0,0091 | 20 | 100000 |
| *Pagellus erythrinus* | Fassatoui et al., 2009 | 0,46 | 0,0389 | 20 | 10 | 0,65 | 0,021 | 20 | 100000 |
| *Serranus cabrilla* | Schunter et al., 2011 | 0,21 | 0,047 | 1 | 1000 | 0,88 | 0 | 1 | 10 |
| *Solea solea* | Bahri-Sfar et al., 2011 | 0,9 | 0,003 | 10 | 100000 | 0,83 | 0 | 10 | 100000 |
| *Solea solea* | Garoia et al., 2007 | 0,49 | 0,1667 | 5 | 10 | 0,49 | 0,0619 | 5 | 100000 |
| *Sparus aurata* | Franchini et al., 2012 | 0,3 | 0,046 | 10 | 10 | 0,36 | 0,0003 | 10 | 1000 |
| *Symphodus tinca* | Carreras et al., 2017 | 0,61 | 0,0194 | 20 | 100000 | 0,45 | 0,0277 | 20 | 100000 |
| *Cerastoderma edule* | Sromek et al., 2019 | 0,94 | 0,004 | 10 | 100000 | 0,96 | 0 | 10 | 10000 |
| *Chiton olivaceus* | Villamor et al., 2014 | 0,83 | 0,1667 | 150 | 10 | 0,72 | 0,0091 | 150 | 10 |
| *Hexaplex trunculus* | Villamor et al., 2014 | 0,94 | 0,0833 | 100 | 10000 | 0,88 | 0,0022 | 100 | 100000 |
| *Hexaplex trunculus* | Marzouk et al., 2017[5] | 0,26 | 0,087 | 500 | 10 | 0,48 | 0,1073 | 500 | 100 |
| *Hexaplex trunculus* | Marzouk et al., 2017[6] | 0,28 | 0,043 | 400 | 100000 | 0,52 | 0,1092 | 400 | 10 |
| *Mytilus galloprovincialis* | Diz and Presa, 2008 | 0,37 | 0,012 | 1 | 1000 | 0,43 | 0,0264 | 1 | 10 |
| *Ostrea edulis* | Launey et al., 2002 | 0,65 | 0,0333 | 150 | 10 | 0,61 | 0,0142 | 150 | 10 |
| *Patella caerulea* | Villamor et al., 2014 | 0,97 | 0,0167 | 60 | 10000 | 0,95 | 0 | 60 | 10000 |
| *Patella rustica* | Sá-Pinto et al., 2012 | 0,35 | 0,0208 | 5 | 10 | 0,44 | 0,0583 | 5 | 100000 |
| *Patella ulyssiponensis* | Sá-Pinto et al., 2012 | 0,76 | 0,025 | 100 | 100000 | 0,86 | 0,0009 | 100 | 100000 |
| *Phorcus turbinatus* | Villamor et al., 2014 | 0,99 | 0,0417 | 150 | 10 | 1 | 0 | 150 | 10 |
| *Ruditapes decussatus* | Gharbi et al., 2011 | 0,48 | 0,005 | 5 | 100000 | 0,22 | 0,0009 | 5 | 1000 |
| *Spondylus spinosus* | Shabtay et al., 2014 | 0,36 | 0,3333 | 1 | 10 | 0,45 | 0,4516 | 1 | 10 |
| *Cymodocea nodosa* | Alberto et al., 2008 | 0,8 | 0,004 | 5 | 100000 | 0,77 | 0 | 5 | 10000 |
| *Posidonia oceanica* | Arnaud-Haond et al., 2007 | 0,57 | 0,001 | 40 | 1000 | 0,58 | 0 | 40 | 100000 |

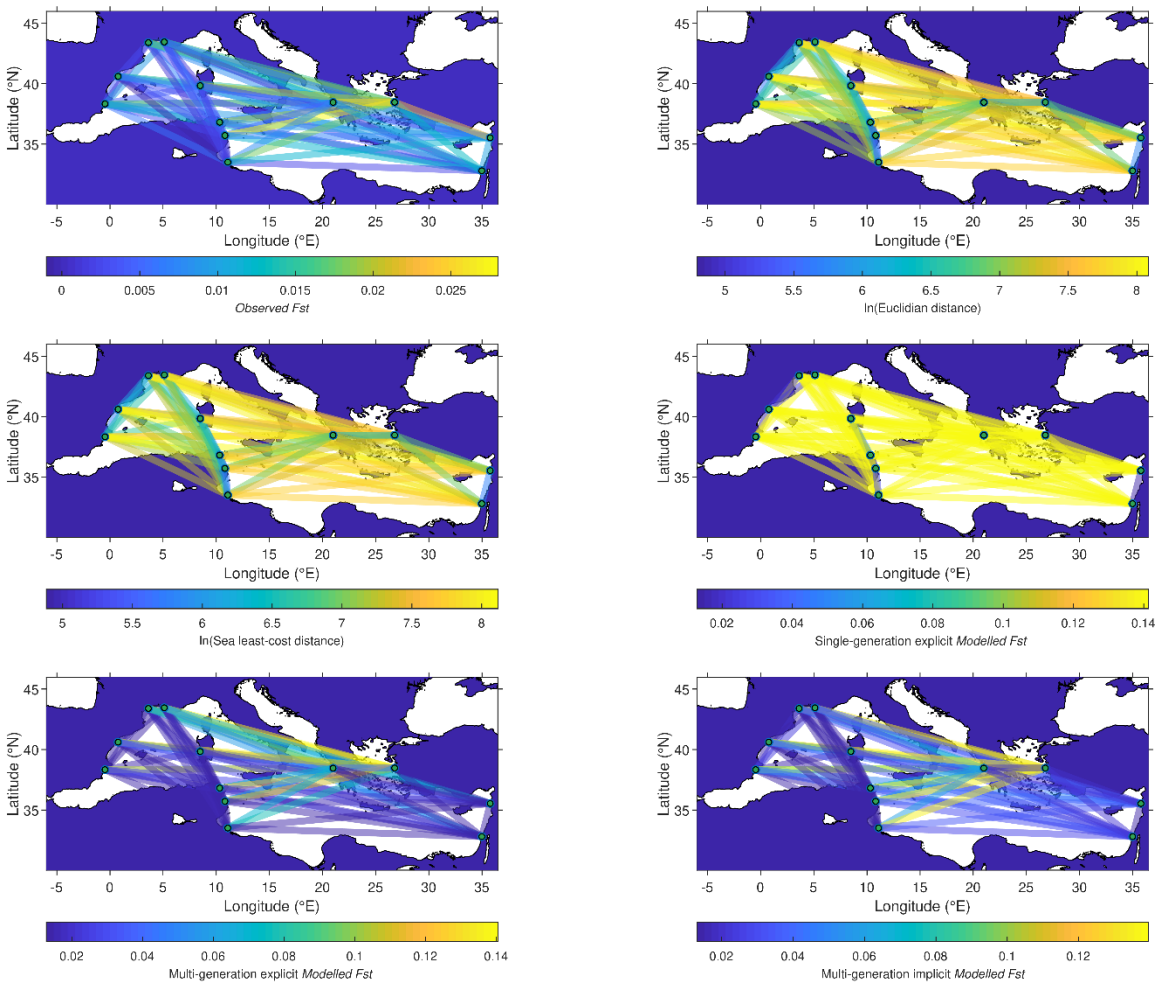


*Supplementary Figure 8:* ***Network representation of*** **observed** ***and*** **modelled** ***genetic structures*** *for* Mugil cephalus*; Durand et al., (2013).* ***a*** $F_{st}^{obs}$ *values,* ***b*** $\log_e$*(Euclidian distance),* ***c*** $\log_e$*(Sea least-cost distance),* ***d*** *single-generation explicit* $F_{st}^{mod}$*,* ***e*** *multi-generation explicit* $F_{st}^{mod}$ *and* ***f*** *multi-generation implicit* $F_{st}^{mod}$*. Similar plots made for each study of our meta-analysis can be viewed at: https://nuage.osupytheas.fr/s/3fj5TidxC4A6Kax*

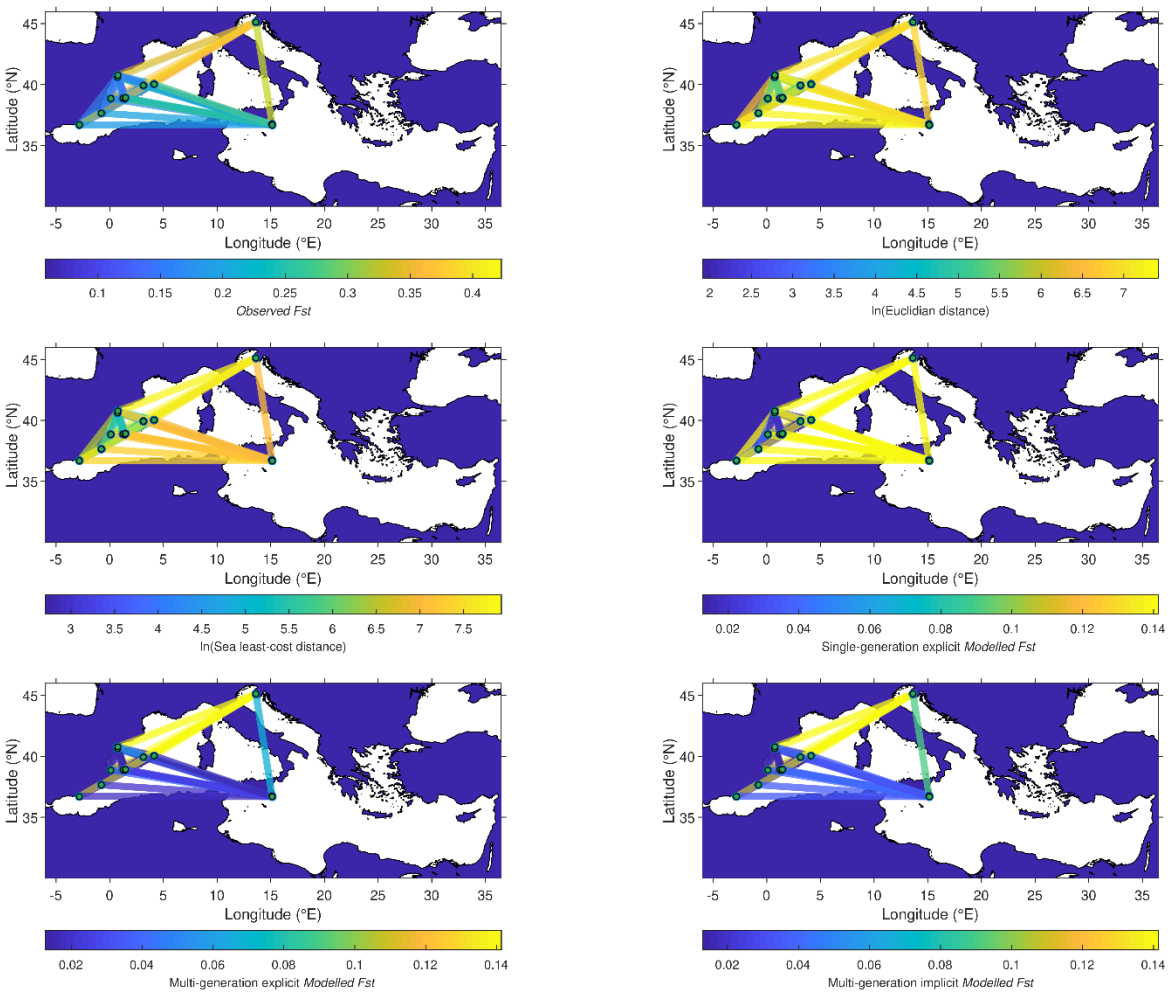


*Supplementary Figure 9:* ***Network representation of*** **observed** ***and*** **modelled** ***genetic structures*** *for* Cymodocea nodosa*; Alberto et al., (2008).* ***a*** $F_{st}^{obs}$ *values,* ***b*** *log$_e$(Euclidian distance),* ***c*** *log$_e$(Sea least-cost distance),* ***d*** *single-generation explicit* $F_{st}^{mod}$*,* ***e*** *multi-generation explicit* $F_{st}^{mod}$ *and* ***f*** *multi-generation implicit* $F_{st}^{mod}$*. Similar plots made for each study of our meta-analysis can be viewed at: https://nuage.osupytheas.fr/s/3fj5TidxC4A6Kax*

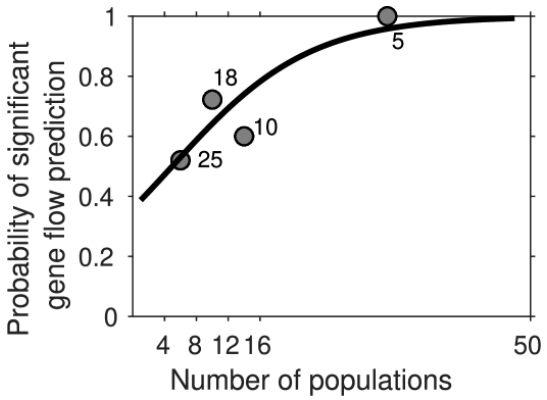


*Supplementary Figure 10:* ***Sensitivity of the multi-generation implicit dispersal model.*** *Probability of significant gene flow predictions (i.e. probability to obtain significant R² between* $F_{st}^{mod}$ *and* $F_{st}^{obs}/(1-F_{st}^{obs})$*) as a function of the number of sampled populations binned in four categories (4-8, 8-12,12-16 and > 16 populations sampled). The thick black line represents the logit model (R² = 0.72***). Source data are provided as a Source Data file.*

# Supplementary Methods 6: Statistical analyses on the impact of species and study characteristics on MLPE linear mixed model predictions

*Supplementary Table 10:* ***Sensitivity of the MLPE linear mixed model predictions of the multi-generation implicit dispersal model for the 58 population genetic studies included in the meta-analysis.*** *We test the sensitivity of the Species characteristics (taxa, PLD and spawning season) and study characteristics (Marker, $F_{st}$ range, Number of populations sampled and Spatial Sampling Representativeness) on* ***a*** *$R^2$ and* ***b*** *p-values either with ANOVA or a linear regression (after a log10 transformation of $R^2$ and p-values). Source data are provided as a Source Data file.*

a

| | **MLPE linear mixed model $R^2$** | | | | |
|---|---|---|---|---|---|
| | *Characteristics* | *Statistic method* | *p-value* | *$R^2$* | *β slope* |
| Species | Taxa | ANOVA | 0.8385 | NaN | NaN |
| | PLD | ANOVA | 0.1362 | NaN | NaN |
| | Spawning season | ANOVA | 0.9624 | NaN | NaN |
| Study | Marker | ANOVA | 0.1832 | NaN | NaN |
| | $F_{st}$ range | log Regression | 0.8966 | 0.0005 | 0.0097 |
| | Nbr of populations | log Regression | 0.0988 | 0.0759 | -0.23 |
| | $D_{btw}$ | log Regression | 0.9792 | 0 | 0.0056 |

b

| | **MLPE linear mixed model p-value** | | | | |
|---|---|---|---|---|---|
| | *Characteristics* | *Statistic method* | *p-value* | *$R^2$* | *β slope* |
| Species | Taxa | ANOVA | 0.1453 | NaN | NaN |
| | PLD | ANOVA | 0.2092 | NaN | NaN |
| | Spawning season | ANOVA | 0.846 | NaN | NaN |
| Study | Marker | ANOVA | 0.6118 | NaN | NaN |
| | $F_{st}$ range | log Regression | 0.0009 | 0.1788 | -10.0746 |
| | Nbr of populations | log Regression | 0 | 0.403 | -31.6825 |
| | $D_{btw}$ | log Regression | 0.9755 | 0 | -0.3246 |

# Supplementary References:


Alberto, F., Massa, S., Manent, P., Diaz-Almela, E., Arnaud-Haond, S., Duarte, C.M., Serrão, E.A., 2008. Genetic differentiation and secondary contact zone in the seagrass Cymodocea nodosa across the Mediterranean–Atlantic transition region. J. Biogeogr. 35, 1279–1294. https://doi.org/10.1111/j.1365-2699.2007.01876.x

Arculeo, M., Pellerito, R., Bonhomme, F., 2010. Isolation and use of microsatellite loci in *Melicertus kerathurus* (Crustacea, Penaeidae). Aquat. Living Resour. 23, 103–107. https://doi.org/10.1051/alr/2010008

Arnaud-Haond, S., Migliaccio, M., Diaz-Almela, E., Teixeira, S., Van De Vliet, M.S., Alberto, F., Procaccini, G., Duarte, C.M., Serrão, E.A., 2007. Vicariance patterns in the Mediterranean Sea: east–west cleavage and low dispersal in the endemic seagrass *Posidonia oceanica*. J. Biogeogr. 34, 963–976. https://doi.org/10.1111/j.1365-2699.2006.01671.x

Aurelle, D., Ledoux, J.-B., Rocher, C., Borsa, P., Chenuil, A., Féral, J.-P., 2011. Phylogeography of the red coral (Corallium rubrum): inferences on the evolutionary history of a temperate gorgonian. Genetica 139, 855–869. https://doi.org/10.1007/s10709-011-9589-6

Baeta, M., Galimany, E., Ramón, M., 2016. Growth and reproductive biology of the sea star Astropecten aranciacus (Echinodermata, Asteroidea) on the continental shelf of the Catalan Sea (northwestern Mediterranean). Helgol. Mar. Res. 70, 1. https://doi.org/10.1186/s10152-016-0453-z

Bahri-Sfar, L., Kaouèche, M., Haffani, M., Ouanes, K., Ben Hassine, O.K., 2011. Genetic population structure of the common sole, *Solea solea* Linnaeus, 1758 (Pisces, Pleuronectiformes) along the southern shores of the Mediterranean Sea (Tunisian coasts). Ital. J. Zool. 78, 157–167. https://doi.org/10.1080/11250003.2010.532513

Baldacconi, R., Nonnis-Marzano, C., Gaino, E., Corriero, G., 2007. Sexual reproduction, larval development and release in Spongia oYcinalis L. (Porifera, Demospongiae) from the Apulian coast. Mar Biol 11.

Bernardi, G., Azzurro, E., Golani, D., Miller, M.R., 2016. Genomic signatures of rapid adaptive evolution in the bluespotted cornetfish, a Mediterranean Lessepsian invader. Mol. Ecol. 25, 3384–3396. https://doi.org/10.1111/mec.13682

Bierne, N., Launey, S., Naciri-Graven, Y., Bonhomme, F., 1998. Early Effect of Inbreeding as Revealed by Microsatellite Analyses on Ostrea edulis Larvae. Genetics 148, 1893–1906.

Borrero-Pérez, G.H., González-Wangüemert, M., Marcos, C., Pérez-Ruzafa, A., 2011. Phylogeography of the Atlanto-Mediterranean sea cucumber Holothuria (Holothuria) mammata: the combined effects of historical processes and current oceanographical pattern: PHYLOGEOGRAPHY OF HOLOTHURIA MAMMATA. Mol. Ecol. 20, 1964–1975. https://doi.org/10.1111/j.1365-294X.2011.05068.x

Boscari, E., Abbiati, M., Badalamenti, F., Bavestrello, G., Benedetti-Cecchi, L., Cannas, R., Cau, A., Cerrano, C., Chimienti, G., Costantini, F., Fraschetti, S., Ingrosso, G., Marino, I.A.M., Mastrototaro, F., Papetti, C., Paterno, M., Ponti, M., Zane, L., Congiu, L., 2019. A population genomics insight by 2b-RAD reveals populations' uniqueness along the Italian coastline in *Leptopsammia pruvoti* (Scleractinia, Dendrophylliidae). Divers. Distrib. 25, 1101–1117. https://doi.org/10.1111/ddi.12918

Boyden, C.R., Russell, P.J.C., 1972. The Distribution and Habitat Range of the Brackish Water Cockle (Cardium (Cerastoderma) glaucum) in the British Isles. J. Anim. Ecol. 41, 719. https://doi.org/10.2307/3205

Caceres-Martinez, J., Robledo, J., Figueras, A., 1993. Settlement of mussels Mytilus galloprovincialis on an exposed rocky shore in Ria de Vigo, NW Spain. Mar. Ecol. Prog. Ser. 93, 195–198. https://doi.org/10.3354/meps093195

Calò, A., Muñoz, I., Pérez-Ruzafa, Á., Vergara-Chen, C., García-Charton, J.A., 2016. Spatial genetic structure in the saddled sea bream (Oblada melanura [Linnaeus, 1758]) suggests multi-scaled patterns of connectivity between protected and unprotected areas in the Western Mediterranean Sea. Fish. Res. 176, 30–38. https://doi.org/10.1016/j.fishres.2015.12.001

Cánovas-Molina, A., Montefalcone, M., Bavestrello, G., Masmoudi, M.B., Haguenauer, A., Hammami, P., Chaoui, L., Kara, M.H., Aurelle, D., 2018. From depth to regional spatial genetic differentiation of Eunicella cavolini in the NW Mediterranean. C. R. Biol. 341, 421–432. https://doi.org/10.1016/j.crvi.2018.09.002

Carlton, J.T., Cohen, A.N., 2003. Episodic global dispersal in shallow water marine organisms: the case history of the European shore crabs *Carcinus maenas* and *C. aestuarii*: Episodic global invasion patterns in shore crabs. J. Biogeogr. 30, 1809–1820. https://doi.org/10.1111/j.1365-2699.2003.00962.x

Carreras, C., García-Cisneros, A., Wangensteen, O.S., Ordóñez, V., Palacín, C., Pascual, M., Turon, X., 2020. East is East and West is West: Population genomics and hierarchical analyses reveal genetic structure and adaptation footprints in the keystone species *Paracentrotus lividus* (Echinoidea). Divers. Distrib. 26, 382–398. https://doi.org/10.1111/ddi.13016

Carreras, C., Ordóñez, V., Zane, L., Kruschel, C., Nasto, I., Macpherson, E., Pascual, M., 2017. Population genomics of an endemic Mediterranean fish: differentiation by fine scale dispersal and adaptation. Sci. Rep. 7, 43417. https://doi.org/10.1038/srep43417

Casado-Amezúa, P., Goffredo, S., Templado, J., Machordom, A., 2012. Genetic assessment of population structure and connectivity in the threatened Mediterranean coral *Astroides calycularis* (Scleractinia, Dendrophylliidae) at different spatial scales: GENETIC STRUCTURE IN *ASTROIDES CALYCULARIS*. Mol. Ecol. 21, 3671–3685. https://doi.org/10.1111/j.1365-294X.2012.05655.x

Coelho, M.A.G., Lasker, H.R., 2016. Larval Dispersal and Population Connectivity in Anthozoans, in: Goffredo, S., Dubinsky, Z. (Eds.), The Cnidaria, Past, Present and Future: The World of Medusa and Her Sisters. Springer International Publishing, Cham, pp. 291–315. https://doi.org/10.1007/978-3-319-31305-4_19

Costantini, F., Carlesi, L., Abbiati, M., 2013. Quantifying Spatial Genetic Structuring in Mesophotic Populations of the Precious Coral Corallium rubrum. PLoS ONE 8, e61546. https://doi.org/10.1371/journal.pone.0061546

Courant, R., Friedrichs, K., Lewy, H., 1928. Über die partiellen Differenzengleichungen der mathematischen Physik. Math. Ann. 100, 32–74. https://doi.org/10.1007/BF01448839

Cuesta, J.A., Rodríguez, A., 2000. Zoeal stages of the intertidal crab Pachygrapsus marmoratus (Fabricius, 1787) (Brachyura, Grapsidae) reared in the laboratory. Hydrobiologia 436, 119–130. https://doi.org/10.1023/A:1026576614590

Dailianis, T., Tsigenopoulos, C.S., Dounas, C., Voultsiadou, E., 2011. Genetic diversity of the imperilled bath sponge Spongia officinalis Linnaeus, 1759 across the Mediterranean Sea: patterns of population differentiation and implications for taxonomy and conservation: GENETIC DIVERSITY OF SPONGIA OFFICINALIS. Mol. Ecol. 20, 3757–3772. https://doi.org/10.1111/j.1365-294X.2011.05222.x

Dalongeville, A., Benestan, L., Mouillot, D., Lobreaux, S., Manel, S., 2018. Combining six genome scan methods to detect candidate genes to salinity in the Mediterranean striped red mullet (Mullus surmuletus). BMC Genomics 19, 217. https://doi.org/10.1186/s12864-018-4579-z

Di Franco, A., Guidetti, P., 2011. Patterns of variability in early-life traits of fishes depend on spatial scale of analysis. Biol. Lett. 7, 454–456. https://doi.org/10.1098/rsbl.2010.1149

Di Franco, A., Qian, K., Calò, A., Di Lorenzo, M., Planes, S., Guidetti, P., 2013. Patterns of variability in early life traits of a Mediterranean coastal fish. Mar. Ecol. Prog. Ser. 476, 227–235.

Diz, A.P., Presa, P., 2008. Regional patterns of microsatellite variation in Mytilus galloprovincialis from the Iberian Peninsula. Mar. Biol. 154, 277–286. https://doi.org/10.1007/s00227-008-0921-3

Durand, J., Blel, H., Shen, K., Koutrakis, E., Guinand, B., 2013. Population genetic structure of Mugil cephalus in the Mediterranean and Black Seas: a single mitochondrial clade and many nuclear barriers. Mar. Ecol. Prog. Ser. 474, 243–261. https://doi.org/10.3354/meps10080

Ernande, B., Clobert, J., McCombie, H., Boudry, P., 2003. Genetic polymorphism and trade-offs in the early life-history strategy of the Pacific oyster, Crassostrea gigas (Thunberg, 1795): a quantitative genetic study: Early life-history strategy in a marine bivalve. J. Evol. Biol. 16, 399–414. https://doi.org/10.1046/j.1420-9101.2003.00543.x

Fassatoui, C., Mdelgi, E., Romdhane, M.S., 2009. A preliminary investigation of allozyme genetic variation and population structure in common pandora (Pagellus erythrinus, Sparidae) from Tunisian and Libyan coasts. Ichthyol. Res. 56, 301–307. https://doi.org/10.1007/s10228-008-0094-6

Félix-Hackradt, F.C., Hackradt, C.W., Pérez-Ruzafa, Á., García-Charton, J.A., 2013. Discordant patterns of genetic connectivity between two sympatric species, Mullus barbatus (Linnaeus, 1758) and Mullus surmuletus (Linnaeus, 1758), in south-western Mediterranean Sea. Mar. Environ. Res. 92, 23–34. https://doi.org/10.1016/j.marenvres.2013.08.008

Franchini, P., Sola, L., Crosetti, D., Milana, V., Rossi, A.R., 2012. Low levels of population genetic structure in the gilthead sea bream, Sparus aurata, along the coast of Italy. ICES J. Mar. Sci. 69, 41–50. https://doi.org/10.1093/icesjms/fsr175

Fratini, S., Ragionieri, L., Cutuli, G., Vannini, M., Cannicci, S., 2013. Pattern of genetic isolation in the crab Pachygrapsus marmoratus within the Tuscan Archipelago (Mediterranean Sea). Mar. Ecol. Prog. Ser. 478, 173–183. https://doi.org/10.3354/meps10247

Fruciano, C., Tigano, C., Ferrito, V., 2011. Geographical and morphological variation within and between colour phases in *Coris julis* (L. 1758), a protogynous marine fish: GEOGRAPHICAL VARIATION IN A PROTOGYNOUS FISH. Biol. J. Linn. Soc. 104, 148–162. https://doi.org/10.1111/j.1095-8312.2011.01700.x

Gaino, E., Baldacconi, R., Corriero, G., 2007. Post-larval development of the commercial sponge Spongia officinalis L. (Porifera, Demospongiae). Tissue Cell 39, 325–334. https://doi.org/10.1016/j.tice.2007.06.006

Galarza, J.A., Turner, G.F., Macpherson, E., Rico, C., 2009. Patterns of genetic differentiation between two co-occurring demersal species: the red mullet (Mullus barbatus) and the striped red mullet (Mullus surmuletus). Can. J. Fish. Aquat. Sci. 66, 1478–1490. https://doi.org/10.1139/F09-098

Garoia, F., Guarniero, I., Grifoni, D., Marzola, S., Tinti, F., 2007. Comparative analysis of AFLPs and SSRs efficiency in resolving population genetic structure of Mediterranean Solea vulgaris: EFFICIENCY OF SSRs AND AFLPs IN FISH POPULATION ANALYSIS. Mol. Ecol. 16, 1377–1387. https://doi.org/10.1111/j.1365-294X.2007.03247.x

Gharbi, A., Zitari-Chatti, R., Van Wormhoudt, A., Dhraief, M.N., Denis, F., Said, K., Chatti, N., 2011. Allozyme Variation and Population Genetic Structure in the Carpet Shell Clam Ruditapes decussatus Across the Siculo-Tunisian Strait. Biochem. Genet. 49, 788–805. https://doi.org/10.1007/s10528-011-9450-8

Gkafas, G., Tsigenopoulos, C., Magoulas, A., Panagiotaki, P., Vafidis, D., Mamuris, Z., Exadactylos, A., 2013. Population subdivision of saddled seabream Oblada melanura in the Aegean Sea revealed by genetic and morphometric analyses. Aquat. Biol. 18, 69–80. https://doi.org/10.3354/ab00490

Goffredo, S., Airi, V., Radetić, J., Zaccanti, F., 2006. Sexual reproduction of the solitary sunset cup coral Leptopsammia pruvoti (Scleractinia, Dendrophylliidae) in the Mediterranean. 2. Quantitative aspects of the annual reproductive cycle. Mar. Biol. 148, 923–931. https://doi.org/10.1007/s00227-005-0137-8

Goffredo, S., Gasparini, G., Marconi, G., Putignano, M.T., Pazzini, C., Zaccanti, F., 2010. Gonochorism and planula brooding in the Mediterranean endemic orange coral Astroides calycularis (Scleractinia: Dendrophylliidae). Morphological aspects of gametogenesis and ontogenesis. Mar. Biol. Res. 6, 421–436. https://doi.org/10.1080/17451000903428488

Goffredo, S., Mezzomonaco, L., Zaccanti, F., 2004. Genetic differentiation among populations of the Mediterranean hermaphroditic brooding coral Balanophyllia europaea (Scleractinia: Dendrophylliidae). Mar. Biol. 145, 1075–1083. https://doi.org/10.1007/s00227-004-1403-x

González-Wangüemert, M., Cánovas, F., Pérez-Ruzafa, A., Marcos, C., Alexandrino, P., 2010. Connectivity patterns inferred from the genetic structure of white seabream (Diplodus sargus L.). J. Exp. Mar. Biol. Ecol. 383, 23–31. https://doi.org/10.1016/j.jembe.2009.10.010

Hammami, I., Bahri-Sfar, L., Kaoueche, M., Hassine, O.K.B., 2007. Genetic characterization of striped sea bream (Lithognathus mormyrus) populations on both sides of a boundary area between eastern and western Mediterranean basins 5.

Hidalgo, M., Rossi, V., Monroy, P., Ser-Giacomi, E., Hernández-García, E., Guijarro, B., Massutí, E., Alemany, F., Jadaud, A., Perez, J.L., Reglero, P., 2019. Accounting for ocean connectivity and hydroclimate in fish recruitment fluctuations within transboundary metapopulations. Ecol. Appl. 0, e01913. https://doi.org/10.1002/eap.1913

Hunter, 1999. BIOLOGY OF THE EUROPEAN SPINY LOBSTER, PALINURUS ELEPHAS (FABRICIUS, 1787) (DECAPODA, PALINURIDEA). Crustaceana 72, 545–565. https://doi.org/10.1163/156854099503609

Kaouèche, M., Bahri-Sfar, L., Hammami, I., Hassine, O.K.B., 2013. Morphological and genetic variations of Diplodus vulgaris along the Tunisian coasts 10.

Kersting, D., Casado, C., López-Legentil, S., Linares, C., 2013. Unexpected patterns in the sexual reproduction of the Mediterranean scleractinian coral Cladocora caespitosa. Mar. Ecol. Prog. Ser. 486, 165–171. https://doi.org/10.3354/meps10356

Kružić, P., Žuljević, A., Nikolić, V., 2008. Spawning of the colonial coral Cladocora caespitosa (Anthozoa, Scleractinia) in the Southern Adriatic Sea. Coral Reefs 27, 337–341. https://doi.org/10.1007/s00338-007-0334-7

Kuo, C.-M., Shehadeh, Z.H., Milken, K.K., 1973. A preliminary report on the development, growth and survival of laboratory reared larvae of the grey mullet, Mugil cephalus L. J. Fish Biol. 5, 459–470. https://doi.org/10.1111/j.1095-8649.1973.tb04475.x

Launey, S., 2002. Geographic Structure in the European Flat Oyster (Ostrea edulis L.) as Revealed by Microsatellite Polymorphism. J. Hered. 93, 331–351. https://doi.org/10.1093/jhered/93.5.331

Lazoski, C., Solé-Cava, A., Boury-Esnault, N., Klautau, M., Russo, C., 2001. Cryptic speciation in a high gene flow scenario in the oviparous marine sponge Chondrosia reniformis. Mar. Biol. 139, 421–429. https://doi.org/10.1007/s002270100542

Macpherson, E., Raventos, N., 2006. Relationship between pelagic larval duration and geographic distribution of Mediterranean littoral fishes. Mar. Ecol. Prog. Ser. 327, 257–265.

Madec, G.: NEMO ocean engine, Note du Pole de modélisation, Institut Pierre-Simon Laplace (IPSL), France, No 27 ISSN No1288-1619, 2008.

Maggio, T., Lo Brutto, S., Garoia, F., Tinti, F., Arculeo, M., 2009. Microsatellite analysis of red mullet Mullus barbatus (Perciformes, Mullidae) reveals the isolation of the Adriatic Basin in the Mediterranean Sea. ICES J. Mar. Sci. 66, 1883–1891. https://doi.org/10.1093/icesjms/fsp160

Marzouk, Z., Aurelle, D., Said, K., Chenuil, A., 2017. Cryptic lineages and high population genetic structure in the exploited marine snail Hexaplex trunculus (Gastropoda: Muricidae). Biol. J. Linn. Soc. 122, 411–428. https://doi.org/10.1093/biolinnean/blx070

Masmoudi, M.B., Chaoui, L., Topçu, N.E., Hammami, P., Kara, M.H., Aurelle, D., 2016. Contrasted levels of genetic diversity in a benthic Mediterranean octocoral: Consequences of different demographic histories? Ecol. Evol. 6, 8665–8678. https://doi.org/10.1002/ece3.2490

Melià, P., Schiavina, M., Rossetto, M., Gatto, M., Fraschetti, S., Casagrandi, R., 2016. Looking for hotspots of marine metacommunity connectivity: a methodological framework. Sci. Rep. 6, 23705.

Milano, I., Babbucci, M., Cariani, A., Atanassova, M., Bekkevold, D., Carvalho, G.R., Espiñeira, M., Fiorentino, F., Garofalo, G., Geffen, A.J., Hansen, Jakob.H., Helyar, S.J., Nielsen, E.E., Ogden, R., Patarnello, T., Stagioni, M., FishPopTrace Consortium, Tinti, F., Bargelloni, L., 2014. Outlier SNP

markers reveal fine-scale genetic structuring across European hake populations ( *Merluccius merluccius* ). Mol. Ecol. 23, 118–135. https://doi.org/10.1111/mec.12568

Morales-Nin, B., Moranta, J., 2004. Recruitment and post-settlement growth of juvenile *Merluccius merluccius* on the western Mediterranean shelf. Sci. Mar. 68, 399–409. https://doi.org/10.3989/scimar.2004.68n3399

Muths, D., Rastorgueff, P.-A., Selva, M., Chevaldonné, P., 2015. Local scale connectivity in the cave-dwelling brooding fish Apogon imberbis. J. Sea Res. 95, 70–74. https://doi.org/10.1016/j.seares.2014.10.009

Oddo, P., Adani, M., Pinardi, N., Fratianni, C., Tonani, M., Pettenuzzo, D., others, 2009. A nested Atlantic-Mediterranean Sea general circulation model for operational forecasting. Ocean Sci.

Ordóñez, V., Pascual, M., Rius, M., Turon, X., 2013. Mixed but not admixed: a spatial analysis of genetic variation of an invasive ascidian on natural and artificial substrates. Mar. Biol. 160, 1645–1660. https://doi.org/10.1007/s00227-013-2217-5

Orth, R.J., Harwell, M.C., Inglis, G.J., 2006. Ecology of Seagrass Seeds and Seagrass Dispersal Processes, in: LARKUM, A.W.D., ORTH, R.J., DUARTE, C.M. (Eds.), SEAGRASSES: BIOLOGY, ECOLOGYAND CONSERVATION. Springer Netherlands, Dordrecht, pp. 111–133. https://doi.org/10.1007/978-1-4020-2983-7_5

Palero, F., Abelló, P., Macpherson, E., Beaumont, M., Pascual, M., 2011. Effect of oceanographic barriers and overfishing on the population genetic structure of the European spiny lobster ( *Palinurus elephas* ): POPULATION GENETICS OF PALINURUS. Biol. J. Linn. Soc. 104, 407–418. https://doi.org/10.1111/j.1095-8312.2011.01728.x

Pallaoro, A., Jardas, I., 2003. Some biological parameters of the peacock wrasse, *Symphodus (Crenilabrus) tinca* (L. 1758) (Pisces: Labridae) from the middle eastern Adriatic (Croatian coast). Sci. Mar. 67, 33–41. https://doi.org/10.3989/scimar.2003.67n133

Paterno, M., Schiavina, M., Aglieri, G., Souissi, J.B., Boscari, E., Casagrandi, R., Chassanite, A., Chiantore, M., Congiu, L., Guarnieri, G., Kruschel, C., Macic, V., Marino, I.A.M., Papetti, C., Patarnello, T., Zane, L., Melià, P., 2017. Population genomics meet Lagrangian simulations: Oceanographic patterns and long larval duration ensure connectivity among Paracentrotus lividus populations in the Adriatic and Ionian seas. Ecol. Evol. 7, 2463–2479. https://doi.org/10.1002/ece3.2844

Pedrotti, M.L., 1993. Spatial and temporal distribution and recruitment of echinoderm larvae in the Ligurian Sea. J. Mar. Biol. Assoc. U. K. 73, 513–530. https://doi.org/10.1017/S0025315400033075

Penant, G., Aurelle, D., Feral, J., Chenuil, A., 2013. Planktonic larvae do not ensure gene flow in the edible sea urchin Paracentrotus lividus. Mar. Ecol. Prog. Ser. 480, 155–170. https://doi.org/10.3354/meps10194

Pérez-Portela, R., Palacín, C., Duran, S., Turon, X., 2007. Biological traits of three closely related species of Pycnoclavella (Ascidiacea) in the Western Mediterranean. Mar. Biol. 152, 1031–1038. https://doi.org/10.1007/s00227-007-0750-9

Raventos, N., 2007. Age, growth and reproductive parameters of the Mediterranean cardinal fish, Apogon imberbis. J. Appl. Ichthyol. 23, 675–678. https://doi.org/10.1111/j.1439-0426.2007.00847.x

Reem, E., Douek, J., Paz, G., Katzir, G., Rinkevich, B., 2017. Phylogenetics, biogeography and population genetics of the ascidian Botryllus schlosseri in the Mediterranean Sea and beyond. Mol. Phylogenet. Evol. 107, 221–231. https://doi.org/10.1016/j.ympev.2016.10.005

Rius, M., Pineda, M.C., Turon, X., 2009. Population dynamics and life cycle of the introduced ascidian Microcosmus squamiger in the Mediterranean Sea. Biol. Invasions 11, 2181–2194. https://doi.org/10.1007/s10530-008-9375-2

Rius, M., Turon, X., Dias, G.M., Marshall, D.J., 2010. Propagule size effects across multiple life-history stages in a marine invertebrate: *Propagule size across life-history stages*. Funct. Ecol. 24, 685–693. https://doi.org/10.1111/j.1365-2435.2009.01668.x

Roberts, S.D., Dixon, C.D., Andreacchio, L., 2012. Temperature dependent larval duration and survival of the western king prawn, Penaeus (Melicertus) latisulcatus Kishinouye, from Spencer Gulf,

South Australia. J. Exp. Mar. Biol. Ecol. 411, 14–22. https://doi.org/10.1016/j.jembe.2011.10.022

Santos, R., Dias, S., Tecelão, C., Pedrosa, R., Pombo, A., n.d. Reproductive biological characteristics and fatty acid profile of Holothuria mammata (Grube, 1840) 8.

Sá-Pinto, A., Branco, M.S., Alexandrino, P.B., Fontaine, M.C., Baird, S.J.E., 2012. Barriers to Gene Flow in the Marine Environment: Insights from Two Common Intertidal Limpet Species of the Atlantic and Mediterranean. PLoS ONE 7, e50330. https://doi.org/10.1371/journal.pone.0050330

Schiavina, M., Marino, I. a. M., Zane, L., Melià, P., 2014. Matching oceanography and genetics at the basin scale. Seascape connectivity of the Mediterranean shore crab in the Adriatic Sea. Mol. Ecol. 23, 5496–5507. https://doi.org/10.1111/mec.12956

Schunter, C., Carreras-Carbonell, J., Macpherson, E., Tintoré, J., Vidal-Vijande, E., Pascual, A., Guidetti, P., Pascual, M., 2011. Matching genetics with oceanography: directional gene flow in a Mediterranean fish species. Mol. Ecol. 20, 5167–5181. https://doi.org/10.1111/j.1365-294X.2011.05355.x

Ser-Giacomi, E., Rossi, V., López, C., Hernandez-Garcia, E., 2015. Flow networks: A characterization of geophysical fluid transport. Chaos Interdiscip. J. Nonlinear Sci. 25, 036404.

Serra, I.A., Innocenti, A.M., Maida, G.D., Calvo, S., Migliaccio, M., Zambianchi, E., Pizzigalli, C., Arnaud-Haond, S., Duarte, C.M., Serrao, E.A., Procaccini, G., 2010. Genetic structure in the Mediterranean seagrass Posidonia oceanica: disentangling past vicariance events from contemporary patterns of gene flow. Mol. Ecol. 19, 557–568. https://doi.org/10.1111/j.1365-294X.2009.04462.x

Shabtay, A., Tikochinski, Y., Benayahu, Y., Rilov, G., 2014. Preliminary data on the genetic structure of a highly successful invading population of oyster suggesting its establishment dynamics in the Levant. Mar. Biol. Res. 10, 407–415. https://doi.org/10.1080/17451000.2013.814790

Soria, G., Tordecillas-Guillen, J., Cudney-Bueno, R., Shaw, W., 2010. Spawning Induction, Fecundity Estimation, and Larval Culture of *Spondylus calcifer* (Carpenter, 1857) (Bivalvia: Spondylidae). J. Shellfish Res. 29, 143–149. https://doi.org/10.2983/035.029.0108

Sromek, L., Forcioli, D., Lasota, R., Furla, P., Wolowicz, M., 2019. Next-generation phylogeography of the cockle *Cerastoderma glaucum* : Highly heterogeneous genetic differentiation in a lagoon species. Ecol. Evol. 9, 4667–4682. https://doi.org/10.1002/ece3.5070

Susini, M.-L., Thibaut, T., Meinesz, A., Forcioli, D., 2007. A preliminary study of genetic diversity in Cystoseira amentacea (C. Agardh) Bory var. stricta Montagne (Fucales, Phaeophyceae) using random amplified polymorphic DNA. Phycologia 46, 605–611. https://doi.org/10.2216/06-100.1

Teixidó, N., Garrabou, J., Harmelin, J.-G., 2011. Low Dynamics, High Longevity and Persistence of Sessile Structural Species Dwelling on Mediterranean Coralligenous Outcrops. PLoS ONE 6, e23744. https://doi.org/10.1371/journal.pone.0023744

Thibaut, T., Bottin, L., Aurelle, D., Boudouresque, C.-F., Blanfuné, A., Verlaque, M., Pairaud, I., Millet, B., 2016. Connectivity of Populations of the Seaweed Cystoseira amentacea within the Bay of Marseille (Mediterranean Sea): Genetic Structure and Hydrodynamic Connections. Cryptogam. Algol. 37, 233–255. https://doi.org/10.7872/crya/v37.iss4.2016.233

Vasconcelos, P., Gaspar, M.B., Joaquim, S., Matias, D., Castro, M., 2004. Spawning of *Hexaplex (Trunculariopsis) trunculus* (Gastropoda: Muricidae) in the laboratory: description of spawning behaviour, egg masses, embryonic development, hatchling and juvenile growth rates. Invertebr. Reprod. Dev. 46, 125–138. https://doi.org/10.1080/07924259.2004.9652616

Vaz, A.C., Scarcella, G., Pardal, M.A., Martinho, F., 2019. Water temperature gradients drive early life-history patterns of the common sole (Solea solea L.) in the Northeast Atlantic and Mediterranean. Aquat. Ecol. 53, 281–294. https://doi.org/10.1007/s10452-019-09688-2

Villamor, A., Costantini, F., Abbiati, M., 2014. Genetic Structuring across Marine Biogeographic Boundaries in Rocky Shore Invertebrates. PLOS ONE 9, e101135. https://doi.org/10.1371/journal.pone.0101135

Wanninger, A., Haszprunar, G., 2002. Chiton myogenesis: Perspectives for the development and evolution of larval and adult muscle systems in molluscs. J. Morphol. 251, 103–113. https://doi.org/10.1002/jmor.1077

Weber, A. a.-T., Mérigot, B., Valière, S., Chenuil, A., 2015. Influence of the larval phase on connectivity: strong differences in the genetic structure of brooders and broadcasters in the Ophioderma longicauda species complex. Mol. Ecol. 24, 6080–6094. https://doi.org/10.1111/mec.13456

Weber, A.A.-T., Stöhr, S., Chenuil, A., 2014. Genetic data, reproduction season and reproductive strategy data support the existence of biological species in Ophioderma longicauda. C. R. Biol. 337, 553–560. https://doi.org/10.1016/j.crvi.2014.07.007

Zitari-Chatti, R., Chatti, N., Elouaer, A., Said, K., 2007. Genetic variation and population structure of the caramote prawn Penaeus kerathurus (Forskäl) from the eastern and western Mediterranean coasts in Tunisia: Genetic variation in Penaeus kerathurus. Aquac. Res. 39, 70–76. https://doi.org/10.1111/j.1365-2109.2007.01874.x

Zulliger, D.E., Tanner, S., Ruch, M., Ribi, G., 2009. Genetic structure of the high dispersal Atlanto-Mediterreanean sea star Astropecten aranciacus revealed by mitochondrial DNA sequences and microsatellite loci. Mar. Biol. 156, 597–610. https://doi.org/10.1007/s00227-008-1111-z